

GEOCHEMICAL ANALYSIS OF GLASS AND GLAZE FROM HASANLU,  
NORTHWESTERN IRAN: CONSTRAINTS ON MANUFACTURING TECHNOLOGY

by

COLLEEN PATRICIA STAPLETON

(Under the Direction of Samuel E. Swanson)

ABSTRACT

Our lack of knowledge of glassmaking technology during the transition between the Bronze and Iron Ages lies partly in the small amount of well-excavated glass artifacts. One site that has produced a range of suitable material is Hasanlu in northwestern Iran, excavated by Robert H. Dyson, Jr., from the University of Pennsylvania. Glass, glaze and faience were analyzed using electron microprobe, laser ablation-inductively coupled plasma-mass spectrometry (LA-ICP-MS), and laser fusion-oxygen isotope analysis. The results show that the glasses from Hasanlu were made using different combinations of quartz sand, alkali feldspar, dolomite, copper ore, copper alloy metal, copper refining slag, antimony ore, and lead ore. The oxygen isotope analyses indicate that more than one geological source of quartz was used to make the glasses. The range in major element compositions and oxygen isotope ratios are large and suggest that the glasses were made in more than one factory. The raw materials and procedures identified for the manufacture of the Hasanlu glasses indicate that glassmakers understood the interaction of materials they used. Many of the glasses from Hasanlu are different in major element composition from those of other 2<sup>nd</sup> millennium BC and early 1<sup>st</sup> millennium BC glasses. These differences suggest that the glasses from Hasanlu were made either near Hasanlu or imported into Hasanlu from an as yet unidentified region. The comparison indicate that at least in the early 1<sup>st</sup> millennium BC, the knowledge of glassmaking probably extended well beyond the boundaries of Mesopotamia and Egypt.

INDEX WORDS: Glass, glassmaking, analysis, microprobe, oxygen isotope, ICP-MS, Hasanlu, Iran, ancient technology, archaeometry, archaeological science, Iron Age, 9<sup>th</sup> c BC, Near East.

GEOCHEMICAL ANALYSIS OF GLASS AND GLAZE FROM HASANLU,  
NORTHWESTERN IRAN: CONSTRAINTS ON MANUFACTURING TECHNOLOGY

by

COLLEEN PATRICIA STAPLETON

B. A., Macalester College, 1986

M. A., University of Texas Austin, 1991

A Dissertation Submitted to the Graduate Faculty of The University of Georgia in Partial  
Fulfillment of the Requirements for the Degree

DOCTOR OF PHILOSOPHY

ATHENS, GEORGIA

2003

© 2003

Colleen P. Stapleton

All Rights Reserved

GEOCHEMICAL ANALYSIS OF GLASS AND GLAZE FROM HASANLU,  
NORTHWESTERN IRAN: CONSTRAINTS ON MANUFACTURING TECHNOLOGY

by

COLLEEN P. STAPLETON

Major Professor: Samuel E. Swanson

Committee: Ervan Garrison  
Alberto Patino-Duce  
Bruce Railsback  
David Wenner

Electronic Version Approved:

Maureen Grasso  
Dean of the Graduate School  
The University of Georgia  
May, 2003

## DEDICATION

This project is dedicated to the people of Hasanlu.

## ACKNOWLEDGEMENTS

My introduction to the world of ancient materials and technology came from the Department of Scientific Research at the British Museum, London, my first professional job. The enthusiasm of the British Museum scientists and the depth of knowledge they possess truly inspired me to continue research in this field. Ian Freestone taught me everything I know, except for the wrong things. Sheridan Bowman provided authoritative and appreciated guidance.

Bob Brill has been a steady source of wisdom and friendship. It was he who suggested I work on glassy materials from Hasanlu.

Regular discussions with Sam Swanson (my advisor) helped to hash out important details of this research, and to understand the practicalities of scientific research and the real world. Mo Ghazi, Rusty Malchow, John Valley, and Mike Spicuzza have been very generous in allowing me to work with them in their labs. I thank my committee members, Dave, Alberto, Bruce, and Erv, for all their critiques, comments, and positive interest in my research.

This project would not have been possible without support from Bob Dyson, Jr., the Hasanlu Project principle archaeologist, and I gratefully acknowledge his helpful comments on this research. Maude de Schauensee has been my constant contact with the Hasanlu Project. Her initial direction and continuing interest in the results of my research have been most encouraging.

Much appreciation also goes to the office staff of the Geology Department, Pat Hancock, Mary Crowe, and Beatrice Stephens. The Department of Geology, the Graduate School, and the Office of Vice President of Research of the University of Georgia, as well as the International Commission on Glass and the Dorot Foundation

(via the American Schools of Oriental Research) have provided me with much appreciated financial funding for this research.

This work really wouldn't have been possible without my parents' original interest in each other. Thanks Mom and Dad.

My grasp on the important things in life, those outside of graduate school, comes from knowing Charlie.

## TABLE OF CONTENTS

	Page
DEDICATION .....	iv
ACKNOWLEDGEMENTS .....	v
CHAPTER	
1 INTRODUCTION.....	1
2 HISTORY OF GLASS MANUFACTURING (LITERATURE REVIEW).....	4
HISTORY OF VITREOUS MATERIALS .....	5
GLASSMAKING RAW MATERIALS AND INDUSTRY ORGANIZATION ..	7
VITREOUS MATERIALS TECHNOLOGY AND EARLY IRON AGE	
POLITICAL CHANGES .....	9
3 REGIONAL SETTING AND HISTORY OF THE ARCHAEOLOGICAL SITE	
OF HASANLU (LITERATURE REVIEW).....	11
HASANLU SITE DESCRIPTION .....	12
POLITICAL HISTORY OF MESOPOTAMIA, IRAN, AND NEIGHBORING	
REGIONS FROM MID-2 <sup>ND</sup> MILLENNIUM BC TO ABOUT 750 BC ....	13
PROCUREMENT AND MOVEMENT OF MATERIALS .....	22
LOCAL AND NON-LOCAL DECORATIVE STYLES OF ARTIFACTS	
FROM HASANLU.....	29
THE SAMPLES OF THIS STUDY .....	30
4 CHEMICAL ANALYSIS OF GLASS ARTIFACTS FROM IRON AGE LEVELS	
AT HASANLU, NORTHWESTERN IRAN.....	38
ABSTRACT.....	39
INTRODUCTION.....	39

	WEATHERING OF ANCIENT GLASSES.....	40
	THE ARCHAEOLOGICAL SITE AND SAMPLES.....	41
	ANALYTICAL METHOD.....	42
	RESULTS AND DISCUSSION.....	44
	CONCLUSION.....	57
5	BATCH MATERIAL PROCESSING AND GLASSMAKING TECHNOLOGY OF 9 <sup>TH</sup> CENTURY B.C. ARTIFACTS EXCAVATED FROM THE SITE OF HASANLU, NORTHWEST IRAN.....	59
	ABSTRACT.....	60
	INTRODUCTION.....	61
	ANALYTICAL METHODS.....	62
	RESULTS AND DISCUSSION.....	62
	CONCLUSIONS.....	67
6	THE RAW MATERIALS USED TO COLOUR 11 <sup>TH</sup> -9 <sup>TH</sup> C BC BLUE TRANSPARENT GLAZES FROM HASANLU, IRAN.....	69
	INTRODUCTION.....	70
	METHODOLOGY.....	71
	RESULTS.....	72
	DISCUSSION.....	74
	CONCLUSIONS.....	75
7	OXYGEN ISOTOPE ANALYSIS OF VITREOUS MATERIALS FROM PERIOD IVB HASANLU AND IMPLICATIONS FOR RAW MATERIAL IDENTIFICATION.....	76
	INTRODUCTION.....	77
	SAMPLES AND ANALYTICAL PROCEDURE.....	79
	RESULTS.....	82

	DISCUSSION.....	85
	CONCLUSIONS.....	97
8	THE MANUFACTURE OF GLASSES AND GLAZES EXCAVATED FROM PERIOD IVB LEVELS (11 <sup>TH</sup> -9 <sup>TH</sup> C B.C.) AT HASANLU, IRAN.....	100
	INTRODUCTION.....	101
	METHODOLOGY.....	104
	RESULTS .....	114
	DISCUSSION.....	115
	CONCLUSIONS.....	148
9	CONCLUSIONS AND RECOMMENDATIONS FOR FUTURE RESEARCH .....	150
	REFERENCES CITED.....	157

CHAPTER 1  
INTRODUCTION

Archaeological evidence indicates that most excavated, larger ancient glass artifacts were manufactured at centers of religious and political power, partly because the technical knowledge and skilled labor required to manufacture glass was difficult to maintain (Grose, 1989; Oppenheim et al., 1970). Early glass objects were valued and often were given as gifts to people of power (Lilyquist and Brill, 1993). The demand for glass probably resulted in a dissemination of glassmaking expertise to areas of wealth and power in Mesopotamia, Egypt, the eastern Mediterranean, and throughout the Mid-East and Near-East. As glassmakers and the knowledge of glassmaking moved, the technology had to adapt to local circumstances, including availability of raw materials for glassmaking, furnace construction and fuel, and interactions with other industries. The resulting glass objects provide a record of the changes in technology and resource utilization experienced by these societies. Unlike objects that quickly decay, for example those of cloth or wood, glass survives more or less intact and provides a record that can be used to measure a complex operation, one that can be used to monitor technological and societal development.

This dissertation presents data obtained from analyses of early Iron Age glass and glazes from the site of Hasanlu, northwestern Iran. Chapters 1 and 9 are the introduction and conclusions, respectively, to this research. Chapter 2 is a literary review of glassmaking history from its beginnings up to the early 1<sup>st</sup> millennium BC. Chapter 3 is a literary review of the archaeological site of Hasanlu and the historical setting in Mesopotamia and the surrounding region from the mid-2<sup>nd</sup> millennium BC to the mid-1<sup>st</sup> millennium BC. The results of various analyses are presented in Chapters 4-9 as a series of papers submitted for publication. Readers are asked to please reference the published papers rather than this dissertation when citing the data and results. Chapter 4 introduces electron microprobe analysis of the Hasanlu material and discusses the benefits of using microanalytical techniques in the analysis of

archaeological manufactured glass. Chapter 5 demonstrates the use of major element data in determining what types of raw materials were used in the glassmaking batches of blue transparent to translucent glasses and glazes, black glasses, and blue opaque glasses from Hasanlu. Chapter 6 introduces the use of laser ablation-inductively coupled plasma-mass spectrometry for trace element analysis on blue glazes from Hasanlu and shows how these data are used to infer the source of colorant used in glassy materials. Chapter 7 describes the use of laser fusing of glass and faience from Hasanlu to evolve oxygen for isotope analysis, and discusses how oxygen isotope composition of archaeological manufactured glass may be used to infer the source of quartz in the glassmaking batch. Chapter 8 describes in detail the raw materials present in the glassmaking batches and possible glassmaking procedures used to manufacture the Hasanlu materials and compares these inferred raw materials and procedures to those describe in 7<sup>th</sup> c BC cuneiform glassmaking texts from Nineveh (Oppenheim et al., 1970).

CHAPTER 2  
HISTORY OF GLASS MANUFACTURING FROM 4<sup>TH</sup> MILLENNIUM BC TO MID-FIRST  
MILLENNIUM BC  
(LITERATURE REVIEW)

## HISTORY OF VITREOUS MATERIALS

The earliest manufactured vitreous materials date to at least as early as the 6<sup>th</sup> millennium BC and are glazes on stone artifacts (Moorey, 1999). A mix of alkalis was applied to the stone surfaces and the whole was heated until a glassy coating formed. A similar process was used to manufacture faience, also called paste and composite, by mixing alkalis with quartz-rich sand or crushed quartz and copper to color it blue (Vandiver, 1983a). Another blue vitreous material, dated to at least as early as the 3<sup>rd</sup> millennium BC, was made by combining quartz, lime, alkalis, and copper to make crystalline Egyptian blue ( $\text{CaCuSi}_4\text{O}_{10}$ ) set in a glass matrix (Tite et al., 1984). Much of this early glassy material is assumed to have been made in imitation of turquoise or lapis lazuli, precious stones in the ancient Near East and eastern Mediterranean (Moorey, 1999). Both glazing and faience are suggested as techniques from which glassmaking developed (Peltenberg, 1987, 1971). However, this is not accepted by all glass researchers, some who have shown that certain colors of glass were made in connection with metallurgical processes (Freestone et al., 2001; Stapleton et al., 1999; Mass et al., 1998; Rehren et al., 1998).

Objects made entirely of glass are found in the archaeological record at least as early as the 25<sup>th</sup> century BC (Moorey, 1999). These early objects are small and relatively rare in the archaeological record. The earliest glass found in the archaeological record is a blue translucent lump of unidentifiable form from Eridu in southern Mesopotamia (Barag, 1970). The earliest glass objects recognized in the archaeological record are small items such as beads. These objects were worked out of cold glass. Open-backed molds made of stone were used by pressing hot, but relatively viscous glass into the mold and letting the glass cool until the finished form could be removed (Grose, 1989). Pale, copper-colored blue glass, and opaque yellow and white glasses were some of the earliest glasses manufactured (Moorey, 1999).

Glassmaking on a large scale appears to have begun around the late 16<sup>th</sup> century BC with the manufacturing of vessels, based on the quantity of glass artifacts found in excavations at Nuzi in northern Mesopotamia (Starr, 1937, 1939). Egypt had an established glassmaking industry by the mid-15<sup>th</sup> c BC (Petrie, 1894; Nicholson, 1995). By this period, the production of core-formed vessels shows that manipulating hot glass had become common. Manufacture of core-formed objects may have been carried out in two ways. In one process, a rod is coated with refractory clay. Wet, crushed glass is then formed around the clay and let to dry, allowing alkalis to effloresce to the surface. This mass is heated until the glass fuses (Giberson, 2002). Decorative elements in glass were added by heating rods over or in a furnace until they became soft, much like modern framewokers use today. In another process, rods of glass may have been heated until fused, then wound around a clay-coated rod. Remnants of the refractory material is found in many core-formed vessels.

Archaeological evidence for the tools and equipment used by ancient glassmakers is not well-known (Nicholson and Henderson, 2002). Only the site of Amarna in Egypt has produced possible evidence for glassmaking furnaces of the 2<sup>nd</sup> and early 1<sup>st</sup> millennium BC (Jackson et al., 1998). Textual evidence comes from four sets of cuneiform tablets found at Nineveh, the 7<sup>th</sup> century capital of Assyria, in Turkey at the Hittite capital of Hattusa, and an unprovenanced tablet (Oppenheim, 1970). The most complete set of texts are those from Nineveh, which are transcriptions of earlier glassmaking texts, probably from about the 17<sup>th</sup> c BC. These texts state what raw materials to use to make glass and probably also to make faience, glaze, and Egyptian Blue. Furnace temperatures are estimated by color of flames. Different types of crucibles and tools are mentioned. It has not been possible to translate many of the technical terms in the texts, such as names for raw material, tools, and materials

produced. Modern scientific analysis of ancient glasses has provided insight into ancient glassmaking.

#### GLASSMAKING RAW MATERIALS AND INDUSTRY ORGANIZATION

Scientific studies of glassy materials have shown that the earliest-dated glass objects have chemical compositions consistent with manufacture using plant ash and quartz. Plant ash provided alkali as a flux added to promote melting in glassmaking mixtures, which are mostly SiO<sub>2</sub> (silica). Additionally, analyses show that ores of copper, cobalt, lead and antimony were processed and used to color the glass. Throughout the Near- and Mid- East, the Mediterranean and Europe, plant ash appears to have been the main source of alkali for glass from the beginnings of glassmaking in the 3<sup>rd</sup> millennium BC until around the 9<sup>th</sup> century BC (Sayre, 1965; Bimson and Freestone, 1987; Lilyquist and Brill, 1993; Moorey, 1999; Hartmann et al., 1997). Cuneiform texts on glassmaking that have been dated to the last half of the 13<sup>th</sup> century BC and the early 7<sup>th</sup> century BC state that the ashes of the *naga* plant should be used to make glass (Oppenheim et al., 1970). A recent study suggests that as early as the 14<sup>th</sup> century BC, Egyptian glassmakers were using a different source of alkali, the mineral natron, taken from evaporite deposits in the Wadi Natrun, Egypt (Shortland and Tite, 2000). It is not yet clear whether other regions were producing natron-type glass at this time.

It has long been accepted that glasses that contain greater than about 1 wt% to 2 wt% each of K<sub>2</sub>O and MgO were made with plant ash (Fig. 2.1), and those with less were made with mineral soda (e.g. Turner, 1956; Brill, 1970a). The evidence for this assumption is mostly circumstantial, since the main archaeological evidence for use of an actual alkali source dates to the Roman period and later (e.g. Nenna et al., 1997). No source of batch material from earlier glass has been positively identified.

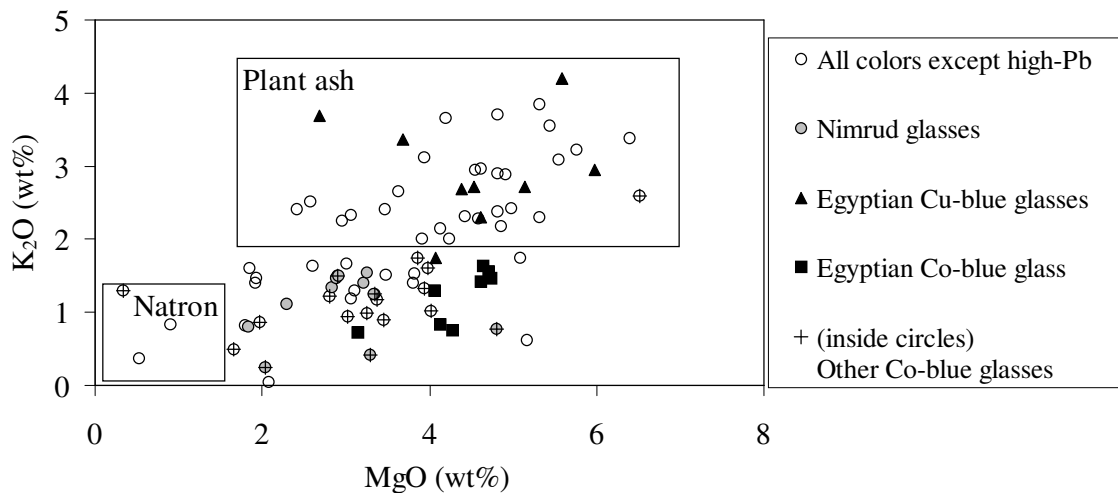


Figure 2.1. Selected Bronze and Iron Age glasses from the East Mediterranean and Near East. High lead in these glasses is related to colorants, and proportionally lowers other oxides. Nimrud glasses were possibly made with mineral alkali. Boxes are guidelines inside of which mineral- and plant ash-glasses typically plot (modified from Lilyquist and Brill, 1993). Egyptian Co-blue glasses are suggested by Shortland and Tite (2000) to be natron-type. Data from Brill (1999), Shortland and Tite (2000), and Lilyquist and Brill (1993).

Previous scientifically studied assemblages of vitreous materials from the Bronze Age and early Iron Age suggest that the quality of glassy material and the organization of manufacturing centers varied according to the political importance of the site. The Bronze Age site of Nuzi (15<sup>th</sup>—14<sup>th</sup> c BC) in northern Iraq was a politically important borderland city of the Mitanni empire. The site is considered to have been a center of large-scale vitreous materials manufacturing because of the narrow range of glass chemical compositions, the variety of glassworking techniques used to form objects, and the wide variety of excavated vitreous materials including glazes, frit (a sintered, polycrystalline body with no glassy coating), faience, and Egyptian blue (Vandiver, 1982, 1983b). Similar conclusions were reached for the Bronze and early Iron Age sites in the Baq'ah Valley and at Beth Shan in modern Israel (McGovern, 1987). Glass from Geoy Tepe and Dinkha Tepe (18<sup>th</sup>—16<sup>th</sup> c BC) in northwestern Iran is considered to have been made in a smaller, less technologically developed, and less organized industry, based

on the limited range of glass colors, coarser inclusions, and larger bubbles (McGovern, et al., 1991; Swann et al., 1993). These northwestern Iranian sites are suggested to be stops along Assyrian trade routes, far from more highly organized vitreous materials manufacturing centers.

## VITREOUS MATERIALS TECHNOLOGY AND EARLY IRON AGE POLITICAL CHANGES

Political and economic changes mark the transition between the late Bronze and early Iron Ages, around the 13<sup>th</sup> to 12<sup>th</sup> century BC, for the dominant eastern Mediterranean civilizations in Egypt, Mesopotamia, Anatolia, and Greece. Little is known of what happened to the glass industry in the east during this transition and prior to about the 7<sup>th</sup> century BC. From about the 9<sup>th</sup> century BC onward, glass with a chemical composition that is characteristic of having been made with mineral alkali is commonly found in the archaeological record, sometimes alongside plant ash glasses (Table 2.1).

Table 2.1. Typical chemical compositions of plant ash glass and natron glass, excluding colorants

	Plant ash glass Egyptian, 14 <sup>th</sup> c BC*	Natron glass Roman, 4 <sup>th</sup> c AD <sup>†</sup> , “aqua”
SiO <sub>2</sub>	68.4	69.4
Al <sub>2</sub> O <sub>3</sub>	0.74	2.64
Fe <sub>2</sub> O <sub>3</sub>	0.48	0.34
CaO	3.22	8.77
MgO	2.69	0.66
Na <sub>2</sub> O	18.3	17.2
K <sub>2</sub> O	3.69	0.64

\*Data from Lilyquist and Brill (1993), analysis #6.

†Data from Brill (1999), Jalame analysis 639.

The spread of the mineral-based glass technology in the Iron Age was possibly related to migration of skilled glassmakers during this period of unrest. Disruption of trade in raw materials or finished glass may have forced glassmakers to use different

sources of alkali. Known resources of plant alkalies may have become scarce, forcing glassmakers to search for appropriate substitutes. Changes in the alkali from a plant to a mineral source could have affected glass recipe preparations, melting temperatures and conditions, or quality of the finished glass. Revisions to the known glassmaking technology probably would have been required. The organization of the glassmaking industry may have changed to accommodate technical changes.

Our lack of knowledge of glassmaking technology during the transition between the Bronze and Iron Ages lies partly in the small amount of published information on well-documented, scientifically excavated glass artifacts and partly in the lack of any thorough scientific study of available material. One site that offers potential is Hasanlu in northwestern Iran (Dyson, 1989a). At this site, a range of well-dated glass and vitreous material artifacts were carefully excavated from Iron Age levels. A number of these artifacts have physical and decorative characteristics that suggest that they were created in culturally distinct regions and are perhaps made from vitreous materials that were manufactured in more than one region (Marcus, 1996). It is proposed that changes and developments in glassmaking technology in the Near East during the Iron Age may be better understood by studying glass and vitreous artifacts from the site of Hasanlu.

## CHAPTER 3

### REGIONAL SETTING AND HISTORY OF THE ARCHAEOLOGICAL SITE OF HASANLU (LITERATURE REVIEW)

## HASANLU SITE DESCRIPTION

The site of Hasanlu is an artificially created mound that rises above the floor of the Solduz Valley, located south of Lake Urmia in northwestern Iran. Today, as in the past, the area around the mound is used for agriculture. The modern climate in the Lake Urmia area is relatively dry with around 30 cm annual rainfall. Local temperatures range from around 32 C in August to around -4 C in January (Voigt, 1977). The archaeological site of Hasanlu is approximately 600 m in diameter with a central high mound of about 25 m height and 200 m width, surrounded by a lower mound. The Hasanlu Project excavations took place from 1956 to 1977 and were directed by Robert H. Dyson from the University of Pennsylvania Museum of Archaeology and Anthropology, and were co-sponsored by the Metropolitan Museum of Art (New York) and the Archaeological Service of Iran (Dyson, 1989a). The occupation layers at Hasanlu record Neolithic 6<sup>th</sup> millennium BC through to the 4<sup>th</sup> c BC occupation (Voigt and Dyson, 1993) with a small re-occupation in the Islamic period. Dyson (1965) describes the features that characterize Periods VI through III (about 1600 BC to 400 BC). The Iron Age identified at Hasanlu begins around 1450 BC, labeled at Hasanlu as Period V (Table 3.1).

Table 3.1 Iron Age of Hasanlu

Iron Age subdivision	Hasanlu Period	Dates (approximate)
Iron I	Hasanlu V	1450 – 1250 BC
Iron II	Hasanlu IVC (terminated by fire)	1250 – 1100 BC
Iron II	Hasanlu IVB (terminated by destruction; samples of this study from Period IVB)	1100 – 800 BC
Iron II	Hasanlu IVA (terminated by fire, abandoned)	800 – 750 BC
Iron III	Hasanlu IIIB	750 – 600 BC

The ruling population in the Iron Age Solduz Valley lived in a number of political centers like Hasanlu, but most people lived on the agricultural land that surrounded these centers. The surrounding hillsides were probably also occupied, as identified from one

Period IV settlement (Dyson, 1989b). At the end of the 9<sup>th</sup> c BC, Hasanlu was sacked and burned by currently unidentified attackers. Period IVB includes the late 9<sup>th</sup> c BC destruction layer and has yielded an abundance of artifacts, including objects made of glass and faience as well as glazed ceramics which are the focus of this study. After the late 9<sup>th</sup> c BC attack, the mound was only sparsely inhabited for about another 50 years (Period IVA). An Urartian settlement occupied the mound in the late 8<sup>th</sup> c BC, Period IIIB (Dyson, 1989b).

Around the time of the major 9<sup>th</sup> c BC destruction at Hasanlu, the nearby kingdom of Urartu in eastern Turkey was trying to expand its influence south to control trade routes to Anatolia, in direct conflict with Assyria. Assyria, recovering from civil war between king Shalmaneser III and rural ruling families, was losing control over Anatolia, Babylon, and western Iran. Objects from Hasanlu show a variety of cultural styles, linking the site to the dominant political powers of the time. Some Period IVB artifacts from Hasanlu appear to have been made in Assyria, while others were made in imitation of Assyrian styles, probably in local workshops (Winter, 1977). Other artifacts showed north Syrian origin or derivation. Many artifacts have stylistic attributes that link them to people of the Iranian plateau (Marcus, 1996). Hasanlu was not an isolated settlement and existed in a boundary area between several cultures (Fig 3.1) that variously influenced what went on at Hasanlu. Detailed bibliographies of articles that discuss Hasanlu are published in Dyson (1965) and Levine and Young (1977).

#### POLITICAL HISTORY OF MESOPOTAMIA, IRAN AND NEIGHBORING REGIONS FROM MID-2<sup>ND</sup> MILLENNIUM BC TO ABOUT 750 BC

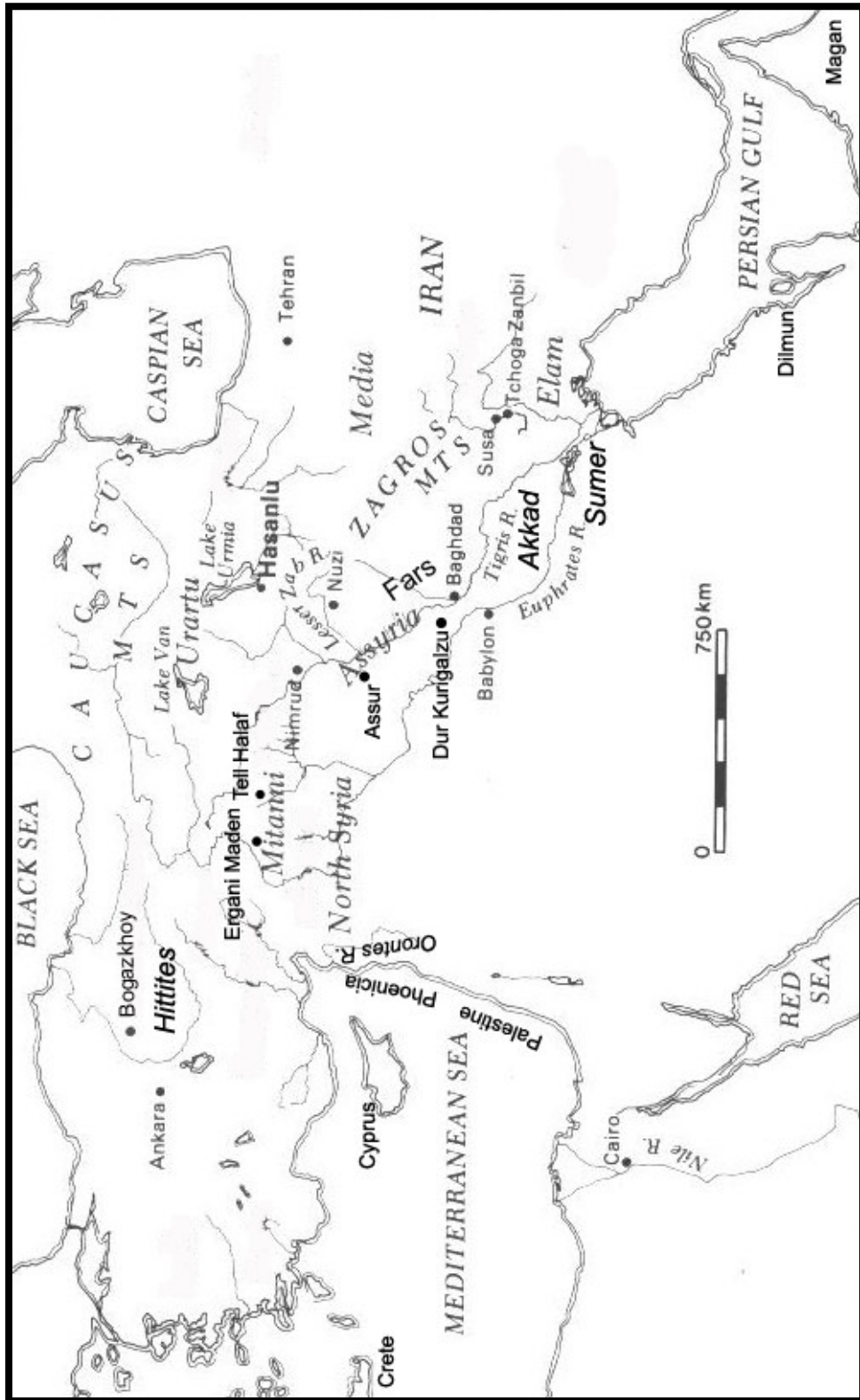
A major change in the political structure of Mesopotamia occurred in 1595 BC when the Hittite king Mursilis I defeated the Babylonian empire (now called the Old Babylonian empire). Mursilis I sacked cities in northern Mesopotamia (cities under Babylonian influence) and then proceeded south with the intention of attacking the city of

Babylon itself. Before he reached Babylon, Mursilis I was called back to Anatolia to defend the Hittite capital. The Old Babylonian dynasty, founded by Hammurabi, which had united Sumer and Akkad (Fig. 3.1), was defeated and no major power existed to take over its former role. This allowed the development of the smaller, regional kingdoms, of the Kassite, Mitannian, and Middle Assyrian empires (Lloyd, 1984). Locations of places and political entities mentioned in this chapter are shown in Fig 3.1.

### **Kassite Kingdom (16<sup>th</sup> c BC – 12<sup>th</sup> c BC)**

The Kassites migrated from Iran into Mesopotamia, part of the movement of Indo-Europeans into Iran (Young, 1967). When Mursilis I and the Hittites left, the Kassites took over the governance of Babylon and adopted the administrative and religious customs along with the Akkadian language of the Old Babylonian Empire (Lloyd, 1984). The strength of the Kassite Empire lay not in military dominance, but in political and economic influence. The Kassites competed with the Hittites, Egyptians, and Assyrians (to the north) for control of trade with the eastern Mediterranean, including Greece. Trade with Egypt brought ivory, wood, and precious metals into the Kassite empire. Other Egyptian connections included political exchanges of ambassadors and intermarriage between Kassite and Egyptian royal families (Knapp, 1988).

Figure 3.1 Location map for some political units and archaeological sites mentioned in the text. Modified from Dyson (1989a).



In the early 14<sup>th</sup> century BC, a new Kassite city was made the capital, Dur-Kurigalzu ('Aqar Quf; Fig 3.1), west of modern Baghdad (Lloyd, 1984; Knapp, 1988). The city of Babylon (Fig 3.1) remained the center of politics, religion, and trade in Mesopotamia. This practice of the Kassites to preserve and rebuild the traditionally important centers of Old Babylonian power, including Ur, Uruk, and Eridu (Fig 3.2), probably contributed to the long, stable period of Kassite rule. The Kassites also had strong influence in the area around the Diyala River (Fig.3.2), a large river system and major transport route in central Mesopotamia up to part of the Iranian highlands. In the 13<sup>th</sup> c BC and 12<sup>th</sup> c BC, the Kassite empire came under increasing attacks from Assyria in the north and Elam (Fig 3.1) in the east and south. In the 13<sup>th</sup> c BC, the Assyrian king Tukulti-Ninurta I sacked the city of Babylon, bringing it under Assyrian control for a short period. The Kassite dynasty was completely defeated around 1157 BC or 1158 BC by the Elamite king Shutruk-Nahhunte (Knapp, 1988; Potts, 1999).

### **Hurrian-Mitannian Kingdom (about 1500 BC – 1350 BC)**

Hurrians first moved into upper Mesopotamia from the north and east at least as early as the late 3<sup>rd</sup> millennium BC. They were neither Semitic nor Indo-European, and their origins are as yet unknown. Small, Hurrian kingdoms were established in upper Mesopotamia led by a strong military class skilled in horsemanship and the use of chariots with two spoked wheels. The Hurrians dominated trade routes between Assyria and the Mediterranean and grew in regional power until they organized into one political entity called the Mitanni Empire (Fig 3.1). One of the largest archaeological excavations of Mitanni culture is Nuzi (Fig 3.1), southwest of modern Kirkuk, Iraq, which existed in the farthest south of the Mitanni Empire. The Mitannians had close political and economic contacts with the Hittites in Anatolia, the Middle Assyrian empire, and Egypt (Lloyd, 1984). By the mid-14<sup>th</sup> century BC, conflict within the ruling royal family caused a

decline in Mitannian military power. Under the Assyrian king Shalmaneser I, the Mitannian Empire was defeated in 1250 BC and came under Assyrian control.

### **Middle and Late Assyrian Empire**

The Middle Assyrian Empire, whose capital was Assur (Fig 3.1), played a dominant role in Mesopotamia in the 14<sup>th</sup> c BC with the military successes of Assur-uballit I (1363-1328 BC) and his later successors, Adad-Nirari I (1307-1275 BC), Shalmaneser I (1274-1245 BC), and Tukulti-Ninurta I (1244-1208 BC), over the Mitannians and Kassites. Tukulti-Ninurta I extended Assyrian control west to the Euphrates River, expelling the Hittites who lived there (Knapp, 1988). The purpose of these military campaigns was to control territory and trade routes to bring metals, ivory, and other materials into resource-poor Mesopotamia. Following the defeat of the Kassites, there were several centuries of political instability, partly instigated by migrating Aramaean and Chaldean, Semitic-speaking tribes (Knapp, 1988).

The Late Assyrian Empire started in the late 10<sup>th</sup> and early 9<sup>th</sup> centuries BC, under king Adad-Nirari II (911-891 BC), Assyria strengthened its position to the north at Tell Halaf (Fig 3.1) and east to Kirkuk. Assyria's next king, Tukulti-Ninurta II, further extended Assyria's boundaries to the north, coming in contact with post-Hittite cultures on the Anatolian plateau and pre-Urartian inhabitants in eastern Turkey. King Assurnasirpal II (883-859 BC) moved the capital of Assyria from Assur north to the junction of the Tigris and Upper Zab rivers at Nimrud (Fig 3.1). In his early military campaigns, Assurnasirpal gained control of Euphrates river crossings towards Aleppo and Syria. This expansion ensured Assyria's access to trade routes to Mediterranean coastal cities (the Levant) and Turkey, rich in metal ores. Assurnasirpal's son, Shalmaneser III (858-824 BC) continued this Assyrian expansion towards the Mediterranean, into Anatolia, Babylonia, and Iran. Campaigns into Iran included raids against the Median kingdom (Fig 3.1), centered around the modern city of Hamadan (Fig 3.2; Roaf, 1995).

Since the early 3<sup>rd</sup> millennium BC, Mesopotamians believed that war between city-states also involved war between the gods of those city-states. For Assyria, the god Assur who was ruler of the gods, was also ruler over the whole of the earth-bound world and thus justified Assyria's aggressive expansion. In order to sever loyalty of local populations to their traditional city-state god and to quell local rebellion in conquered territory, Assyria had instituted a policy of mass deportation, moving whole cities or districts of people, and replacing them with other deported populations (Knapp, 1988). Assyrian governors were appointed by the king to newly conquered lands, ensuring strong centralized control by the king. Partly because of vicious Assyrian military punishments and deportation practices, western states formed military coalitions against the campaigns of Shalmaneser III. In 853 BC, Shalmaneser III abandoned a fight on the Orontes River (Fig 3.1) against such a coalition of states in the region from Cilicia to Israel. In response to the strong centralized control of land and the power held by appointed governors, the rural ruling families and free citizens rebelled against Shalmaneser III, demanding that land and power be more evenly distributed. A four year long civil war ensued, ending with suppression of the rebels. However, dissension remained and throughout Assyrian provinces, and between about 825 BC and 750 BC, five subsequent Assyrian rulers could not regain control of the whole empire. In the north, the newly formed Urartian kingdom (Fig 3.1) was extending its influence towards Syria and inhibiting Assyrian access to Anatolia (Knapp, 1988). In 745 BC, a new dynasty was established in Assyria by Tiglath-pileser III (745-727 BC). He instituted administrative reforms that brought the ruling families under control and continued with Assyria's deportation and punishment policies. Tiglath-pileser III (745-727 BC) stopped the Urartian advance and re-established control over Assyria's provinces in the north and extended the borders to as far west as Egypt. Tiglath-pileser III also established

outposts along trade routes in order to stay in close and constant contact with provincial governors (Lloyd, 1984; Knapp, 1988).

## **Iran**

The kingdom of Elam (Fig 3.1) in southwest Iran was one of the dominant powers throughout the 3<sup>rd</sup> and 2<sup>nd</sup> millennium BC in the Near East. The Middle Elamite period (approx. 1500-1100 BC) is marked by the political and religious unification of highland Anshan (Fars) and lowland Susa (Khuzistan) (Fig 3.1; Potts, 1999). The Middle Elamite kingdom peaked in the mid 2<sup>nd</sup> millennium BC under king Untash-Napirisha (approx. 1340-1300 BC) (Curtis, 1995). In this period, the city of Susa was expanded and the new city of Tchoga Zanbil (Fig 3.1) was established. Relations with the Kassite empire included diplomacy based on intermarriage of the ruling royal families. In the 12<sup>th</sup> c BC, the Elamite king Shutruk-Nahhunte defeated the Kassites and his son Kutir-Nahhunte continued to carry out military raids in Mesopotamia. Nebuchadnezzar I (1125-1104 BC) ended the Middle Elamite dynasty in a raid on Susa (Curtis, 1995). For about 300 years following this defeat, there is little textual or archaeological evidence of the activities of the Elamites (Potts, 1999). During this period (approx. 1100-744 BC), it appears that they supported Babylonian rebels against Assyria, a coalition that continued on into the following period, leading to more intense military conflict between Assyria and Elam and the eventual complete destruction of the city of Susa.

In the late 12<sup>th</sup> c BC, Indo-Iranian speaking tribes migrated into the eastern foothills of the Zagros Mountains (Fig 3.1; Curtis, 1995). Also during this period, two changes appear throughout sites in these Iranian highlands and farther east into Iran. New pottery forms, especially in a grey fabric, were introduced and the dead were buried in cemeteries. At Hasanlu Period V (1450-1250 BC), these changes were also accompanied by new clothing and personal ornaments, and differences in architecture and building plans from preceding periods (Dyson and Voigt, 1989; Dyson, 1977).

## **Urartu**

Starting around the middle of the 9<sup>th</sup> c BC, the Kingdom of Urartu formed in eastern Anatolia from small states centered on the eastern side of Lake Van (Fig 3.1; Zimansky, 1985). By the late 9<sup>th</sup> c BC, at about the time that Assyria was dealing with rebels from powerful rural families, Urartu expanded its influence to west of the Euphrates and acquired control of trade routes to Anatolia and its metal resources (Knapp, 1988). The geographically divided and isolated inhabitants of eastern Turkey appear to have grouped together to form the political state of Urartu because of potential military incursion from Assyria (Knapp, 1988). In the mid-8<sup>th</sup> c BC, Urartu was defeated and lost control over its newly acquired areas by the Assyrian king Tiglath-Pileser III (Knapp, 1988). Urartu continued in existence until around the beginning of the 6<sup>th</sup> c BC.

## **Summary**

By the end of the 9<sup>th</sup> c BC, Assyria and Urartu, the major political and military powers near Hasanlu, were vying with each other for control of trade routes and natural resources. Hasanlu existed on a borderland between Assyria and Urartu, although the exact nature of the activities of these kingdoms in the region around Hasanlu are not clear. The Medians to the south of Hasanlu were targets of Assyrian expansion in the mid-9<sup>th</sup> c BC. The kingdom of Elam in southern Iran had joined with Babylon to fight against Assyria throughout the 9<sup>th</sup> c BC, but were defeated in the mid-8<sup>th</sup> c BC. Assyrian-made artifacts were found in the Period IVB level at Hasanlu and shows that the inhabitants had some connection with Assyria. No Urartian objects have been found in the Period IVB levels, except perhaps for helmets, which may in fact be local. The objects at Hasanlu that were made in local styles and in styles associated with the cultures of the Iranian plateau (Winter, 1977; Marcus, 1996) show that Hasanlu was not an isolated settlement dependent on a dominant power for its existence and livelihood. Hasanlu was in contact with cultures other than Assyria.

## PROCUREMENT AND MOVEMENT OF MATERIALS

In the 2<sup>nd</sup> and early 1<sup>st</sup> millennium BC, Mesopotamia was not rich in resources other than bitumen and agricultural products. Metals, stone, wood, and other resources were imported from surrounding regions (Moorey, 1999). Many of the physical routes of trade had been well-established by the 2<sup>nd</sup> millennium BC (Fig. 3.2). Archaeological remains imply that large quantities of raw materials and finished goods moved into Mesopotamia, but that comparatively little export of goods out of the region occurred. This is probably a skewed interpretation, however, since Mesopotamia's most important products for export or trade were agricultural goods (Lamberg-Karlovsky and Sabloff, 1995), perishable items which would not likely survive into the archaeological record. The following summary is, therefore, biased to trade into Mesopotamia.

Materials and objects moved into and out of Mesopotamia and surrounding regions as plunder from military campaigns, taxes paid to ruling empires via local governors, diplomatic gifts, and trade. Movement was complex and depended on tithes owed or demanded, diplomatic relations, and practicalities of transport. Many materials were supplied from more than one region. A complete discussion of the intricacies of the procurement and movement of materials is far beyond the scope of this dissertation and only a summary is offered here. Moorey (1999) offers the most comprehensive survey of archaeological, textual, and scientific data on Mesopotamian materials written to date. Mesopotamian exchange with Western Asia is interpreted from textual and archaeological data by Potts (1994). More in depth discussions of sources and movement of materials and of trade mechanisms in and around Mesopotamia through the early 1<sup>st</sup> millennium BC are found in Beale (trade mechanisms, 1973), Yoffee (1981), Winter (carved ivory distribution, 1976), Pigott (metallurgy in Iran and Western Asia, 1999), Herrmann (1968, lapis lazuli), and Lamberg-Karlovsky (1988, chlorite vessels).

Figure 3.2. Location of trade routes (dot-dashed lines) between Mesopotamia and Western Asia, archaeological sites, and modern cities (modified from Potts, 1994).



For Mesopotamians, Iran was a resource-rich region. Gold, silver, and copper were mined and worked on the Iranian plateau (Potts, 1994). Stone for statuary and vessels, and semi-precious stones also came from Iran. Bitumen and bituminous limestone were mined and used in Susa (Elam) for decorative purposes, taking advantage of the malleability of hot bitumen (Potts, 1994). The site of Shar-i Sohka in eastern Iran (Fig 3.2) was active in the production of stone vessels including those made of calcite and of chlorite, which have been found in Mesopotamian contexts (Potts, 1994; Lamberg-Karlovsky and Sabloff, 1995). Volcanic tuff from Kerman (central-south Iran, Fig 3.2) and Birjand in the Iranian highlands was used to make cylindrical vessels (Potts, 1994). Carnelian was mined mainly from placer deposits in Iran (Potts, 1994). Turquoise was probably mined near Kerman, Nishapur, and Herat (Fig 3.2) in Afghanistan close to the eastern border of Iran (Potts, 1994; Beale, 1973).

The Persian Gulf and Western Asia, identified here as areas east of modern Iran, are linked in trade with Mesopotamia through the use of water transportation routes. Beginning in the 3<sup>rd</sup> millennium BC, archaeological evidence indicates that materials derived from regions in contact with the Persian Gulf and the Indus River, namely Oman, Bahrain, Afghanistan, and India, become more common than those derived from the Iranian plateau (Potts, 1994). The regions of Dilmun, Magan, and Meluhha are mentioned as being in contact with 3<sup>rd</sup> millennium BC Sumer primarily as trading partners through sea routes, except for one mention that Naram-Sim briefly conquered Magan (Potts, 1994). Magan was a source of large quantities of copper, and is possibly the region of modern Oman (Fig 3.1), where copper smelting occurred in the 3<sup>rd</sup> millennium BC (Potts, 1994). Oman probably also supplied diorite and gabbro for statuary and landmarks denoting property boundaries and royal edicts (Potts, 1994). Oman was where certain types of grey, low-relief carved chlorite vessels (*série récente* type) were made and transported to Sumer (Potts, 1994). Dilmun is more confidently

assigned to the region of Bahrain (Fig 3.1; Potts, 1994) and was probably a major trading center for raw materials and goods rather than a source region these materials (Knapp, 1988). Several written texts in the Near East mention “Dilmun copper” or copper that arrived from Dilmun which, based on historical, archaeological, and geological data, was probably mined in Oman, shipped to Bahrain, and then traded to Mesopotamia. Meluhha was the source of ivory, ebony, gold, tin, copper, lapis lazuli, carnelian, wood, and possibly peacocks (Potts, 1994), a combination of goods consistent with source areas in the Indus River (Fig 3.2) and modern Afghanistan, an area encompassed by the Harappan civilization and its successors (Potts, 1994). Also from the east, lapis lazuli was imported into Mesopotamia mainly as raw chunks of material (Potts, 1994), probably extracted from mines around Kerano-Munjan, Badakhshan (Potts, 1994) and near Shortugai I on the Oxus River (Potts, 1994), or possibly from farther south at Chagai southwest of Quetta (Fig 3.2; Potts, 1994). Cuneiform textual evidence says that lapis lazuli came into Mesopotamia via Meluhha (Potts, 1994). Modern geologic data is not yet detailed enough to determine other potential sources of lapis lazuli. Carnelian was mined from Gujarat and Afghanistan and imported into Mesopotamia as raw material and finished objects (Potts, 1994).

From the west and north, Anatolia provided copper, tin, silver, and obsidian to Mesopotamia (Renfrew et al., 1966; Potts, 1994). During the second half of the 2<sup>nd</sup> millennium BC, the Hittites had tight control over the rich mineral resources of Anatolia. Movement of these materials into Mesopotamia was limited partly because of Hittite control, but also because of the difficulty of overland transport (Knapp, 1988). Syria was also a source of stone for statuary, landmarks, and building material (Potts, 1994). In Syria and Phoenicia (Fig 3.1), elephant ivory was carved into plaques, bowls, furniture, and other objects. Both styles have been found in northern Mesopotamia, but have different distributions in the eastern Mediterranean. Syrian ivory objects have been

found in excavations in Anatolia, Greece, Crete, and Syria, whereas Phoenician ivory objects have been found in western Turkey, Crete, Cyprus, and modern Israel (Winter, 1976).

### **Copper and Copper Alloys as Example of Material Movement**

Copper and copper alloys were important metals used to make utilitarian objects. Numerous copper ores were mined and smelted in the ancient Near East, including ores from eastern Anatolia at Ergani Maden (Fig 3.1), the Caucasus, Oman (Magan), Feinan in southern Palestine, Khedri mountains in Rajasthan, as well as on the Iranian plateau near Anarak (east of Isfahan), Tal-i Iblis (south-central Iran), Tepe Ghabristan, Shahdad, Malyan, and Shahr-i Sokhta (Fig 3.2; Potts, 1994). In the 2<sup>nd</sup> millennium BC, copper ore in Iran was mined and worked and was, theoretically, available to Mesopotamia and surrounding regions (Potts, 1994). However, the material accrued a considerable cost as it was transported across Iran, over the Zagros mountains, and through states that were not always friendly. Iran, thus, was probably not a consistent or reliable source of material. Textual references and chemical data indicate that the main source of copper for Mesopotamia changed sometime in the mid-3<sup>rd</sup> millennium BC from the Iranian plateau to Oman (Magan) (Potts, 1994). This more consistent source of copper for Mesopotamia, at least in the 2<sup>nd</sup> millennium BC, was mined in Magan and transported through Dilmun via water routes deep into Mesopotamia. This made Magan copper much less expensive than Iranian or Anatolian copper (Potts, 1994). Individual shipments of Dilmun copper at this period are recorded up to about 100 kg (Potts, 1994). Resource-rich states which Sumer claimed as provinces are mentioned in royal Sumerian inscriptions and their important economic features are pointed out: copper mountains in Magan, silver mountains in Keban, Turkey, and cedar forests in Lebanon (Potts, 1994). Iranian resources, on the other hand, are only mentioned in literary texts, not official or royal documents.

Some of the earliest copper alloys in Mesopotamia and surrounding regions were arsenical alloys (Tylecote, 1976). However, low arsenic contents in many so-called alloys indicate that the addition of arsenic may not be intentional but may originate from the copper ores. A cuneiform word for arsenic has yet to be identified (Potts, 1994). Iranian copper ores near Anarak (Fig 3.2) in central Iran are the major arsenic deposits in the modern Near East, and arsenic-bearing copper ores occur in Rajasthan and Armenia (Fig 3.2; Potts, 1994). Copper ore from Oman is generally thought to contain less than 0.4 wt% As, however, “raw copper” and artifacts from Bronze Age Oman contain up to 7 wt% As (Potts, 1994). Another early copper alloying metal was antimony. Iran, Anatolia, and the antimony-rich copper deposits of the Caucasus were possible sources for this metal. However, the distribution of antimony in many of these early “alloys” is similar to that of arsenic. For a group of metal objects from one site, the Sb content ranges from less than 0.1 wt% Sb up to 5 wt% Sb (Thornton et al., 2002), suggesting that there was no real control on the amount of antimony added to copper for alloying. Antimony in these metals may have its origins in the copper ores.

Tin was a known metal to 2<sup>nd</sup> millennium BC miners and metal workers. Metallic tin is identified in Early Dynastic II/III (c. 2600 BC) Fara texts (Potts, 1994). Near Eastern copper ores contain up to about 0.05 wt% Sn (Potts, 1994), well below the amount of tin found in these early tin bronzes, which typically contain greater than about 5 wt% Sn. Until the end of the 3<sup>rd</sup> millennium BC, objects made of tin bronze appear to occur mainly in Mesopotamian and southern Iranian contexts, and not in Oman, Bahrain, northern or highland Iran, nor Afghanistan (Potts, 1994). However, tin is attested to have come from east of Mesopotamia and southern Iran in 3<sup>rd</sup> millennium BC texts. These texts also associate tin with lapis lazuli and carnelian, stones which purportedly also originated in the east. Early 2<sup>nd</sup> millennium BC references indicate that tin continued to be supplied from the east into Mesopotamia, through Susa (Fig 3.1; Potts,

1994). The eastern geological sources for tin ores have not been satisfactorily identified. To date, no tin ores have been identified in Iran or Mesopotamia (Potts, 1994; Muhly 1985; Muhly et al., 1991). Tin ores that were worked in antiquity have been recognized in Afghanistan south of the city of Herat and in the Zeravshan Valley of Uzbekistan, (Potts, 1994). Tin was being smelted from tin ore in the Kestel mine in the Taurus Mountains, Turkey and may have been an important source for Mesopotamia's bronze industry. At Kestel, mining and tin processing has been dated to as early as the 3<sup>rd</sup> millennium BC (Yener et al., 1989; Yener and Vandiver, 1993; Yener, 2000).

#### LOCAL AND NON-LOCAL DECORATIVE STYLES OF ARTIFACTS FROM HASANLU

Heavy destruction occurred during the attack on Hasanlu at the end of the 9<sup>th</sup> c BC, but no reconstruction was carried out at the settlement afterwards although there was a small squatter settlement. Buildings had burned and collapsed and buried victims of the fires as well as the material remains of the inhabitants. Much of the excavated material from Hasanlu comes from this destruction layer, Period IVB (Table 3.1). Even though Hasanlu has been studied since at least 1940 (Stein, 1969), the relationships that Hasanlu had in the early Iron Age with other cultures and political entities is not yet clear. Study of the architecture of Period V and IV Hasanlu shows no relationship with sites to the east in Central Asia (Dyson, 1989b). Chemical and petrographic analysis of Period V pottery from Hasanlu demonstrates there was a tradition of local crafts industries, even for new styles introduced in Period V (Bedal et al., 1995). Bronzeworking as represented by materials and molds from Hasanlu is discussed in de Schauensee (1988) who suggests that there may have been a local or regional bronzeworking industry. Pigott (1980, 1999) discusses the presence and use of iron at Hasanlu and describes the unusual use of iron and bronze pieces in individual objects, a decorative style not common in Mesopotamia.

A local style of decorative elements has been recognized in a variety of artifacts excavated from level IVB at Hasanlu. The artifacts include ivory plaques, bronze and iron plaques, cylinder seals and vessels of faience, a silver beaker, and glazed ceramic tiles (Muscarella, 1966; Winter, 1976, 1977; Marcus, 1991). Objects made in other regions include cylinder seals and ivory plaques from Assyria, and fragments of ivory objects from North Syria (Winter, 1977). Assyria appears to have had the greatest impact on the local material culture because the largest number of artifacts from a foreign culture at Hasanlu IVB levels are Assyrian and much of the local style appears to have been taken from Assyrian cultural and artistic traditions (Winter, 1977). The Assyrian influence is consistent with political and trade patterns. North Syria also exerted considerable influence on the styles found at Hasanlu. The existence of a local style at Hasanlu implies that there were craftsmen in and around Hasanlu making such objects (Winter, 1977). Crucibles, molds, hematite balls (possibly a polishing tool for bronze) and other evidence for metalworking were found in three separate places in Hasanlu IVB levels (de Schauensee, 1988). However, it is not clear whether any materials, such as bronze, glass or ceramic glazes, were manufactured at Hasanlu directly from raw materials.

#### THE SAMPLES OF THIS STUDY

The archaeological artifacts from the Iron Age Period IVB levels of Hasanlu are unique and irreplaceable because of the scarcity of materials from this period and this region. No other accessible collections of glassy materials are known from this period, either from museums or excavations (Lightfoot and Arslan, 1992; Lightfoot, 1989; C. Lightfoot, personal communication). Investigation of the technology that was used to manufacture the vitreous artifacts from Hasanlu has yielded some information about its association with Assyria and other cultures. Glass and glassy materials from Hasanlu

have been studied by von Saldern (1966), Marcus (1991, 1996), Brill (1999), Moorey (1999), and de Schauensee (2001).

The University of Pennsylvania's collection of glass, glazed ceramics, and faience objects from Hasanlu was examined by Maude de Schauensee and C. P. Stapleton and a representative selection of about 80 artifacts was chosen for sampling. The artifacts are typical of the colors and types of vitreous materials that were manufactured prior to about the 13<sup>th</sup> century BC and after about the 7<sup>th</sup> century BC (Oppenheim et al., 1970), and can be used to investigate what happened to glass manufacturing techniques in the early Iron Age. During excavations at Hasanlu, artifacts of vitreous materials were found in cemetery burials, in storage in temple or administrative buildings burned during the late 9<sup>th</sup> c BC attack, and on human and horse remains also caught in the attack. Find locations for the artifacts can be related to Dyson's (1989b) description of the distribution of artifacts in the destructions layer of the Period IVB buildings. Vitreous materials artifacts were found in Burned Building II (BB II), BB III, BB IV, BB IVE, BB V, and BB VIIE. Building BB II appears to have included storage areas and may have been a temple (Dyson and Voigt, 2003), perhaps used as a local treasury, and many beads and hollow glass tubes were found here. The second story of building BB IV may have been a living area. Horses that had been killed were found in buildings BB V and BB IVE. BB III contained a main reception hall, kitchens, store rooms and a courtyard with horse remains. The Double Gate Building on the west is possibly part of a stable. Museum registration numbers, descriptions of artifacts, colors sampled, and find locations for the artifacts are listed in Table 3.2.

### **Glass**

Of the artifacts made completely of glass, there are fragments of thin-walled (3 mm) and thick-walled (approx. 10-15 mm) vessels, and of 4-sided, thick-walled, hollow tubes, possibly architectural features or furniture fittings. The hollow tubes are made of

opaque pale blue (turquoise) glass that is homogeneous in color and contains few macroscopic inclusions or bubbles. Thousands of glass beads were found at Hasanlu, from temples or administrative buildings, houses, victims' bodies, and cemetery burials. The colors of the glasses sampled from the beads include pale blue opaque (turquoise), dark blue translucent, white opaque, yellow opaque, black, and blue transparent to translucent (tp-tl). Both monochrome and polychrome beads were found. The glasses of the beads contain many bubbles and inclusions, and do not appear to be as well made as the blue opaque glasses. Forty-five artifacts yielded samples suitable for chemical and isotopic analysis. For polychrome artifacts, samples were removed from as many colors as was possible.

### **Glazed Ceramics**

Samples of glaze were removed from fragments of nine ceramic vessels. Most of the glazes are blue to green transparent to translucent glazes. Glaze from two bridge-spouted vessels of a type known only from Hasanlu, and probably locally-made, were analyzed. These glazes are assumed to be examples of vitreous material manufactured at Hasanlu against which other samples in this study may be compared. Polychrome glazes analyzed from a vessel decorated in Assyrian-style, but probably not made in Assyria, include blue transparent, yellow opaque, and white opaque.

### **Faience**

Faience is a glassy material sometimes referred to as paste, composite or, incorrectly, as frit. Faience is composed mainly of quartz grains held together by thin threads of glass or almost entirely surrounded by a glass matrix, and a surface glaze is usually present. The 29 faience objects in this study include beads, vessels, and wall tiles.

Table 3.2 List of Samples

UPenn. Museum Registration Number+	Object Type	Colors Sampled*	Field Number	Notes	Excavation Location**	Period / Date
<b>OBJECTS MADE OF GLASS</b>						
61-5-54	tube, square	blue opq	HAS 60-299	square lt? bl glass tube frag.	BB II Rm 5 (SW quadrant) CC30(5)[1]/23\	Period IVB late 9th c BC
65-31-280	tube, square	blue opq	HAS 64-84	square dk bl glass tube frag.	Between S. end BB II and Fortification wall CC32(4)/20\	Period IVB late 9th c BC
65-31-282	tube, square	blue opq	HAS 64-679	square lt? bl glass tube frag.	BB II Rm 7a CC31(4)[2]/278\	Period IVB late 9th c BC
65-31-283	tube, square	blue opq	HAS 64-680	square bl glass tube frag. Three thin copper/bronze strips inserted into glass at or near corners at broken end.	BB II Rm 7a CC31(4)[2]/279\	Period IVB late 9th c BC
65-31-728e	tube, square	blue opq		frag. square turquoise glass tube	BB II Rm 7a CC31(4)[2]	Period IVB late 9th c BC
65-31-728f	tube, square	blue opq		frag. square turquoise glass tube	BB II Rm 7a CC31(4)[2]	Period IVB late 9th c BC
65-31-992	tube, square	blue opq	HAS S64-81	square lt bl? glass tube frag	BB II Rm 7a CC31(4)[2]	Period IVB late 9th c BC
65-31-993	tube, square	blue opq	"used to have incorrect # HAS 64-479"	square glass tube frag		Period IVB late 9th c BC
73-5-782	fragment of ?	blue opq	HAS 72-S6	turq glass frag.	BB IVE Rm 4 V30N(1A)[10]	Period IVB late 9th c BC
58-4-61b	bead	black	HAS 57-169	b) 1 broken black glass bead	East Cemetery SK 30 VIB burial 20	Period IV
61-5-89h-1	bead	black	HAS 60-813	h-1) black ball bead, eyes missing	BB II Rm 14 floor Y26(5)[6]/147\	Period IVB late 9th c BC
61-5-89h-2	bead	blue/green	HAS 60-813	h-2) blue/green bead	BB II Rm 14 floor Y26(5)[6]/147\	Period IVB late 9th c BC
61-5-89h-3	bead	black base with white	HAS 60-813	h-3) black bead w/white spiral	BB II Rm 14 floor Y26(5)[6]/147\	Period IVB late 9th c BC
61-5-89i-3	bead	black	HAS 60-813	i-3) black bead	BB II Rm 14 floor Y26(5)[6]/147\	Period IVB late 9th c BC
61-5-95a (bag 1 of 3)	bead	blue/green base with yellow & black	HAS 60-900	1 blue/green ball bead w/raised spiral yellow/black "eyes"	BB II Rm 5 North center SK 138 or 153 AA30(4)[3] burial 13 or 128 /181a,b\	Period IVB late 9th c BC
61-5-95b (bag 1 of 3)	bead	green base with yellow & black	HAS 60-900	1 green ball bead with flat spiral yellow/black eyes	BB II Rm 5 North center SK 155 AA40(4)[3] burial 30/191\	Period IVB late 9th c BC
61-5-95c (bag 2 of 3)	bead	black	HAS 60-900	c) large black ball bead	BB II Rm 5 North center SK 138, 153 or 155, AA30(4)[3] burial 13,28 or 30	Period IVB late 9th c BC
61-5-95d (bag 2 of 3)	bead	black base with white	HAS 60-900	d) small black ball w/white spiral eyes	BB II Rm 5 North center SK 138,153 or 155, AA30(4)[3] burial 13,28 or 30	Period IVB late 9th c BC
63-5-269a	bead	black base with ?	HAS 62-946	black glass bead with raised applied eyes	BB III Rm 7 Q24(3)[3]/121\	Period IVB late 9th c BC

Table 3.2 Continued

UPenn. Museum Reg. Number+	Object Type	Colors Sampled*	Field Number	Notes	Excavation Location**	Period / Date
63-5-270a (bag 1 of 2)	bead	green/blue	HAS 62-702	1 green/blue ball bead, broken	BB III Rm 12 Q23(3)[5]/43\	Period IVB late 9th c BC
63-5-276a	bead	green/blue	HAS 62-411	1 green/blue ball bead, broken	BBII Rm 5 (NE corner) SK262 AA31(4)[5] burial 8/51\ next to skeleton	Period IVB late 9th c BC
63-5-280a	bead	green base with yellow and white	HAS 62-52	green glass bead with yellow and white stripes & yellow/white hatched band around holes	BB III Rm 5 R23(3)[2]/26\	Period IVB late 9th c BC
65-31-247a	bead	black base with white	HAS 64-267	a)1 broken black bead w/white spiral	East Cemetery 486 burial 1/7\	SK VIG(5) Period IV
65-31-267a	bead	dk blue	HAS 64-337	1 dk blue bead frag	East Cemetery 494 burial 4/26\	SK VIH(5) Period IV
65-31-273a	bead	blue/green base with yellow & black	HAS 64-147	frag of blue/green ball bead w/yellow/black spiral eyes	BB VII E Rm 5 R23(3)[1]/20\	Period IVB late 9th c BC
65-31-396d (bag 2 of 6)	bead	blue	HAS 64-803	d)1 frag blue ball bead	BB II Rm 10 BB32(4)[1]/8\	Period IVB late 9th c BC
65-31-396e (bag 2 of 6)	bead	black base with white	HAS 64-803	e) black ball bead w/white eyes	BB II Rm 10 BB32(4)[1]/8\	Period IVB late 9th c BC
65-31-396f (bag 2 of 6)	bead	black base with white	HAS 64-803	f) black ball bead w/white eyes	BB II Rm 10 BB32(4)[1]/8\	Period IVB late 9th c BC
65-31-396g (bag 2 of 6)	bead	black base with white	HAS 64-803	g) black ball bead w/white eyes	BB II Rm 10 BB32(4)[1]/8\	Period IVB late 9th c BC
65-31-396h (bag 2 of 6)	bead	black base with white	HAS 64-803	h) black ball bead w/white eyes	BB II Rm 10 BB32(4)[1]/8\	Period IVB late 9th c BC
65-31-397a	bead	multicolors	HAS 64-22	1 multicolor glass bead, domed	BB III Rm 6 Q24(4)/137\	Period IVB late 9th c BC
65-31-728c	bead	black base with white		c)1 black glass bead w/white circle pattern	BB II Rm 7a CC31(4)[2]	Period IVB late 9th c BC
73-5-293b	bead	blue/green	HAS 72-N220	b) 1 bl/gr bead frag	Period V house, 2 hearth, S22(7)[10]/26\ Bldg. inside	Rm Period V ca. 1450-1250 BC
73-5-305a	bead	multicolor	HAS 72-N318	incomplete patterned multicolor glass bead, domed	Fortification wall, west side of Citadel T20E(3)[3]/21\ Below BB IE Y28/29(+)[4]/5\ Period V house, 2 hearth S22(7)[10]/31\ Period V house, 2 hearth S22(7)[10]/31\ BBIVE Rm 3 W31(1)[3]/27\ Period IVB late 9th c BC	Period IIIA? ca. 6th-5th/4th c BC
73-5-341a	bead	black	HAS 72-N164	black ball bead, damaged	Below BB IE Y28/29(+)[4]/5\ Period V house, 2 hearth S22(7)[10]/31\ Period V house, 2 hearth S22(7)[10]/31\ BBIVE Rm 3 W31(1)[3]/27\ Period IVB late 9th c BC	Period V ca. 1450-1250 BC
73-5-350a	bead	black ?base & white	HAS 72-N221	a)1 frag black/white striped bead	Period V house, 2 hearth S22(7)[10]/31\ Period V house, 2 hearth S22(7)[10]/31\ BBIVE Rm 3 W31(1)[3]/27\ Period IVB late 9th c BC	Rm Period V ca. 1450-1250 BC
73-5-350b	bead	blue/green, bright	HAS 72-N221	b) 1 frag bright bl/gr bead	Period V house, 2 hearth S22(7)[10]/31\ Period V house, 2 hearth S22(7)[10]/31\ BBIVE Rm 3 W31(1)[3]/27\ Period IVB late 9th c BC	Rm Period V ca. 1450-1250 BC
73-5-559a	bead	blue/green	HAS 72-N31	a)1 frag blue/green	BBIVE Rm 3 W31(1)[3]/27\ Period IVB late 9th c BC	Period IVB late 9th c BC

Table 3.2 Continued

UPenn. Museum Reg. Number+	Object Type	Colors Sampled*	Field Number	Notes	Excavation Location**	Period / Date
73-5-559c	bead	colorless? base with green/blue	HAS 72-N31	c) chip from 1 clear? glass beads w/green/blue stripe	BBIVE Rm 3 W31(1)[3]/27\	Period IVB late 9th c BC
73-5-559d	bead	blue/green	HAS 72-N31	d) frag. medium blue/green bead	BBIVE Rm 3 W31(1)[3]/27\	Period IVB late 9th c BC
73-5-559e	bead	blue/green	HAS 72-N31	e) frag lt. blue/green bead	BBIVE Rm 3 W31(1)[3]/27\	Period IVB late 9th c BC
73-5-559f	bead	multicolor	HAS 72-N31	f) sample from patterned multi burned domed glass bead	BBIVE Rm 3 W31(1)[3]/27\	Period IVB late 9th c BC
73-5-781	bead	blue opq	HAS 72-S7	turq glass bead frag.	S23 ashes	Period IV
75-29-199a	bead	dk blue (?whole bead)	HAS 74-N520	a) cobalt frag. of glass bead	BB V Rm 3 Y33(4)[2]lot 17/88\	Period IVB late 9th c BC
75-29-307a	bead	blue/green base with yellow and black	HAS 74-N663a	blue/green sub-round glass bead w/hatched yellow and black lines on boss and whorls around perforations. Yellow, bl/gr glass, samples from damaged area	BB VI Rm 1 (SE corner) W23(4)[7]/118\	Period IVB late 9th c BC
<b>GLAZED CERAMIC</b>						
60-20-344	sherd	blue tp	1959 season on tag in storage box but probably 1958 excavation season	sherd, glazed, blue	East edge of Citadel XI(3)[4]ash pit	by type-Period IVB late 9th c. BC
60-20-346	bridge-spouted vessel	blue tp	probably 1959 season	bridge-spouted sherd, glazed	BB II probably corner, Rm 5	Period IVB late 9th c BC
60-20-347	vessel sherd	blue tp	1959 season on tag in box but may be 1958 season of excavation	body sherd, glazed	East edge of Citadel XI(2)	
60-20-348	Assyrian style vessel	blue tp, yellow opq, white opq	1959 season	Assyrian style polychrome glazed vessel sherds	Building unknown BB28	Period IVB late 9th c BC
60-20-349	vessel foot sherd	blue tp	probably 1958 season of excavation	vessel foot sherd, glazed	East edge of Citadel XI(3)[4] ash pit	by type Period IVB late 9th c BC
61-5-906	vessel	blue tp		bowl, glazed, broken	BB II Rm 1, 2 or N. center Rm 5, AA30(4)	Period IVB late 9th c BC
61-5-913	footed vessel	blue tp		fragmentary footed glazed ceramic pot	BB II Rm 1 or Lower Courtyard in front of Rm 1, Z30(4-5)/112b\	Period IVB late 9th c BC
63-5-64	bridge-spouted vessel	blue tp	HAS 62-1011	spouted vessel, broken, glazed, poor condition	BB III Rm 11 P23(3)[1]/19\	Period IVB late 9th c BC
93-4-154	animal vessel	blue tp	pd IVB, unstratified	animal vessel frag., glazed	+	by type Period IVB late 9th c BC

Table 3.2 Continued

UPenn. Museum Reg. Number+	Object Type	Colors Sampled*	Field Number	Notes	Excavation Location**	Period / Date
<b>FAIENCE OBJECTS</b>						
59-4-52	sherd		HAS 58-27 (see 73-5-276)	carved sherd, glazed	U27/U28(5)	Period IVB late 9th c BC
59-4-86	boss		HAS 58-348	boss with incised lines and circles; sample from damaged edge, composite	BB IW Rm 2 Z27(3)[1]/92\	Period IVB late 9th c BC
60-20-341	vessel		pd IV	sm vessel frag	AA29/102\ sherd dump	by type-Period IVB late 9th c. B.C.
60-20-342	vessel			sm vessel, glazed	Building unknown AA29(1-3)	Period IVB late 9th c BC
60-20-345	vessel		BB II (HAS IV) (1959 season tag in box)	jar neck sherd, glazed	BB II Rm unknown CC28	Period IVB late 9th c BC
61-5-53	tube, wall tile?		HAS 60-309	glazed comp. body tube frag. of wall tile?, perforated near base	BB II Rm 5 (SW quadrant) CC30(5)[1]/33\	Period IVB late 9th c BC
61-5-55	wall tile knob?		HAS 60-460	wall tile knob?, glazed	BB II probably Rm 2 AA30(4)[1]/13\	Period IVB late 9th c BC
61-5-896	vessel		HAS 60-1094	sherds of fluted bowl, glazed	Lower Court below BB II, Rm 1 Z30(4)[5]/113\	Period IVB/ late 9th c BC
61-5-89h-4	bead		HAS 60-813	h-4) white frit w/incised lines	Y26(5)[6]/147\ BB II Rm 14 floor	Period IVB late 9th c BC
61-5-923	vessel		XXXVIII[1]	sm dish frag, glazed, bl, wh. Incised.	BB II NE corner or Rms 13 or 14 BB29[1]	Period IVB late 9th c BC
61-5-924	boss		HAS 60-268	one half sm boss, blue glazed	Courtyard? east of fragmentary bldg west of BB II Rm 18 CC28(5)[1]/35\	Period IVB late 9th c BC
65-31-299a	vessel sherd (wasters?)		HAS 64-529	a)rim sherds, carinated vessel-wasters?, turquoise? glazed	BB II Rm 5 (south quadrant) CC31(4)[4]/186\	Period IVB late 9th c BC
65-31-396a (bag 3 of 6)	bead		HAS 64-803 A,B	a) 1 turquoise comp bead w/crosshatch design	BB II Rm 10 BB32(4)[1]/8\	Period IVB late 9th c BC
65-31-396b (bag 3 of 6)	bead		HAS 64-803 A,B	b) 1 white barrel bead	BB II Rm 10 BB32(4)[1]/8\	Period IVB late 9th c BC
65-31-396c (bag 3 of 6)	bead		HAS 64-803 A,B	c) 1 white paste short barrel w/crosshatching	BB II Rm 10 BB32(4)[1]/8\	Period IVB late 9th c BC
65-31-728d	bead			d) 1 paste bead	BB II Rm 7a CC31(4)[2]	Period IVB late 9th c BC
65-31-96	vessel		HAS 64-314	sm. vessel (sample from frags. not in reconst)	BB II Rm 5 (SE quadrant) CC31(4)[4]/88\	Period IVB late 9th c BC
65-31-99 (original label: 65-31-994)	wall tile		HAS 64-801	wall tile with knob, glazed	BB II Rm 7 (behind Rm 6) BB31(5)[3]/201\	Period IVB late 9th c BC
71-23-198a	bead		HAS 70-383	glazed rectangular comp body bead w/notched edges & crosshatched pattern, broken	BB II Rm 7 (behind Rm 6) CC31[1]/72\	Period IVB late 9th c BC

Table 3.2 Continued

UPenn. Museum Reg. Number+	Object Type	Colors Sampled*	Field Number	Notes	Excavation Location**	Period / Date
71-23-609	vessel		bag labeled HAS 70-glazed and frit sherds, drawn	sm footed vessel frag, glazed		by type Period IVB late 9th B.C.
71-23-610	vessel			sherd of sm vessel, glazed	BB V Rm 4b Y31(3)[8]	Period IVB late 9th c BC
73-5-220	cylinder (wall tile?)		HAS 72-N286	sherd of cylindrical object, glazed	BB V Rm 6 AA32(4)[6]/11\	Period IVB late 9th c BC
73-5-276	sherd		HAS 72-N52 (see 59-4-52)	carved sherd, glazed	BB IVE Rm 3 W31(4A)[1]/45\	Period IVB late 9th c BC
73-5-296a	bead		HAS 72-N321	frag comp body bead, small, notched edge, crosshatch pattern	Period V house Rm 2 R22"S. balk" /30\	Period V ca. 1450/1350-1100 B.C.
73-5-785	sherd		HAS 72-S3	sherd, glazed	BB II Rear Kitchen DD30(5)[4]	Period IVB late 9th c BC
75-29-271a	bead		HAS 74-N184	comp. body tube bead, crosshatch design	BBIVE Rm 3 V31E(3)[3]lot 22/179\	Period IVB late 9th c BC
75-29-438	vessel		HAS 74-N91	vessel frag?, glazed	BB IVE Rm 3 V31E slump lot 1/61\	Period IVB late 9th c BC
75-29-439	vessel		HAS 74-N166	jar neck, glazed	BB IVE Rm 3 V31E(3)[3]lot 18/149\	Period IVB late 9th c BC
75-29-788	sherd		HAS 74-S62A	turq glazed composite body sherd	BB IVE Rm 3 V31E(3)[3]lot 22 S#4	Period IVB late 9th c BC

+In text, Museum registration numbers do not include "bag x of x". UPenn: University of Pennsylvania.

\*Some samples were too corroded for analysis and are not reported in subsequent chapters.

\*\*BB: Burned Building (Dyson, 1989a).

Abbreviations: bl: blue; comp: composite (faience); frag: fragment; gr: green; opq: opaque; tp: transparent; turq: turquoise; sm: small; wh: white.

## CHAPTER 4

### CHEMICAL ANALYSIS OF GLASS ARTIFACTS FROM IRON AGE LEVELS AT HASANLU, NORTHWESTERN IRAN

---

Stapleton, C. P. and Swanson, S. E. (2002) *Journal of Glass Technology*, 2002, v. 43C, 151-157. Reprinted here with permission of publisher.

## ABSTRACT

Ancient glasses often contain mineralogical and chemical inhomogeneities, and are not well-suited to bulk analysis. Electron microprobe analysis (EMPA) is being used to characterize a group of colored glasses from the site of Hasanlu located southwest of Lake Urmia in northwestern Iran. The results show that the glasses are  $\text{Na}_2\text{O-CaO-SiO}_2$  with about 18—25 wt%  $\text{Na}_2\text{O} + \text{K}_2\text{O}$ . Back-scattered electron imaging reveals networks of weathered fractures leached of Na. Identification of crystalline phases was done using the imaging and analysis capabilities of EMPA. The glasses contain partially reacted natural minerals such as feldspars, spinels and possible clay or mica that will be used to identify batch material sources. High temperature devitrifying phases including diopside, wollastonite, and a calcium sodium silicate were also found. Round alkali sulfate inclusions were identified as crystallized immiscible liquids (gall or scum), the abundance and distribution of which will be used in interpreting manufacturing steps and glass chemical composition variations. These results emphasize the need for microanalysis as the initial step in characterizing early ancient glass, with EMPA being the technique recommended in this paper.

## INTRODUCTION

Analytical research on ancient glasses has involved a wide variety of analytical techniques, most often with the goals of interpreting ancient technology and relationships between glassmaking centers, as well as identifying glass trade routes. Analysis of bulk samples has yielded much information on the history of glass and has formed the framework on which current investigations are based (Caley, 1962). Many modern glass researchers analyze bulk samples by a variety of techniques including atomic absorption (AA), inductively-coupled plasma mass spectrometry (ICP-MS), instrumental neutron activation analysis (INAA), and X-ray fluorescence (XRF). With the development of micro-analytical techniques, glass researchers have applied electron

microscopy (EMPA) with either wavelength (WD) or energy dispersive (ED) spectrometers (Brill and Moll, 1963; Henderson, 1988; Verità et al., 1994; Stapleton et al., 1999), lasers (laser ablation-ICP-MS; Saitowitz et al., 1996), and proton-induced X-ray excitation (PIXE; Swann et al., 1993) to the investigation of ancient glasses.

Measurements made with microanalytical techniques have demonstrated that within a single sample of ancient glass, significant mineralogical and chemical inhomogeneities can exist (Santopadre and Verità, 2000). Microanalysis can avoid these inhomogeneities during routine analysis. Additionally, microanalytical techniques can be used to identify these same inhomogeneities which can aid in determining glass batch materials or manufacturing steps. Microanalysis is suited to the unique nature of archaeological glass, one that often requires sampling to be minimal and, if possible, essentially non-destructive. Such samples may also need to be analyzed multiple times by different techniques. The purpose of this paper is to emphasize the utility of electron microprobe analysis (EMPA) as a first step in the analytical investigations of small, ancient glass fragments.

## WEATHERING OF ANCIENT GLASSES

Alteration by weathering is a common feature of ancient glasses (Newton and Davison, 1989), and its effects should be considered when designing an analytical program for these high alkali materials. Glass can corrode in the presence of small amounts of water, causing changes to the original chemical composition and phases present. This is especially problematic for archaeological glasses, most of which have high alkali compositions, commonly with 15—20 wt%  $\text{Na}_2\text{O} + \text{K}_2\text{O}$  (Brill, 1999). Archaeological glass artifacts often spend long periods of time in damp or water-logged conditions buried in sediments or under water, or sitting on display in uncontrolled atmospheric conditions. Even glass found in regions with dry climates shows signs of weathering by water. In the first stage of typical water corrosion of glass, Group I

cations, especially Na<sup>+</sup> and K<sup>+</sup>, are leached out of a glass and replaced by water, probably as H<sub>3</sub>O<sup>+</sup> (Newton and Davison, 1989). In addition, ions contained in water can be adsorbed and promote the growth of new phases during the weathering of glass. Extensive corrosion is more common in intensely coloured and opaque glasses, as well as in glasses made prior to the middle 1<sup>st</sup> millennium BC, which are more heterogeneous than later glasses (Freestone, 2001b).

Any plan for a chemical analytical program for ancient glass characterization must allow for the analysis of major and minor elements (< 1 wt%), while avoiding corroded areas of glass. The imaging capability of the electron microprobe can be used to resolve and avoid hydrated or otherwise altered areas of a sample during routine analysis.

#### THE ARCHAEOLOGICAL SITE AND SAMPLES

The glass artifacts chosen for this study were excavated from Iron Age levels at the site of Hasanlu in northwestern Iran. Dr. Robert H. Dyson, Jr. of The University of Pennsylvania Museum of Archaeology and Anthropology has carried out excavations at this site located southwest of Lake Urmia (formerly, Lake Rezaiyeh) in the Solduz Valley in the province of Azerbaijan (Dyson, 1989a). The site is presently about 600 m wide, consisting of an artificial mound about 25 m high and 200 m in diameter bordered by a lower mound. Much of the excavated material was found in Period IVB levels, dated to the very end of the 9<sup>th</sup> century BC. At that time, the settlement was attacked and totally destroyed by burning.

The glass artifacts of this study excavated from the 9<sup>th</sup> century BC Iron Age levels are part of the collections of The University of Pennsylvania Museum of Archaeology and Anthropology. The Museum object registration numbers are noted in this paper by the designation UPenn., for example UPenn. 63-5-280a. The artifacts include small objects such as beads and inlays in small vessels. Sampling of objects was limited to

removal of small volumes of glass from already damaged areas, which included material that had been partly affected by weathering. Samples as small as a fraction of a millimeter were collected for analysis.

## ANALYTICAL METHOD

### **Microprobe analysis of high alkali glass**

High alkali glasses are susceptible to alkali loss under an electron beam from overheating of the glass by the beam. This can result in lower values of volatilized elements and in greater values of more refractory elements like Si and Al. Heat damage from the electron beam is minimized through a combination of measures. Defocusing the beam spreads the concentration of heat energy over a larger area and decreases the local temperature rise. Using a low beam current also contributes to a decrease in the amount of heat energy generated. Lower beam currents decrease analytical precision and increase detection limits. Because damage begins almost immediately when the beam hits the sample, shorter counting times are not helpful. However, using very long counting times, even with a low beam current, significantly increases the reported values of Si and decreases the reported values of Na.

Another behavior associated with electron beam analysis of glasses is the diffusion of alkalis around the analyzed area in response to an electrostatic field produced by the negatively charged electron beam (Reed, 1996). A space-charge layer can develop near the surface of the sample and attract positive  $\text{Na}^+$  ions to the area being analyzed. This increases the intensity of Na X-ray counts and causes an apparent increase in the reported value of  $\text{Na}_2\text{O}$ .

### **Electron microprobe analytical conditions**

A JEOL 7300 microprobe with four wavelength dispersive spectrometers was used in this study. Accelerating voltage was 15 kV, with a beam current of 2 nA as measured in a Faraday Cup, and a beam diameter of 20  $\mu\text{m}$  (0.02 mm). Calibration for

each element was carried out for 20 seconds at peak and backgrounds levels. Synthetic Na<sub>2</sub>O-CaO-SiO<sub>2</sub> glasses were used as standards for Na and Si, and natural and synthetic mineral standards were used for the remaining elements.

Calibration was performed before each run of analyses. A number of glass standards that are replicates of ancient glasses, including Corning A and Corning B, were regularly analyzed for each run. The Corning glasses are commonly used by researchers in museums, universities, and government laboratories as analytical standards for quality control comparisons with archaeological samples in studies of ancient vitreous materials (Henderson, 1988; Verità et al., 1994; Vandiver, 1983b; Brill, 1999).

During analysis, counting times on peaks and backgrounds were 20 seconds for each element. For each analysis, a peak search for Si was automatically carried out to account for drift in this element, which is the most abundant component in the Hasanlu glasses. The two major elements, Na and Si, were measured at the very beginning of each analysis, although the Si peak measurement lagged by about 20 seconds to 40 seconds because of the Si peak search. The ZAF routine devised by Armstrong (1984) was chosen to calculate corrections factors. Geller software dQuant, a Windows version of Tracor Northern software, was used as the interface between microprobe and user.

For each sample, at least three points of the glass matrix were analyzed, and the average of these analyses are then used to represent the glass in comparative discussions and graphs (see Henderson, 1988, and Verità et al., 1994 for similar analysis strategy).

### **Sample preparation**

A minimal amount of sample preparation was carried out because the loss of material during standard grinding and polishing would have been unacceptable for the small fragments of Hasanlu samples. Selected samples were fastened with double-

sided cellotape to the base of a container, then back-filled with epoxy resin. After hardening, the resin block was removed from the container and ground with either 400 or 600 grit silicon carbide sandpaper until the fragments were just visible on the ground surface. No water or other lubricant was used at this stage. This process was stopped as soon as all fragments were visible because further grinding removed a significantly large portion of glass. A paper towel or soft tissue with a few drops of acetone or methanol was then used to wipe off the surface. Subsequently, either hand-held or mechanical polishing was performed with a 6  $\mu\text{m}$  diamond grit suspended in oil or as paste. At about 10 second intervals, the surface was wiped with soft tissue and acetone or methanol and examined for a good finish. This procedure was repeated for 1  $\mu\text{m}$  and 0.25  $\mu\text{m}$  diamond grits. Longer polishing times in between examination usually proved to be unnecessary and to remove more glass than was desirable. Absolutely no water was used during polishing or grinding.

## RESULTS AND DISCUSSION

Totals for analyses used in this study are those that are between 97 wt% and 106 wt%. Some high totals are related to one analytical run that gave high Si values on both Corning standards and Hasanlu glasses, with totals at about 104—105 wt% for Corning B and about 101 wt% for Corning A. Other high totals may be related to analyses where more than one phase was present, especially those where sulfide or antimonate inclusions were present. Normally, totals on the Corning A and B standard glasses ranged from about 97 wt% to 102 wt%.

Reproducibility and accuracy of the Corning glass standards analyses are reported in Table 4.1. Measured values of  $\text{Na}_2\text{O}$  of the standards were consistently higher (average 3% relative) than the recommended values, and may account for some of the high totals. This generally higher  $\text{Na}_2\text{O}$  is possibly an affect of the electron beam

on the glass matrix (Reed, 1996). No corrections have been applied to any of the microprobe data in this report. However, analyses were normalized prior to graphing.

Table 4.1 Analytical Precision and Accuracy of Glass Standards

	Corning A				Corning B			
	Recommended composition (Brill, 1999)	This study (mean of 7)	Standard deviation	RSD	Recommended composition (Brill, 1999)	This study (mean of 16)	Standard deviation	RSD
SiO <sub>2</sub>	66.56	67.66	0.58	0.9	61.55	62.23	0.49	0.8
TiO <sub>2</sub>	0.79	0.84	0.14	16.2	0.089	0.21	0.02	9.1
Al <sub>2</sub> O <sub>3</sub>	1.00	0.92	0.05	5.4	4.36	4.45	0.30	6.8
FeO	0.98	1.05	0.26	24.7	0.31	0.38	0.18	49.1
MnO	1.00	0.91	0.20	21.8	0.25	0.40	0.22	55.3
MgO	2.66	2.75	0.12	4.4	1.03	1.08	0.09	8.0
CaO	5.03	5.10	0.14	2.7	8.56	8.95	0.40	4.5
Na <sub>2</sub> O	14.3	14.75	0.37	2.5	17.0	17.60	0.61	3.5
K <sub>2</sub> O	2.87	2.66	0.08	2.9	1.00	1.01	0.07	6.8
P <sub>2</sub> O <sub>5</sub>	0.13	bd			0.82	0.91	0.32	35.7
SO <sub>3</sub>	0.16	bd			0.54	0.44	0.08	18.1
Cl	0.10	0.10	0.02	23.4	0.20	0.18	0.04	25.4
Sb <sub>2</sub> O <sub>5</sub>	1.75	1.79	0.12	6.7	0.46	0.54	0.09	16.8
CuO	1.17	1.20	0.18	15.3	2.66	2.93	0.47	16.1
PbO	0.12	bd			0.61	bd		
CoO	0.17	bd			0.046	bd		

RSD - relative standard deviation (100\*(stand deviation / mean))

bd - below detection

Precision as relative standard deviation (RSD, 100\* standard deviation / mean) is better than about 10% for major elements, except CuO which is about 15%, and better than about 20% to 55% for minor (< 1 wt%) elements. The cause of the large RSD for minor elements lies mainly in the low count rates produced by the low beam current.

Detection limits range between about 0.3 wt% and 0.05 wt%.

### Hasanlu glass chemistry and colorants

The Hasanlu glasses from this study are all of the Na<sub>2</sub>O-CaO-SiO<sub>2</sub> type. The glasses contain about 17—21 wt% Na<sub>2</sub>O, about 2—8 wt% CaO, and 56—72 wt% SiO<sub>2</sub>, with about 1.5—6 wt% MgO and 1.5—4 wt% K<sub>2</sub>O (except for two blue translucent

glasses), and about 1—6 wt% Al<sub>2</sub>O<sub>3</sub> (Table 4.2). The remainder of each glass is composed mainly of Ti, P, Cl, S, and Fe, and various concentrations of Cu, Sb, and Pb, depending on the colorant.

Table 4.2 Microprobe analyses of selected unweathered and weathered glasses from Hasanlu (wt%)\*

UPenn. Museum registration no.	Color analyzed	<i>n</i>	SiO <sub>2</sub>	TiO <sub>2</sub>	Al <sub>2</sub> O <sub>3</sub>	FeO	MgO	CaO	Na <sub>2</sub> O	K <sub>2</sub> O	P <sub>2</sub> O <sub>5</sub>	SO <sub>3</sub>	Cl	Sb <sub>2</sub> O <sub>5</sub>	CuO	Total
<b>unweathered glass</b>																
HAS 63-5-276a	blue tp	9	63.90	0.31	3.26	1.43	2.81	8.24	17.43	2.17	0.45	0.43	0.45	bd	1.00	101.87
HAS 65-31-992	turquoise	3	67.33	0.21	2.35	0.58	4.57	5.22	17.51	1.55	0.23	0.58	0.32	1.75	2.03	104.23
HAS 65-31-396f, bag 2 of 6	black	4	65.70	0.20	2.00	13.04	2.08	1.65	16.39	0.76	bd	bd	0.30	bd	bd	102.12
<b>weathered glass</b>																
HAS 63-5-270a, bag 1 of 2	blue tp	1	60.35	0.51	4.72	2.50	2.38	0.93	2.28	4.37	bd	bd	0.30	0.77	1.30	77.91
HAS 75-29-442	turquoise	1	73.10	bd	0.69	bd	2.21	0.34	0.43	2.14	bd	0.35	0.32	1.84	2.79	84.20
HAS 73-5-559d	black	1	73.63	0.28	1.98	0.75	2.66	5.14	bd	1.41	0.72	0.39	0.95	bd	bd	87.15
HAS 63-5-280a	white opq	1	56.44	0.22	5.87	1.22	4.03	7.84	2.06	3.70	bd	bd	0.40	6.55	0.44	87.56

\* values listed are means of *n* analyses on a single sample

see text for analytical conditions

bd - below detection

na - not analyzed

MnO, SnO<sub>2</sub>, PbO, and CoO were also analyzed but do not occur above detection limits in these samples

tp - transparent; opq - opaque

Except for the 2 blue translucent glasses, the glasses are Na<sub>2</sub>O-CaO-SiO<sub>2</sub> with high K<sub>2</sub>O and MgO contents, indicating that they are of the plant ash variety (Brill, 1970a). The 2 exceptions contain less than about 1.5 wt% each of K<sub>2</sub>O and MgO. The wide range in K<sub>2</sub>O and MgO values is a common feature of groups of early glasses found at individual sites in the Near East (Vandiver, 1982, 1983b; Swann et al., 1993). The Hasanlu glasses contain generally higher Al<sub>2</sub>O<sub>3</sub> than other early Near Eastern glasses. A small group of blue translucent and black Hasanlu glasses contain significantly lower CaO than other late Bronze Age and early Iron Age glasses from the Near East.

The colors of glass found in the Hasanlu artifacts of this study include transparent to translucent blue, blue opaque (commonly called turquoise), white opaque, yellow opaque, and black (dark brown). Using the electron microprobe imaging and

analysis capabilities, in conjunction with what is known of ancient glass coloring technology, the Hasanlu colorants were identified. All of the glasses contain crystalline phases that color and/or opacify, except for the transparent to translucent blue glasses. These latter glasses are colored by  $\text{Cu}^{2+}$  dissolved in the glass matrix. The blue opaque (turquoise) glasses are colored in the same way, but also contain calcium antimonate crystals, which inhibit light from passing through the glass and thus make it opaque. The euhedral shape and unbroken state that some calcium antimonate crystals exhibit indicate that this phase was probably struck, or grown, from the glass melt and was probably not added as a separate constituent to batch materials. White opaque glasses are colored and opacified by calcium antimonate crystals but do not contain dissolved coloring ions at concentrations high enough to cause coloration. Another antimonate compound, yellow lead antimonate, colors and opacifies the yellow opaque glasses. Hasanlu black glasses are colored by polymetallic sulfides composed mainly of Cu and Fe, but some also contain Pb and Sb. The sulfides are very small, rounded droplets, most are less than 1  $\mu\text{m}$  in diameter, with some that are larger and composed of several phases. The shape, sizes and compositions of these sulfide droplets suggest that they may have originated in material left over from a partially processed ore.

### **Weathering of the Hasanlu glasses**

Many samples contain fractures along which weathering has taken place. The alteration that occurs along these fractures is not always easily visible, even with the aid of a light microscope. Figure 4.1 is a back-scattered electron image (BSI) of a black glass sampled from a bead (UPenn. 63-5-280a). The image shows altered glass existing along fractures which probably acted as conduits for water to infiltrate the sample. Analysis of one point from an altered area yields about 4 wt%  $\text{Na}_2\text{O}$ , about a 15 wt% absolute loss in  $\text{Na}_2\text{O}$  from the unaltered glass. In this particular part of the sample (Figure 4.1), the proportion of weathering along fractures appears to be small, but is

about 10% by area of the whole and represents a significant total loss of Na from this area of glass. A bulk analysis of this glass would give a Na<sub>2</sub>O value of about 1.5 wt% lower than that of the original.

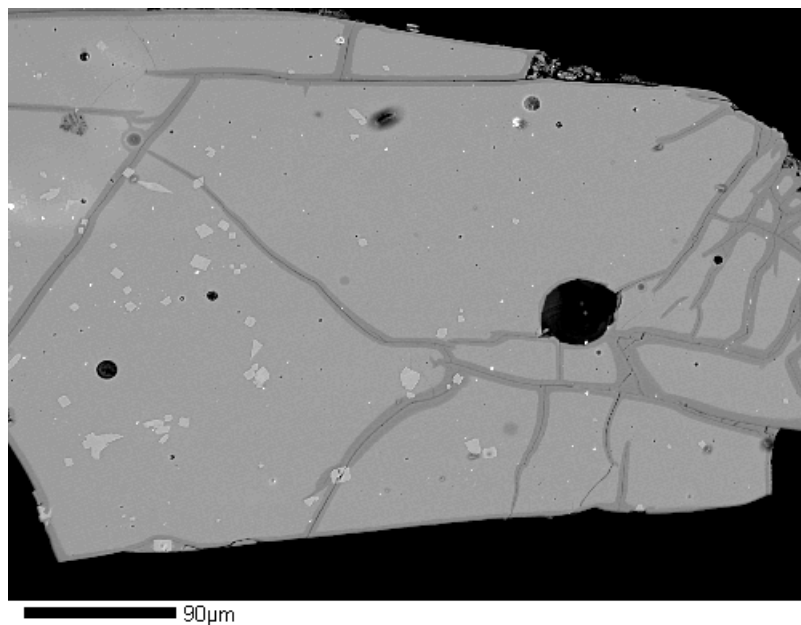


Fig 4.1. Back-scattered electron image (BSI) of black glass. Different levels of gray indicate areas of different chemical compositions. The glass matrix is medium gray and comprises most of this image. The linear darker gray features are areas of weathered glass, probably originally fractures along which water traveled. Euhedral crystals (lighter gray) are silicates of Ca, Mg, Fe, and/or Na. The smallest, white inclusions are sulfides of Cu and Fe, but some also contain different amounts of Pb and Sb. These sulfides color the glass black. Circular, black areas are gas vesicles. Bead, UPenn. 63-5-280a. Scale bar is 90  $\mu$ m.

Hasanlu samples that appeared to be completely weathered were prepared for microprobe examination in order to examine the patterns of weathering and to search for unaltered areas of glass. Figure 4.2 is a BSI that shows complicated patterns of weathering in a black glass sampled from a bead fragment (UPenn. 65-31-273). The glass seems to have experienced an initial stage of weathering, represented by sub-parallel layering, and a later stage of weathering, appearing in the BSI as mid-gray regions around fractures which cut across the sub-parallel layering. The later stage

probably occurred under different chemical environmental conditions than the initial weathering. Figure 4.2 also illustrates the small regions of unweathered glass that may still exist in a sample, regions that an electron microprobe is capable of imaging and analyzing.



Fig 4.2. BSI of black glass. The only area of unweathered glass is present in the lower right and appears as a lighter gray area, about 100  $\mu\text{m}$  wide, containing white inclusions of Cu, Fe, and Pb sulfides. The remainder of the sample exhibits layering that typically develops during weathering. Sulfide inclusions in the weathered area appear to have been unaffected by weathering. Circular to oval areas are gas vesicles, some now with polishing/grinding material inside. Bead, UPenn. 65-31-273. Scale bar is 100  $\mu\text{m}$ .

Glasses of certain colors appear to be more readily weathered than others.

Figure 4.3 is a BSI that shows a fragment of a blue glass bead with an attached decorative stripe of opaque white glass. The opaque white glass now consists almost completely of alternating layers of compositionally different materials, indicative of intense weathering. It is possible that the glass matrix of the white opaque stripe is depleted in Ca compared to the blue glass because the calcium antimonate crystals that color and opacify were probably struck from this glass. As a result, this white opaque

glass is less stable in the presence of water. The stability of the blue opaque (turquoise) glasses may be the affect of the  $\text{Cu}^{2+}$  ion acting as a stabilizer in the place of  $\text{Ca}^{2+}$ .

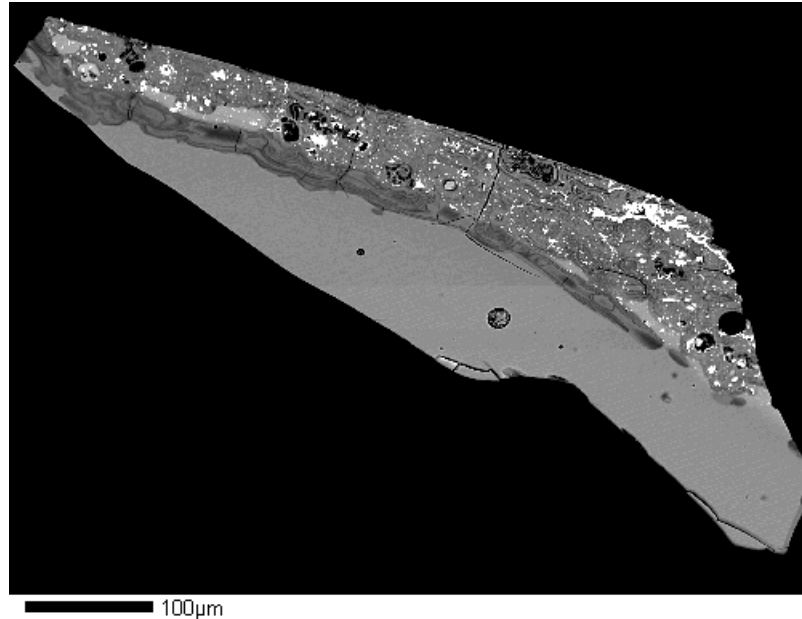


Fig 4.3. BSI of blue transparent (lower, mid-gray area) and opaque white (upper layer with white inclusions) glass. The opaque white glass is almost entirely weathered. The blue glass exhibits weathering only along the contact with the white glass. The white inclusions in the opaque white glass are calcium antimonate crystals. Bead, UPenn. 63-5-276a. Scale bar is 100  $\mu\text{m}$ .

Some crystalline colorants are less susceptible to weathering than the surrounding glass matrix. The sulfide droplets that color the black glasses and the calcium antimonate crystals that color the blue opaque (turquoise) and white opaque glasses are apparently unaffected by the weathering processes that have altered their surroundings (Figures 4.4 and 4.5). Electron microprobe analysis can identify these crystalline phases, and thus original colors can be identified. In hand sample or using a light microscope, weathered glass of any color often appears white.

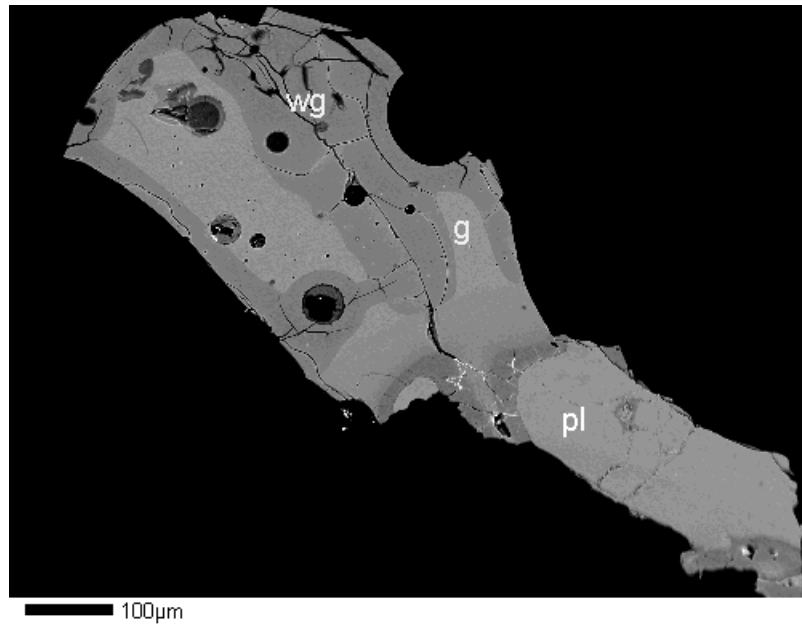


Fig 4.4. BSI of blue translucent glass with plagioclase feldspar grain (pl, entire phase in lower right, mid-gray). The glass is weathered (wg) around the rim and part of the interior. Unweathered glass (g) contains about 3 wt%  $\text{Al}_2\text{O}_3$ . Between the glass and the plagioclase is a glass with about 10 wt%  $\text{Al}_2\text{O}_3$  (slightly darker gray zone), and an area of altered plagioclase (very dark gray zone). The white phase filling the fractures in the altered plagioclase is MnO rich, probably a post-burial deposit. Bead, UPenn. 63-5-280a.

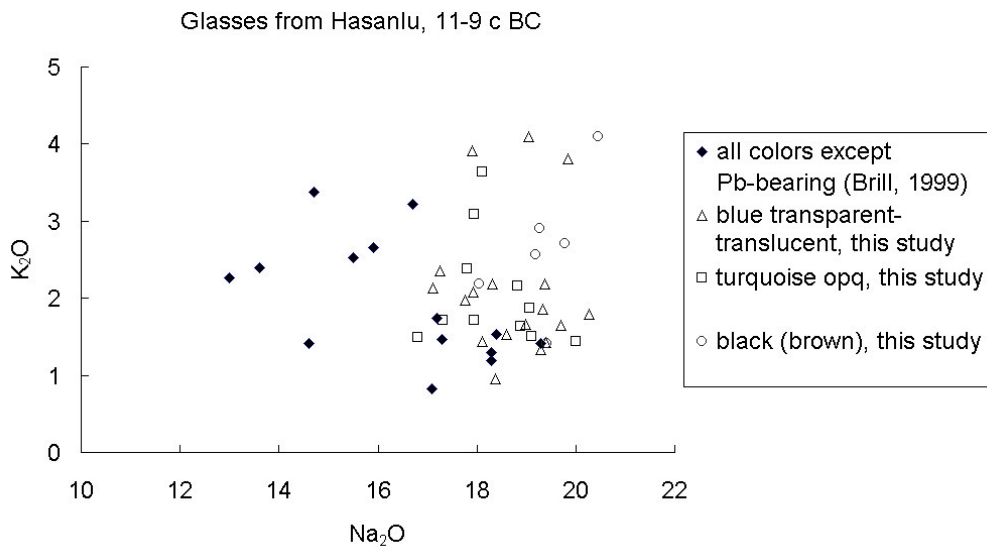


Fig 4.5. Comparison of bulk glass analyses of glass artifacts from Hasanlu with microprobe analyses from this study. Lower  $\text{Na}_2\text{O}$  values in bulk analyses may be the result of incorporation of some weathered glass. Greater than about 1.5 wt% each of MgO and  $\text{K}_2\text{O}$  suggests a plant ash source for the alkalis; less suggests a mineral (natron) source.  $\text{SiO}_2$  reported by difference from 100 for bulk analyses (Brill, 1999); microprobe data normalized to 100% for comparison. Lead-bearing glasses not included in this graph.

In a few of the Hasanlu glass fragments, material has been deposited into fractures and vesicles after the original objects were discarded. Analysis of filling in a fracture of a transparent blue glass (Figure 4.4) shows that it is Mn rich, containing up to about 4 wt% MnO. There is no Mn in the feldspar, and the glass contains only about 0.6 wt% MnO, suggesting that Mn leached from the weathered glass was redeposited into the fractures.

### **Chemical composition of weathered areas**

A few areas of weathered glass from the Hasanlu glasses have been analyzed, yielding totals of much less than 100 wt%. These weathered areas contain much less Na<sub>2</sub>O than unweathered glass and have correspondingly higher SiO<sub>2</sub> (Table 4.2). Back-scattered electron imaging of these areas show compositionally different layers, alternating on scales of less than 10 um up to at least 30 um, typical of weathered glass (Figure 4.2).

A previous investigation of a group of 21 glass artifacts from Hasanlu was carried out by two different bulk analytical methods (either AA or ICP spectroscopy; Brill, 1999). About half of those samples contain lower Na<sub>2</sub>O than the glasses from this study (Figure 4.5). Even taking into account the sodium analytical problems encountered with the electron microprobe in this study, a number of the bulk analyses yielded unusually low Na<sub>2</sub>O. Some of the glasses from the earlier investigation are described as being partly weathered (Brill, 1999). The lower Na<sub>2</sub>O values reported in the bulk analyses may be the result of the inclusion of weathered glass. The compositions of the glasses are more consistently and accurately identified using the electron microprobe.

### **Chemical and mineralogical inhomogeneities**

#### *Devitrifying phases*

High temperature phases in the Hasanlu glasses include diopside (CaMgFeSiO<sub>3</sub>), wollastonite (CaSiO<sub>3</sub>), and a calcium sodium silicate (not devitrite).

These phases exist as euhedral, well-formed crystals, indicative of growth from the melt and are on the order of 10—30  $\mu\text{m}$  long.

#### *Original and partially reacted batch inclusions*

Quartz, plagioclase feldspar, alkali feldspar, spinel and altered alumino-silicates occur as inclusions in a number of Hasanlu glasses. These naturally-occurring minerals were probably incorporated into the glasses as part of the batch and thus are indicators of the types of materials used in the glassmaking process. The quartz grains appear to be stable, while the feldspar grains exhibit disequilibrium textures, suggesting that they were in reaction with the glass melt. A translucent blue glass (UPenn. 63-5-280a) contains a large grain of plagioclase feldspar  $((\text{Ca},\text{Na})(\text{Al},\text{Si})_2\text{O}_8)$  which has a reaction rim of about 20  $\mu\text{m}$  (Figure 4.4). The composition of the glass closest to the reacted rim of the plagioclase grain is enriched in  $\text{Al}_2\text{O}_3$  and slightly depleted in  $\text{Na}_2\text{O}$  compared to the bulk glass. A blue opaque (turquoise) glass (UPenn. 65-31-992) contains an alkali feldspar grain which also exhibits a disequilibrium texture with the bulk glass (Figure 4.6), although the zone of chemical transition is much smaller than that in the previous example. This same sample also contains large grains of quartz up to 200  $\mu\text{m}$  across, and a smaller apatite grain, about 50  $\mu\text{m}$  long. The translucent blue glass of another sample (UPenn. 73-5-559e) contains a partially reacted phase with high MgO (approx. 22 wt%), FeO (approx. 8 wt%), and  $\text{Al}_2\text{O}_3$  (approx. 23 wt%) and low  $\text{SiO}_2$  (approx. 34 wt%) that originally may have been a mica or clay mineral (Figure 4.7). This area is about 100  $\mu\text{m}$  across, indicating a relatively large original grain size. Feldspars and micas or clay minerals are not commonly found in the mature, pure quartz sands used for glassmaking.

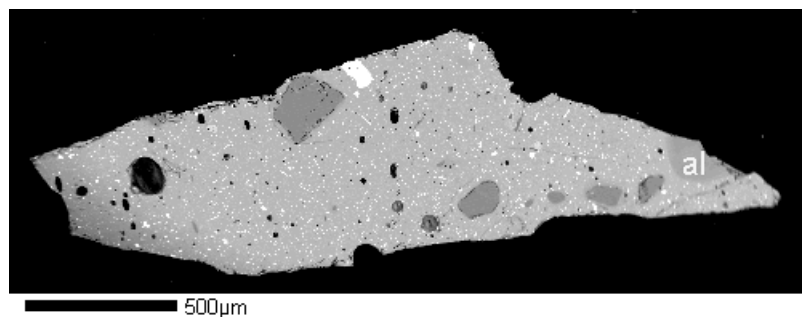


Fig 4.6. BSI of blue opaque (turquoise) glass. White inclusions are calcium antimonate crystals. Dark gray, angular to rounded inclusions are quartz. Mid-gray phase in right is alkali feldspar (al). Round apatite grain occurs in upper left (bright gray). Hollow, 4-sided tube, UPenn. 65-31-992. Scale bar is 400 um.

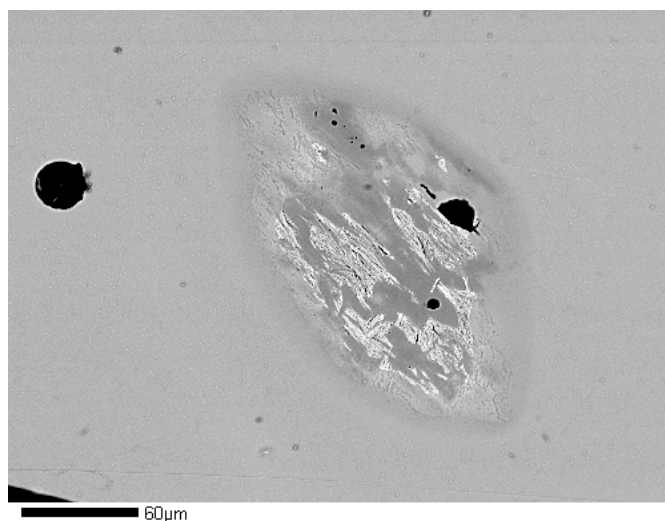


Fig 4.7. BSI of blue translucent glass. Inclusion at center is probably partly reacted batch phase that exhibits crystallographically controlled dissolution. High MgO, Al<sub>2</sub>O<sub>3</sub>, and FeO and low SiO<sub>2</sub> contents suggest that this phase was originally a mica or clay mineral. Bead, UPenn. 73-5-559e. Scale bar is 60 um.

Two blue glass beads excavated from an earlier-dated level at Hasanlu were investigated to compare them with the 9<sup>th</sup> century BC glasses. The major element compositions of the two earlier-dated glasses are not distinctly different from the 9<sup>th</sup> century BC glasses. However, both of the earlier glasses contain small spinel ((Mg,Fe)(Cr,Al)<sub>2</sub>O<sub>4</sub>) mineral grains, on the order of 20 um by 10 um as identified using an electron microprobe. Spinel has not yet been found in any of the 9<sup>th</sup> century BC glasses. This mineralogical difference suggests that the earlier-dated, spinel-bearing

glasses were made from different sources of materials than the later glasses, even though the basic types of materials may have been the same.

#### *Sulfate inclusions*

Round inclusions of alkali sulfate, mainly sodium sulfate, occur in at least half of the glass samples examined to date. Alkali sulfate inclusions have been found in all colors of Hasanlu glass, but do not exist in every sample examined. These sulfate inclusions at first glance are similar in appearance to gas vesicles filled with deposits from grinding and polishing or from post-burial water precipitates (Figure 4.8). The alkali sulfate inclusions range in size from a few microns up to about 100  $\mu\text{m}$  in diameter. The larger inclusions show crystal forms (Figure 4.9) and have structures unlike the layering that is common to minerals precipitated from water. Analysis of some sulfate inclusions also yield small amounts of chlorine, and one inclusion shows the cubic crystal habit of halite ( $\text{NaCl}$ ). The round or spherical shape of these inclusions, in combination with their chemistry, indicates that they were probably immiscible liquid inclusions within the silicate glass melts. This material may be found in modern glassmaking operations floating on the surface of glass melts and is referred to as gall or scum.

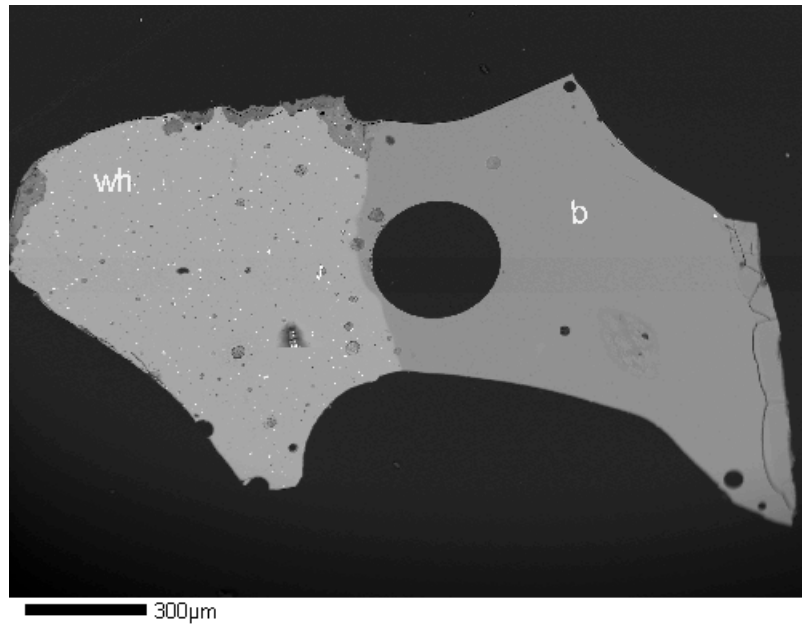


Fig 4.8. BSI of white opaque (wh) and blue translucent (b) glasses. Round, darker gray inclusions in white opaque glass are crystallized sulfate inclusions. No sulfate inclusions exist in this blue glass, except for one that is close to the contact with the white opaque glass, where it may have its origin. Bead, UPenn. 73-5-559e. Scale bar is 300  $\mu\text{m}$ .

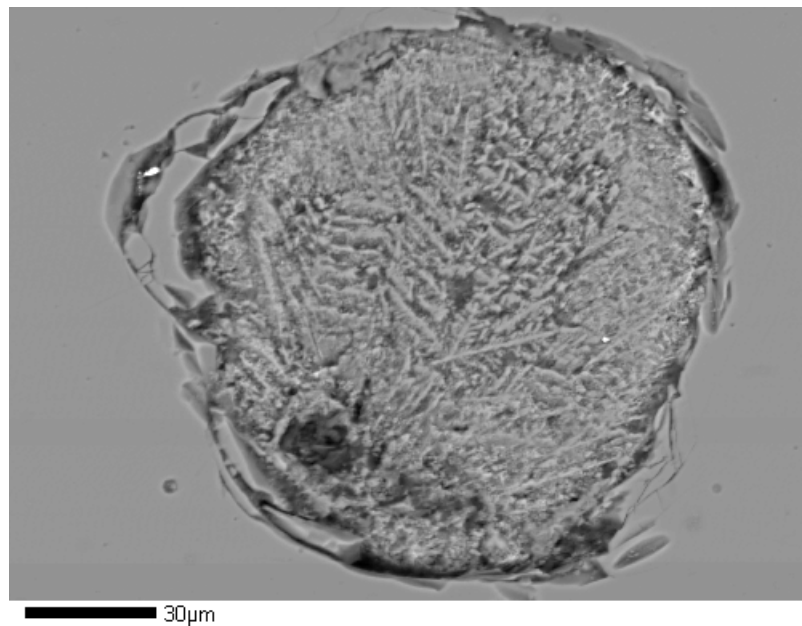


Fig 4.9. BSI of crystallized sulfate inclusion in blue translucent glass. Bead, UPenn. 61-5-95b, bag 1 of 3. Scale bar is 30  $\mu\text{m}$ .

These types of inclusions have not been reported or described in the archaeological science literature on ancient glasses, and thus possibly do not exist in other ancient glass samples. However, sodium sulfate is very soluble in water, and the use of water is a common part of many sample preparation techniques. The case may be made that no sulfate inclusions have been reported because they were dissolved during sample preparation procedures. The authors of this paper strongly recommend using alcohol in the place of water during sample cleaning in order to preserve any possible sulfate phases.

The presence of phases such as the alkali sulfate inclusions are important to the interpretation of glassmaking technology. In some of the Hasanlu glasses, there are very large sulfate inclusions, while in other glasses the sulfate inclusions are small in both size and number. This difference may be the result of using different source materials or of washing the latter glass in water at some stage in the manufacturing process, a step described in some early glassmaking texts to rid the glass of unreactive salts (Neri, 1662). The existence of sulfates in these glasses may also allow for a more clear understanding of batch melting reactions and explain the wide variation in chemical compositions of the glasses produced.

## CONCLUSION

The glasses from Hasanlu are broadly similar to other late Bronze Age and early Iron Age glasses (Vandiver, 1982, 1983b; Swann et al., 1993; Brill, 1999), but made from different sources of materials. Most of the Hasanlu glasses appear to have been made with alkali derived from plant ashes. The range in CaO contents suggests that the glasses from Hasanlu were made from more than one recipe.

When designing an analytical program for ancient glass and other vitreous materials, the analyst should keep in mind that almost all ancient glasses show some signs of weathering. This should probably be expected because the vast majority of

ancient glasses are high alkali glasses which are very easily weathered. Intensely colored, opaque glasses and glasses made prior to the middle 1<sup>st</sup> millennium BC appear to weather to a greater degree than weakly colored and later glasses. The former glasses are more heterogeneous than the latter and water can move into the glasses more easily along grain boundaries in the heterogeneous glasses. Analyses of weathered glass are not useful in interpreting ancient glass technology because the chemical changes that have happened are not predictable and it is not possible to back-calculate the amount of material that has been lost from a weathered area of glass. This is particularly true of ancient glasses made prior to about the middle 1<sup>st</sup> millennium BC because the original chemical compositions are not consistent from one glass to the next. Bulk analysis of early glasses is more likely to produce erroneous results than microanalysis. Electron microprobe analysis has the advantage of enabling the researcher to image a sample in real time and identify unaltered, unweathered areas of glass for analysis.

The analyst additionally should be aware that information that is very helpful in interpreting ancient glass technology and glass trade relationships goes beyond bulk chemical compositions. Consideration should be given to collecting data on colorant chemistry and phases, unreacted and partially reacted batch inclusions, and high temperature crystalline phases. All of this information, including bulk chemical analyses, can be gathered using an electron microprobe with an attached quantitative chemical analytical system.

## CHAPTER 5

### BATCH MATERIAL PROCESSING AND GLASSMAKING TECHNOLOGY OF 9<sup>TH</sup> CENTURY B.C. ARTIFACTS EXCAVATED FROM THE SITE OF HASANLU, NORTHWEST IRAN

---

Stapleton, C. P. and Swanson, S. E. (2002) *Materials Issues in Art and Archaeology VI*  
(P. B. Vandiver, M. Goodway, and J. L. Mass, Eds.), Materials Research Society  
Symposium Proceedings v. 712, 315-321. Reprinted here with permission of publisher.

## ABSTRACT

The site of Hasanlu is located southwest of Lake Urmia (Lake Rezaiyeh) in the province of Western Azerbaijan, northwest Iran. Excavations carried out by Dr. R. H. Dyson, Jr. of the University of Pennsylvania from 1957 to 1977 of the Iron Age levels at Hasanlu yielded a large number of glass beads, as well as glass vessels, and glass furniture inlays or wall fittings. Sampling of many of these pieces was limited to weathered areas, requiring the use of a micro-analytical technique to characterize the glass. Electron microprobe and wavelength dispersive analysis were used to characterize the chemical compositions of the glasses of Hasanlu. The glasses are soda-lime-silica in composition, containing about 17-21 wt% soda and 2-8 wt% lime. Of 51 glasses analyzed to date, 47 contain about 1-6 wt% of magnesia and 1-4 wt% potash, indicative of a plant ash source of alkali. Four glasses contain less than 1 wt% each of magnesia and potash, suggesting that these may have been made with a mineral alkali source like natron.

At least 35 glasses contain inclusions of partly reacted batch materials. In blue transparent to translucent, black translucent, and yellow opaque glasses, large, 0.2 mm diameter, droplets of alkali sulfates exhibit features that indicate they were an immiscible liquid coexisting with a surrounding silicate liquid. These sulfate droplets, which appear to be relatively common in the glasses found at Hasanlu, are probably the scum or "gall" that can form during melting of poorly prepared plant ash. Remnants of original raw colorants occur in a few glasses. Many of the black glasses contain polymetallic sulfides of different combinations of lead, copper, antimony, and iron. These inclusions and the glass chemistry are used to interpret the origin and processing of the batch materials, and the conditions under which the materials were melted.

## INTRODUCTION

The history of glassmaking in the late 2<sup>nd</sup> millennium BC and early 1<sup>st</sup> millennium BC is not well known, partly because few scientific excavations have yielded glass. Prior to this period, glass was made with a mix of plant ash and quartz (Oppenheim et al., 1970). In Mesopotamia, this recipe appears to have been used in the 7<sup>th</sup> century BC and later in the 1<sup>st</sup> millennium BC (Brill, 1999) through the Islamic period (Freestone and Stapleton, 1998), and well into the 20<sup>th</sup> century AD (Brill, 1972a). Along the eastern Mediterranean and in Egypt, from about the 9<sup>th</sup> century BC onward, glass with a chemical composition that is characteristic of having been made with mineral alkali and sand is commonly found in the archaeological record, sometimes alongside plant ash glasses (e.g. Sayre, 1965, and Hartmann et al., 1997). This type of glass may have been made as early as the 15<sup>th</sup> century BC in Egypt (Shortland and Tite, 2000). The co-occurrence of both glass types in later times may be the result of the techniques used to make specific colors. For example, some copper-colored red opaque glasses required the addition of carbon-bearing plant ash to reduce copper from  $\text{Cu}^{2+}$  to  $\text{Cu}^{\circ}$  or  $\text{Cu}_2\text{O}$  (Freestone, 2001a) The existence of these red glasses from the 2<sup>nd</sup> millennium BC through to the 1<sup>st</sup> millennium AD suggests a technologically conservative approach to making such glasses.

One archaeological site that offers the potential to investigate early 1<sup>st</sup> millennium BC glassmaking is Hasanlu in northwestern Iran (Dyson, 1989a). At this site, a range of well-dated glass and vitreous material artifacts were carefully excavated from Iron Age levels. The glass objects found include vessels, hollow tubes possibly used as furniture inlays or wall fittings, and thousands of beads. Glazed ceramic, faience and Egyptian blue artifacts were also excavated from the Iron Age levels. The purpose of this paper is to use the major element compositions and crystalline inclusions in the finished glass

objects to identify the raw materials and the basic processing they underwent before being added to the glassmaking batch.

## ANALYTICAL METHODS

Electron microprobe analysis (EMPA) was used to chemically and mineralogically characterize 3 colors of glass: blue opaque (turquoise), blue transparent to translucent, and black. The problems associated with electron microprobe analysis of high alkali glass, and the analytical conditions and sample preparation for this study are further discussed in Stapleton and Swanson (2002a; Chapter 4). In order to compare the main raw ingredients of these glasses, the compositions have been recalculated to include oxides that are assumed to have been derived mainly from the alkali and silica raw ingredients. The discussion in this paper is based on compositions recalculated to include only SiO<sub>2</sub> and Al<sub>2</sub>O<sub>3</sub> from the silica component, and Na<sub>2</sub>O, MgO, K<sub>2</sub>O, and CaO from the alkali component, unless otherwise indicated.

## RESULTS AND DISCUSSION

The Hasanlu reduced compositions show that these glasses contain about 17—22 wt% Na<sub>2</sub>O, 2—9 wt% CaO, 0.7—5 wt% K<sub>2</sub>O, and 0.8—7 wt% MgO. The compositions (Table 5.1) are broadly similar to other Bronze and early Iron Age glasses.

Table 5.1. Examples of chemical compositions of glasses from Hasanlu (means of *n* analyses).

UPenn. #	<i>n</i>	SiO <sub>2</sub>	TiO <sub>2</sub>	Al <sub>2</sub> O <sub>3</sub>	FeO	MnO	MgO	CaO	Na <sub>2</sub> O	K <sub>2</sub> O	P <sub>2</sub> O <sub>5</sub>	SO <sub>3</sub>	Cl	Sb <sub>2</sub> O <sub>5</sub>	CuO	Total
Blue transparent to translucent																
61-5-89h2	10	59.01	0.21	4.95	0.53	<0.3	4.68	5.53	20.16	3.87	0.34	0.38	0.69	0.32	0.94	101.63
61-5-95a	3	64.33	0.27	2.49	1.35	0.34	3.42	7.41	18.11	2.02	0.30	<0.30	0.55	<0.3	1.39	101.97
75-29-199a	4	71.95	<0.2	0.80	0.56	<0.3	0.85	4.67	19.04	0.98	0.29	0.59	0.27	2.55	1.08	103.63
Black																
63-5-280a	5	56.12	0.31	5.29	3.05	<0.3	5.93	5.43	20.18	2.70	0.60	1.31	0.81	2.42	0.94	105.11
65-31-273a	5	60.49	0.21	1.75	8.06	<0.3	2.60	5.00	18.10	2.19	0.40	0.82	0.72	<0.3	<0.4	100.34
65-31-396h (bag 2 of 6)	3	62.96	<0.2	1.35	15.15	<0.3	0.72	4.02	15.13	0.67	<0.3	<0.30	0.28	<0.3	<0.4	100.28
Opaque pale blue (turquoise)																
65-31-728f	4	61.43	<0.2	2.88	0.66	<0.3	4.49	5.65	19.06	1.65	0.29	0.47	0.27	1.83	2.22	100.89
65-31-280	4	59.38	0.41	9.41	3.10	<0.3	2.74	4.08	18.06	2.42	<0.30	0.43	0.58	<0.3	0.85	101.47
65-31-280	2	62.80	<0.2	2.58	0.54	<0.3	4.10	6.46	19.35	1.89	0.40	0.54	0.44	1.15	1.20	101.43



Alumina ( $\text{Al}_2\text{O}_3$ ) may be used to distinguish between a basically pure quartz source, which contains very little  $\text{Al}_2\text{O}_3$ , and quartz sand, which usually contains  $\text{Al}_2\text{O}_3$ -bearing minerals such as feldspars. However,  $\text{Al}_2\text{O}_3$  can enter the glass batch unintentionally with other components such as the colorants, as appears to be the case with the black Hasanlu glasses (Figure 5.2), and with kiln and crucible materials, which contain considerable amounts of  $\text{Al}_2\text{O}_3$ .

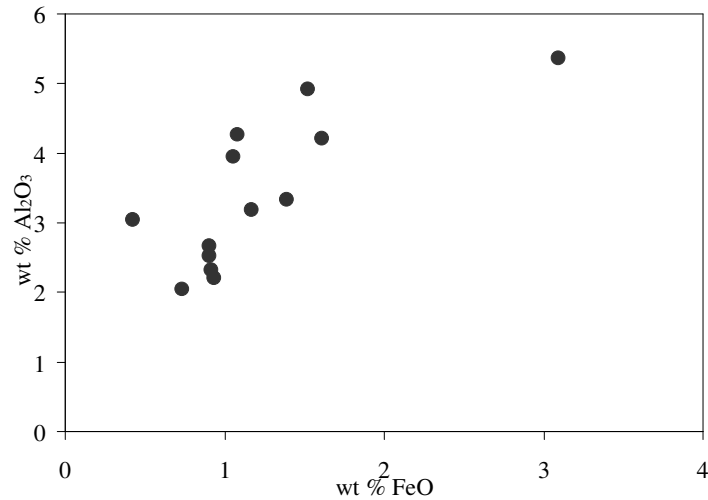


Figure 5.2. Some black glasses from Hasanlu exhibit a positive correlation between FeO and  $\text{Al}_2\text{O}_3$ , suggesting that these 2 oxides entered the glass in the same batch material. The black glasses are colored by mixed copper-iron sulfides that occur as < 1  $\mu\text{m}$  spheres.

The  $\text{Al}_2\text{O}_3$  in the blue transparent to translucent glasses does not show any correlation with the copper colorant and may be used to investigate the relationship between the alkali and the silica batch materials. The low MgO Hasanlu glasses may have been made with a smaller amount of alkali batch material than the high MgO glasses (open triangles, Figure 5.3). The slight positive correlation between  $\text{Al}_2\text{O}_3$  and MgO in these low MgO glasses is more pronounced with the addition of  $\text{K}_2\text{O}$  to MgO, suggesting that at least some of the  $\text{Al}_2\text{O}_3$  in these lower MgO glasses was associated with  $\text{K}_2\text{O}$  in the batch materials. Alkali feldspar in one of the batch materials would account for the positive correlation.

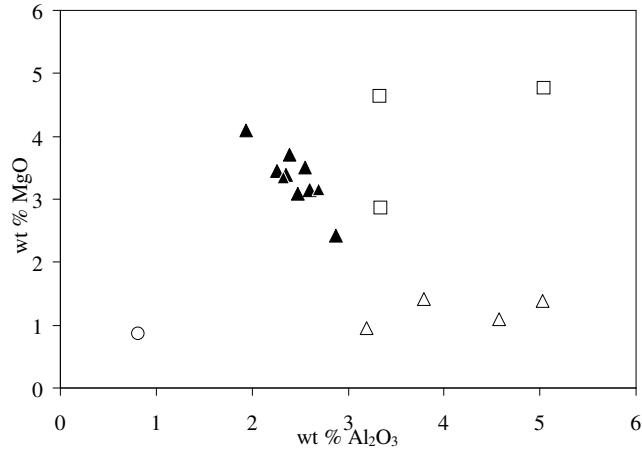


Figure 5.3. Blue transparent to translucent glasses with the lowest MgO (open triangles) contain generally higher Al<sub>2</sub>O<sub>3</sub> than other blue transparent to translucent glasses. This suggests that the batch materials for these glasses were composed of a greater proportion of the silica batch material (which contained most of the Al<sub>2</sub>O<sub>3</sub>) than the alkali batch material. Symbols same as Figure 5.1.

The negative correlation between MgO and Al<sub>2</sub>O<sub>3</sub> in the higher MgO glasses (closed triangles, Figure 5.3) is an indication that these 2 components entered into the glass in separate batch materials. Figure 5.4 shows that a feldspar- or clay-bearing sand was the probable source for Al<sub>2</sub>O<sub>3</sub> in these glasses.

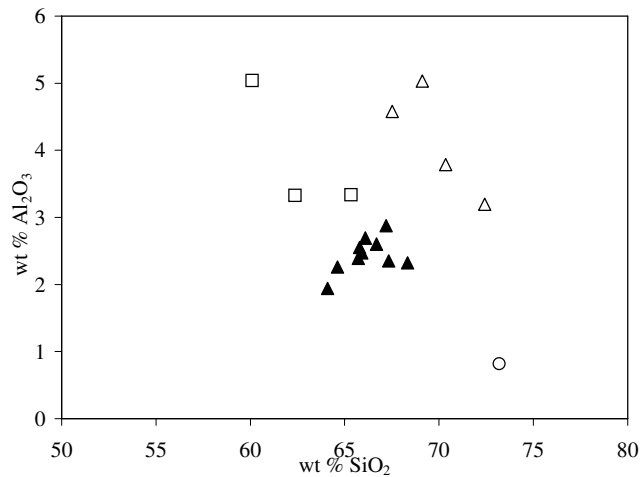


Figure 5.4. Blue transparent to translucent glasses in the higher MgO group (closed triangles) show a positive correlation between SiO<sub>2</sub> and Al<sub>2</sub>O<sub>3</sub>, 2 oxides that characterize “impure” sands, which typically contain feldspar or clay minerals as major secondary phases along with quartz. This suggests that all of the Al<sub>2</sub>O<sub>3</sub> in the glasses of the high MgO group was derived from the silica batch source (impure sand). Symbols same as Figure 5.1.

Two blue transparent to translucent beads excavated from an earlier-dated level at Hasanlu were investigated to compare them to the 9<sup>th</sup> century BC beads. The major element compositions are similar to those of the 9<sup>th</sup> century BC glasses, suggesting that the same type of glassmaking raw materials were used in the earlier period. Both of the earlier beads contain spinel ((Mg,Fe)(Cr,Al)<sub>2</sub>O<sub>4</sub>) mineral grains, one of which is Cr-bearing. In addition, the spinel grains contain copper, which has probably diffused in from the copper-bearing silicate melt. In natural settings, spinel is one of the first minerals to weather from a rock. The spinel entered these glasses either as part of the copper ore material or as part of a sand that was close to the source rock of the spinel mineral grains. The apparent lack of spinel in the 9<sup>th</sup> century BC beads suggests that the earlier-dated, spinel-bearing glasses were made with sand or copper ore from a different source than the 9<sup>th</sup> century BC beads.

Alkali sulfate phases are found in 33 out of 47 glasses examined for such inclusions, and occur in all color of glasses. These inclusions are on the order of 10 um to 40 um in diameter in the black and blue transparent to translucent glasses, but are <10 um in diameter in the opaque blue (turquoise) glasses. An Mg-Si crystalline phase and a Ca-K-P-S crystalline phase were found in 2 blue glasses. Similar phases have been identified in plant ashes obtained from the wood of modern plants (Smedley et al., 2001), and are surmised to represent original, but partly-reacted plant ash in the glasses of Hasanlu.

Rare, small inclusions of calcium antimonate have been found in 2 blue transparent to translucent glasses, suggesting that these glasses may have some association with the blue opaque (turquoise) or white opaque glasses, both of which are opacified by calcium antimonate crystals. It is possible that some opaque blue (turquoise) or white glass was recycled into the transparent to translucent blue glasses. However, the rare occurrence of the antimonate crystals in these transparent to

translucent blue glasses indicates that the proportion of recycled material, if any, would have been very small. Copper, as  $\text{Cu}^{2+}$  dissolved in the glass matrix, is the colorant for both the opaque and the transparent to translucent blue glasses.

The black glasses are colored by  $<1\mu\text{m}$  diameter spheres of mixed copper-iron sulfides. Some black glasses also contain mixed copper-iron-lead-antimony sulfides. These types of phases are not typical geologic ores, but can be formed during smelting of ores. Slags of smelted iron ores do not usually contain copper, but copper ore slags often contain iron as well as antimony and sulfur. It is possible that the colorants of the black and blue transparent to translucent glasses from Hasanlu were derived from slags smelted from copper ores. The ores used for the black glasses would have been sulfidic ores, rather than carbonate or oxide ores. The opaque blue (turquoise) glasses do not contain the metal oxide inclusions that glasses in the other 2 color groups contain.

Some glass samples contain glass with different chemical compositions. These heterogeneous glasses may be the result of mixing of a base glass with the coloring agent. For example, a sample of opaque pale blue (turquoise) glass from a thick-walled, four-sided rod (UPenn. 65-31-280, Table 5.1), has 2 different compositions. The higher  $\text{SiO}_2$  glass also contains calcium antimonate crystals that opacify the glass. The mixing may have been done to extend a limited supply of the given glass or it may be the way in which those colors of glass were made.

## CONCLUSIONS

All of the blue transparent to translucent, black and opaque blue (turquoise) glasses from Hasanlu probably were made with alkali derived from plant ash. The low  $\text{K}_2\text{O}$  and  $\text{MgO}$  contents of several of the blue transparent to translucent and black glasses are possibly the result of smaller proportions of plant ash mixed with the silica batch material. The high  $\text{Al}_2\text{O}_3$  content of the blue transparent to translucent and opaque blue (turquoise) glasses and the presence of feldspar and spinel grains suggest

an impure sand was used as the silica source for these glasses. The copper colorant of most of the blue transparent to translucent glasses was probably an iron-bearing copper carbonate or oxide ore, or slag from processing such an ore. The presence of mixed copper-iron-lead-antimony sulfides that color the black glasses suggests that slag from processed sulfidic copper ore was used in these glasses.

The blue opaque (turquoise) glasses have generally lower FeO than the other 2 color groups, and do not contain the metal oxide inclusions that the other glasses contain. Fewer and generally smaller alkali sulfate inclusions are found in the opaque blue (turquoise) glasses than in the other colored glasses. The batch materials of these opaque blue (turquoise) glasses were probably more carefully prepared than those of the black and blue transparent to translucent glasses. Further analytical studies on the trace element compositions may yield information that will more clearly define the silica source as well as the colorant sources.

## CHAPTER 6

### THE RAW MATERIALS USED TO COLOUR 11<sup>TH</sup>—9<sup>TH</sup> C BC BLUE TRANSPARENT GLAZES FROM HASANLU, IRAN

---

Stapleton, C. P. and Swanson, S. E., Ghazi, A. M. (2002) Submitted to *Journal of Geoarchaeological and Bioarchaeological Studies* .

## INTRODUCTION

Our lack of knowledge of glassmaking technology during the transition between the Bronze and Iron Ages lies partly in the small amount of well-excavated glass artifacts. One site that has produced a variety of suitable material is Hasanlu in northwestern Iran, excavated by Robert H. Dyson, Jr., from the University of Pennsylvania (Dyson, 1989a). At the very end of the 9<sup>th</sup> century BC (Period IVB), Hasanlu was completely destroyed by unknown attackers and thereafter remained unoccupied for a period of perhaps 50 to 100 years. The archaeological artifacts from the Period IVB (Iron Age II) levels of Hasanlu are unique and irreplaceable because of the scarcity of materials from this period and this region. Artifacts made of glassy materials excavated from this level are reported in von Saldern (1966), Dyson and Voigt (1989), de Schauensee (2001), and Marcus (1991, 1996). The artifacts excavated include beads, hollow tubes, and vessels made of glass, beads and seals made of faience, beads and tiles of Egyptian Blue, as well as glazed ceramics. Blue transparent glazed and unglazed vessels with a spout attached to the vessel body by a bridge found in the Period IVB levels are unique to Hasanlu. Only the blue transparent glazes of two bridge-spouted vessels will be discussed in this brief paper.

In glassy materials, the colouring ion or compound is often easily identified from chemical analysis, but the form or phase in which the colourant was initially added to the glaze or glass batch is not directly evident. Chemical signatures of the original host phase, along with the colourant, will have been carried into the finished product. Correlations of colourants with trace elements are used here to interpret the source material (ores, metals, slag) of the colourants added to the glaze batches to yield the blue transparent colour.

## METHODOLOGY

### **Electron Microprobe**

The microprobe analytical conditions used for these glazes are discussed in detail Stapleton and Swanson (2002a; Chapter 4). Polished samples of the blue transparent glazes were analyzed for major and minor elements using electron microprobe analysis at the Geology Department of the University of Georgia. Beam conditions were 15 kV, 2.0 nA, 20  $\mu\text{m}$  beam diameter, and 20 second counting times for each element. Sodium and silicon were analyzed first and at the same time to reduce sodium migration from electron beam heat damage. Reproducibility, measured from repeat analyses on standard glass Corning B are better than about 2% relative for oxides present at greater than 10 wt%, better than about 10% for the remaining oxides except FeO, which is around 40%. The glazes were examined in back-scattered electron mode for homogeneity. From these examinations, representative areas were chosen for analysis.

### **Laser Ablation-Inductively Coupled Plasma-Mass Spectrometry (LA-ICP-MS)**

The samples prepared for electron microprobe analyses were also analyzed by LA-ICP-MS at the Geology Department at Georgia State University. The instruments used were a New Wave-Merhcantek 213 nm Nd-YAG laser and a high resolution Finnigan MAAT Element 2 high magnet ICP-MS. Laser parameters were set at 20 Hz rep rate (laser pulses/second), 25  $\mu\text{m}/\text{second}$  raster speed, 100  $\mu\text{m}$  raster spacing, 100  $\mu\text{m}$  laser spot diameter. The laser fluence was between about 1.2  $\text{J}/\text{cm}^2$  and 1.5  $\text{J}/\text{cm}^2$ . Corning A and Corning B standard glasses were used as calibration standards because their chemical matrices closely match those of the Hasanlu glasses. The recent re-evaluations reported in Rising (1999) are used here as the calibration values. York 76-C-145 was used as the calibration standard for arsenic because this element is not reported in the recent re-evaluation of the Corning standards. A gas blank was

measured at the beginning of a run. Corning B was analyzed at the beginning of a run and in between sample changes to check for precision, accuracy, and instrumental drift.

Isotopes of As, Sn, Zn, Pb, Ag, Sr, and Ba were analyzed using LA-ICP-MS were. Only Sn, As, Zn, Pb, and Ag are presented and discussed in this paper.

## RESULTS

The two glazes of this study were sampled from bridge-spouted vessels UPenn. 60-20-346, and UPenn. 63-5-64. Imaging in BSI mode reveals that the glazes contain numerous large vesicles and angular inclusions of quartz up to 200  $\mu\text{m}$  in the longest dimension. Imaging also shows that the glazes contain occasional inclusions of needle-shaped crystals of a tin phase (Figure 6.1), probably tin oxide, and rare calcium silicate crystals. In addition, the glazes are partially weathered. Other than these features, the glass matrices of the glazes appear to be chemically homogeneous. Electron microprobe imaging allowed unweathered areas to be specifically chosen for major and minor element analysis. The results yield compositions of about 64–67 wt%  $\text{SiO}_2$ , 12–17 wt%  $\text{Na}_2\text{O}$ , 6–4 wt%  $\text{CaO}$ , 3–4 wt%  $\text{K}_2\text{O}$ , and 1–2 wt%  $\text{MgO}$  (Table 6.1). The glazes also contain about 1.7–2 wt%  $\text{Al}_2\text{O}_3$ , 0.6–0.7 wt%  $\text{FeO}$ , 0.5–0.6 wt%  $\text{P}_2\text{O}_5$ , 0.8–1.2 wt%  $\text{Cl}$ , and small amounts of manganese and sulphur. Copper occurs at about 3–5 wt%  $\text{CuO}$ .

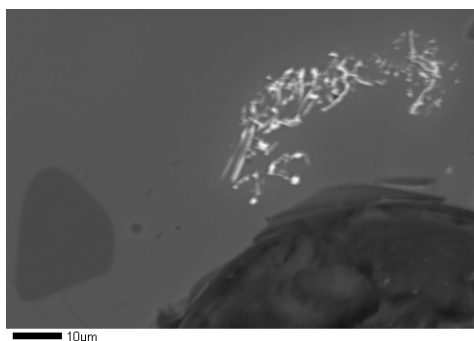


Fig 6.1. BSI image of blue glaze from a bridge-spouted vessel (UPenn. 60-20-346). The acicular crystal shapes of the tin-rich phase indicated that this phase formed in the glaze. The rounded inclusion in the lower left of the image is a quartz grain. Sample UPenn.63-5-64 contains similar inclusions. Scale bar is 10  $\mu\text{m}$ .

Table 6.1 Results of Microprobe and LA-ICP-MS Analyses (wt%)

microprobe data		SiO <sub>2</sub>	Al <sub>2</sub> O <sub>3</sub>	FeO	MnO	MgO	CaO	Na <sub>2</sub> O	K <sub>2</sub> O	Sb <sub>2</sub> O <sub>5</sub>	CuO	P <sub>2</sub> O <sub>5</sub>	SO <sub>3</sub>	Cl	
UPenn. #	n =														
60-20-346	avg	7	66.93	1.69	0.71	<0.3	1.32	6.21	12.46	4.09	0.31	3.14	0.50	0.35	0.75
	sd	7	3.02	0.47	0.21		0.23	1.09	0.71	0.15		0.45	0.12		0.15
63-5-64	avg	3	64.13	1.95	0.61	0.34	1.57	4.38	17.11	3.27	<0.3	4.95	0.56	0.35	1.16
	sd	3	0.98	0.08	0.12		0.02	0.20	0.34	0.15		0.26	0.13		0.11
LA-ICP-MS data		Zn66	As75	Ag107	Sn118	Pb208	Total (microprobe and LA-ICP-MS)								
UPenn. #															
60-20-346	nd	0.008	0.000	0.153	0.019		98.62								
63-5-64		0.037	0.006	0.001	0.142	0.088	100.63								

Average (avg) and standard deviation (sd) calculated for microprobe data only  
n: number of analyses used in the average and standard deviation  
Ti was sought by microprobe analysis but was not detected above 0.2 wt% TiO<sub>2</sub>  
nd: not detected

It was not possible to entirely avoid weathered areas during LA-ICP-MS analysis because of the need to collect a statistically useful number of counts. Some weathered areas in the glaze on sample UPenn. 63-5-64 were ablated in part of the analysis. Studies have shown that some minor ions and colouring compounds are not as profoundly affected by weathering as is sodium, which can decrease by almost 100% from its original value. The software used in the LA-ICP-MS analysis allows the operator to examine the data as a function of time. It is therefore possible to identify spikes or depletions in each element/isotope as the laser moved over the analysis area and associate those spikes or depletions with weathered areas. For this reason, it is believed that the trace element data presented for UPenn. 63-5-64 are of the same order of magnitude as in completely unweathered glaze. In the future, however, effort will be made to analyze only uncorroded areas for comparison to other published data.

Tin is present in both glazes at around 0.15 wt% Sn (Table 6.1). Zinc is present in only one glaze (UPenn. 63-5-64) at about 0.04 wt% Zn and may be associated with lead, which is higher in this sample at about 0.09 wt% Pb. Arsenic is lower than tin in both glazes, around 0.007 wt% As. Silver is below detection limits in one glaze and is very low at about 0.0006 wt% Ag in the other.

## DISCUSSION

The high levels of copper in the glazes indicate that they are coloured by copper, as  $\text{Cu}^{2+}$ , the most common colourant in 2<sup>nd</sup> and 1<sup>st</sup> millenium BC glasses and glazes. To determine the form in which the copper was added, arsenic, tin, zinc, lead, and iron, elements associated with copper in common ores, in metal alloys, and in slags from copper smelting and melting operations, were compared with copper. The average molar ratio of Cu:Fe in these glazes is 4:1 and 8:1, although individual analyses deviate from these ratios. The Cu:Fe ratios of the glazes are significantly higher than that for the common copper ore mineral chalcopyrite, which contains iron and has 1:1 Cu:Fe ratio. The low iron content of the glazes is considered to be a background amount, added to the glazes from the silica or alkali sources.

The glazes contain more tin than any of the blue glasses analyzed from Hasanlu. The tin phase seen in these glazes has not been found in any of the blue *glasses* from Hasanlu. The wt% ratios of Cu:Sn for these glazes is 1:0.04 and 1:0.08 which are about the same as for two bronze artifacts excavated from Hasanlu (snaffle bit, UPenn. 65-31-185; lion pin, UPenn. 61-5-182) which have Cu:Sn ratios of about 1:0.05 and 1:0.15 (de Schauensee, 1988). The As:Cu wt% ratio is 0.002 and 0.003, also comparable to that of the two analyzed bronzes from Hasanlu, which have As:Cu ratios of about 0.001 and 0.003. The relatively high tin and the proportion of tin to copper in the glazes suggests a relation to bronze, perhaps directly from bronze alloy. Pigott (1999) points out that tin bronzes with 5-12% tin were common in Iron Age Iran, although arsenic-bronzes and other arsenic-copper alloys were still in use in Iran at Tepe Yahya, for example (Thornton et al., 2002).

Fragments of fresh bronze metal could have been added to the glaze batch, as metallic copper will readily dissolve in alkali glazes. Bronze which had been roasted or pickled to form copper carbonate or to otherwise oxidise the metallic copper before

adding it to a glaze batch may have been more advantageous than copper alloy because it would have already been oxidised to  $\text{Cu}^{2+}$ .

## CONCLUSIONS

The colourant in the blue transparent glaze from two bridge-spouted vessels is  $\text{Cu}^{2+}$ . For the glazed, bridge-spouted vessels that are unique to Hasanlu, the source of the copper appears to have been derived from a manufactured metal alloy similar to bronze artefacts excavated from Hasanlu, rather than from a copper mineral or copper-bearing slag. The different amounts of lead, tin, arsenic, and copper, and the different Cu:Sn and Cu:As ratios of these two glazes suggest that the copper did not originate from the exactly the same piece of metal alloy. This is consistent with the bronze artefacts from Hasanlu, which also exhibit differences in their chemistry. It has not yet been possible to determine if fragments of fresh metal were added to the glaze batch, or if the metal was first roasted or pickled to oxidise the copper and then added to the batch.

While it was relatively straight-forward to identify the actual colouring agent in these glazes using instrumental analysis, the source of the colourant became apparent only after combining the chemical data with information from archaeological sources, an important collaboration for any archaeometrist.

CHAPTER 7.  
OXYGEN ISOTOPE ANALYSIS OF VITREOUS MATERIALS FROM PERIOD IVB  
HASANLU AND IMPLICATIONS FOR RAW MATERIAL IDENTIFICATION

---

Stapleton, C. P., Swanson, S. E., Valley, J. W., and Spicuzza, M. J.

To be submitted to *Archaeometry*.

## INTRODUCTION

There is considerable variation in the oxygen isotope ratios of archaeological glasses manufactured during the last four thousand years (Brill, 1970b). The oxygen isotope composition of a glass can be calculated from the oxygen isotope ratios of the raw materials that went into its manufacture. Brill (1970b; 1988a) and Brill et al., 1999) reported on a series of experimental glasses prepared using natron as the alkali source. The oxygen isotope compositions of the batch materials (natron, quartz sand) and the resulting glass were measured. Oxygen isotope compositions measured in the prepared glass correspond well with the predicted compositions based on batch materials. This study by Brill indicates that the oxygen isotope composition of batch materials are unchanged during the glass making process. To date, no similar studies are available using plant ash as the alkali source in the batch materials.

Throughout the Near East and Middle East, plant ash appears to have been the main source of alkali (sodium) for glass from the beginnings of glassmaking in the 3<sup>rd</sup> millennium BC until around the mid-1<sup>st</sup> millennium BC (Sayre, 1965; Moorey, 1999). Cuneiform texts on glassmaking that date to the 13th c BC and 7th c BC state that the ashes of the *naga* plant should be used to make glass (Oppenheim et al., 1970). Islamic glasses known to have been made with ashes of *salicornia*, which is a salt-tolerant plant, typically contain greater than about 1.5 wt% each of MgO and K<sub>2</sub>O (Brill, 1970a; Henderson, 2002; Freestone and Stapleton, 1998). Most glasses made prior to the mid-1<sup>st</sup> millennium BC are consistent with these compositional characteristics (Fig 7.1) and are believed to have been made with plant ash (Turner, 1956; Sayre, 1965). From the mid-1st millennium BC onward, glass that contains low MgO and K<sub>2</sub>O is commonly found in the archaeological record, sometimes alongside plant ash glasses. These glasses usually contain less than about 1 wt% each of MgO and K<sub>2</sub>O (Fig 7.1) and were probably made with a sodium-rich evaporite mineral such as natron (Na<sub>2</sub>CO<sub>3</sub> · 10H<sub>2</sub>O) (Turner,

1956; Brill, 1970a). Experimental glassmaking replications using quartz and either plant ash or natron as the sodium raw material corroborate the analyses of genuine ancient mineral-based glasses (Brill, 1988a).

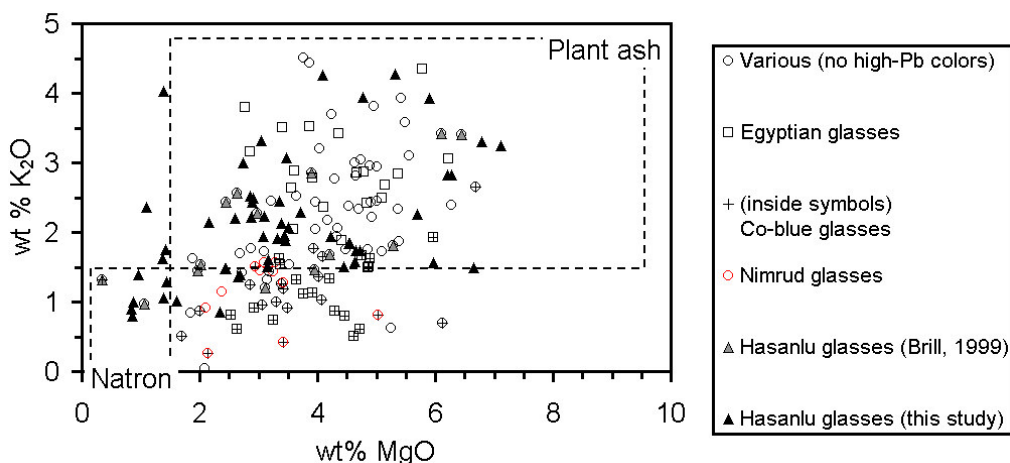


Fig 7.1. Selected glasses from the east Mediterranean and Near East made prior to the mid-1<sup>st</sup> millennium BC. Dashed lines enclose compositions typical of glasses made with plant ash or with natron and are based on analyses of glasses known to have been made with these materials (Brill, 1999). Most of the glasses with low K<sub>2</sub>O but high MgO (to the right of the “natron” box) are dark blue, colored by cobalt, and are suggested to have been made with natron and a high-MgO colorant (Shortland and Tite, 2000). High-lead glasses are not included.

Some 2<sup>nd</sup> and early 1<sup>st</sup> millennium BC glasses from regions where plant ash was traditionally used to make glass contain lower-than-expected MgO and K<sub>2</sub>O values, less than 1.5 wt% (Fig 7.1). Stapleton et al. (Chapter 8) propose that the low MgO-K<sub>2</sub>O glasses from Hasanlu were made not with natron, but with smaller proportions of plant ash, yielding glasses with lower levels of MgO and K<sub>2</sub>O. The scientifically excavated site of Hasanlu in northwestern Iran (Dyson, 1989a) offers a chance to study early 1<sup>st</sup> millennium BC plant ash glasses made and other technologically similar vitreous materials such as faience and ceramic glazes. A destruction layer at the Hasanlu site, Period IVB dated to the very end of the 9<sup>th</sup> c BC (Dyson and Muscarella, 1989), contains an abundance of vitreous artifacts. Faience found at Hasanlu is composed of quartz held together by a glass matrix and is typically composed of greater than 80 wt% SiO<sub>2</sub>.

The main raw material used to make both glass and faience is SiO<sub>2</sub>. This study presents results of oxygen isotope analyses from archaeological glass and faience from Hasanlu and results from modern experimental glass made with plant ash and quartz as part of this study. The purpose of this study is to determine the utility of oxygen isotopes in identifying raw materials used in manufacturing the vitreous materials found at Hasanlu.

#### SAMPLES AND ANALYTICAL PROCEDURE

Two experimental glasses, #6 and #7, were made using plant ash and quartz. The batch materials for the glasses were quartz from Spruce Pine, North Carolina and plant ashes from the collection of Dr. Robert H. Brill (Brill, 1999). The chemical compositions of the plant ashes used are described in Brill (1999), Table XXIV C, analysis 1326 (chinan, Iraq) in glass #6 and 1330 (tezab, Kandahar) in glass #7. The plant ash used in experimental glass #6 was acquired as dried plant in a souq in Baghdad (Brill, 1999). The plant was fired first in a slow burn, then held at temperatures between 700—900 C for 1—4 hrs. The ash used for glass #7 was bought by Robert H. Brill in 1968 in a soap shop in Kandahar, Afghanistan and was already a sintered mass when bought (Brill, 1999). Quartz was obtained from Zemex Minerals Corp. in Spruce Pine, North Carolina. The quartz is a first-stage separate from crushed granite and contains rare grains of epidote and garnet. Based on the reported bulk plant ash compositions and essentially pure quartz (100 wt% SiO<sub>2</sub>), mixes of ash and quartz were prepared to make glasses with theoretical compositions of 65 wt% SiO<sub>2</sub>. Both samples were placed in a cold furnace and ramped up at 2 C / minute to 1100 C, soaked for 10 hours at 1100 C, and then cooled by shutting off the furnace power. The furnace atmosphere was open to air. Experimental glasses were analyzed with the electron microprobe at the University of Georgia (analytical procedures are discussed in detail in Stapleton and Swanson, 2002a; Chapter 4). Imaging of the glasses using an electron

microscope showed that the glasses were homogeneous and that no immiscible phases were present.

Small samples of archaeological faience and glass from Hasanlu, northwestern Iran, were obtained from The University of Pennsylvania Museum of Archaeology and Anthropology in cooperation with Robert H. Dyson, Jr. and Maude de Schauensee. A group of faience vessels (UPenn. 65-31-299a) that had been fused together during manufacture were found at Hasanlu. It is unlikely that these vessels traveled far from where they were fired in the kiln, and thus were probably made at Hasanlu. A sample from one of these vessels was analyzed for oxygen isotope ratios and the result is used here as an example of what should be expected as the "local" oxygen isotope composition. In total, sixty-one samples from 56 archaeological artifacts were analyzed. In all, 11 blue transparent to translucent glasses, 12 black glasses, 7 blue opaque glasses, 1 white opaque glass, 29 faience bodies, and 1 thick surface glaze from a faience artifact were analyzed. Samples came from 21 glass beads, 6 glass hollow tubes, 9 faience beads, 14 faience vessels, 1 knobbed wall tile, 3 tubes (possibly from wall tiles), and 2 bosses (seals). Replicate analyses were carried out on ten samples. Using an optical microscope, unweathered areas of samples were selected for analysis. However, microprobe imaging demonstrates that some weathering occurs in most glass samples, and it is expected that the samples contained some weathered regions.

The samples were prepared and analyzed in the Stable Isotope Laboratory (SIL) at the Department of Geology and Geophysics, University of Wisconsin (Madison). All samples were crushed in a mortar and pestle with enough alcohol added to contain fragments as they splintered during crushing. The crushed sample was removed using a stainless steel scoop, placed in an oven and dried. The dried sample was then placed into a clean nickel cup reaction vessel and weighed. Between 1.1 mg and 2.5 mg of sample was used in each analysis. The prepared samples were stored in an oven until

analysis. The alcohol and oven preparation steps probably reduced the amount of free water in the samples, thus reducing the input of secondary water from weathering into the oxygen isotope analysis. Standards were prepared in the same way. Sample preparation techniques are also described in detail in Eisenheimer and Valley (1992) and Kohn et al. (1993).

For analysis, about 30 nickel reaction vessels filled with dried, crushed standards or samples are placed into an air-lock chamber and put under vacuum. In a separate compartment for fluorination, one sample is put into a holder and  $\text{BrF}_5$  is introduced into the compartment and is heated with a 10.6  $\mu\text{m}$  IR laser to evolved oxygen. During heating, the sample sinters and forms into a sphere, then becomes almost completely volatilized under the heat of the laser. Usually, some sample remains un-volatilized in the reaction vessel, probably highly refractory components such as  $\text{CaF}_2$  (Valley et al., 1995). The oxygen evolved is sent through a conventional oxygen isotope analysis line and converted to  $\text{CO}_2$ . The analytical procedures and the experimental derivation of the analytical accuracy and precision for this procedure are described in detail in Valley et al. (1995) and Spicuzza et al. (1998). The standard used was UWG-2, a powdered single garnet prophyroblast prepared by the University of Wisconsin SIL with a recommended  $\delta^{18}\text{O}$  of 5.8 ‰ (Valley et al., 1995). Five analyses of between 1.6 mg and 2.5 mg of standard UWG-2 were analyzed at the beginning of each day, which was also the beginning of each run. To account for memory effects, the first standard analysis of each day was not included in the standardization. The precision of the standard analyses is better than about  $\pm 0.10$  ‰. Replicate analyses on archaeological materials yielded errors of 0.02—0.23 ‰.

Samples available for oxygen isotope analysis from 5 artifacts were limited and weighed less than optimum, between 0.4 mg and 1 mg each. Analyses of 1.0 mg to 0.4

mg of standard UWG-2 were run before analysis of these low-weight samples. All five of the standards analyses were used in the standardization for the low-weight samples.

## RESULTS

Oxygen isotope analyses are reported in Table 7.1 in per mil (‰) relative to SMOW. Archaeological samples are grouped by type of material and secondly by color (blue tp-tl glass, blue opaque glass, white glass, blue glaze on faience, faience).

Table 7.1. Oxygen Isotope Ratios of Vitreous Materials from Hasanlu

Object	UPenn. Sample #	Sample wt. (mg)	<i>n</i>	$\delta^{18}\text{O}$ (‰) SMOW	stddev*
<i>Black glasses</i>					
bead	75-29-307a	1.7		16.2	
bead	61-5-95c	1.6		13.5	
bead	73-5-350a	2.6		14.1	
bead	65-31-247a	2.30		13.8	
bead	63-5-280a	0.8		12.8	
bead	73-5-305a	0.8		13.2	
<b>bead</b>	<b>63-5-269a</b>	<b>1.73</b>	<b>3</b>	<b>14.9</b>	<b>0.2</b>
bead	58-4-61b	1.22		12.3	
<b>bead</b>	<b>61-5-89h3</b>	<b>1.85</b>	<b>2</b>	<b>15.9</b>	<b>0.02</b>
bead	65-31-396g	2.7		14.2	
bead	65-31-396h	1.6		14.2	
<i>Blue transparent-translucent glasses (blue tp-tl)</i>					
bead	75-29-199a	2.5		17.3	
bead	73-5-559e	1.8		15.6	
<b>bead</b>	<b>65-31-396d</b>	<b>1.8</b>	<b>2</b>	<b>15.7</b>	<b>0.2</b>
bead	63-5-280a	1.5		17.3	
<b>bead</b>	<b>73-5-559c</b>	<b>1.7</b>	<b>2</b>	<b>15.0</b>	<b>0.1</b>
bead	73-5-350b	1.7		14.1	
bead	73-5-293b	2.0		14.1	
bead	65-31-273a	1.6		13.7	
bead	75-29-307a	2.2		13.9	
<b>bead</b>	<b>65-31-267a</b>	<b>2.2</b>	<b>3</b>	<b>14.8</b>	<b>0.2</b>
bead	63-5-270a	2.5		14.7	
<i>Blue opaque (turquoise) glasses</i>					
hollow tube	65-31-280	2.3		15.3	
hollow tube	65-31-728e	2.1		14.4	
hollow tube	65-31-728f	0.4		12.7	
hollow tube	65-31-283	0.4		14.0	
hollow tube	65-31-993	1.6		14.8	
hollow tube	73-5-782	1.5		15.1	
<b>bead</b>	<b>73-5-781</b>	<b>1.6</b>	<b>2</b>	<b>17.1</b>	<b>0.1</b>

Table 7.1. Continued

Object	UPenn. Sample #	Sample wt. (mg)	<i>n</i>	$\delta^{18}\text{O}$ (‰) SMOW	stddev*
<i>White opaque glass</i>					
bead	73-5-559e	2.4		14.3	
<i>Faience glaze blue transparent (tp)</i>					
faience: boss (one half)	61-5-924	1.1		13.8	
<i>Faience</i>					
<b>bead barrel</b>	<b>65-31-396b</b>	<b>2.2</b>	<b>2</b>	<b>10.7</b>	<b>0.2</b>
boss w/incised lines, circles	59-4-86	2.3		11.7	
vessel, sherd	71-23-610	2.2		12.1	
carved sherd	73-5-276	1.0		12.9	
<b>jar neck</b>	<b>75-29-439</b>	<b>1.9</b>	<b>2</b>	<b>13.1</b>	<b>0.1</b>
carved sherd	59-4-52	1.9		13.4	
jar neck sherd	60-20-345	2.5		13.5	
bead w/incised lines	61-5-89h4	1.7		13.6	
boss (one half)	61-5-924	1.7		13.6	
vessel(?) frag	75-29-348	1.7		13.9	
bead crosshatch	73-5-296a	2.1		13.9	
tube, wall tile(?) frag	61-5-53	2.1		14.0	
vessel	60-20-342	2.3		14.1	
sherd	73-5-785	2.4		14.2	
footed vessel	71-23-609	2.3		14.3	
sherd	75-29-788	1.7		14.4	
vessel	65-31-96	2.0		14.7	
bead, rectangular	61-23-198a	2.5		14.7	
bead, barrel	65-31-396c	1.5		14.7	
vessel frag	60-20-341	2.4		15.2	
bead crosshatch, tube	75-29-271a	1.8		15.4	
bead	65-31-728d	2.0		15.9	
over-fired vessels	65-31-299a	1.6		16.2	
bead w/cross hatch design	65-31-396a	2.0		16.2	
cylindrical object, sherd of	73-5-220	nr		18.1	
dish frag, incised	61-5-923	2.5		18.2	
wall tile knob?	61-5-55	1.9		18.2	
cylinder frag	65-31-99	2.5		18.4	
fluted bowl, sherd	61-5-896	1.7		18.9	
<i>Experimental Glasses</i>					
Run 6 glass (#6)		2.4		10.3	
Run 7 glass (#7)		2.1		10.5	
<i>Spruce Pine Quartz</i>					
Split 2		nr		11.3	
Split 1		nr		11.4	

\*Data in **bold** are averages of *n* repeat analyses. \*\*stddev: standard deviation of averaged data. See text for discussion of analytical technique, accuracy and precision. Tp-tl: transparent-translucent; turq opq: turquoise opaque (blue opaque) frag:fragment.

## Experimental Glasses #6 and #7 and Spruce Pine quartz

Analysis of the two samples of Spruce Pine quartz yielded 11.3 ‰ and 11.4 ‰ (Table 7.1). The  $\delta^{18}\text{O}$  values of the two experimental glasses, #6 and #7 made with Spruce Pine quartz, are 10.3 ‰ and 10.5 ‰, respectively (Table 7.1).

## Archaeological samples

The  $\delta^{18}\text{O}$  values of the Hasanlu glasses range from 12.3 ‰ to 17.3 ‰ while the faience artifacts have a wider range from 10.5 ‰ to 18.9 ‰ (Table 7.1). The single faience glaze analyzed (blue transparent, UPenn. 61-5-924) has a  $\delta^{18}\text{O}$  value of 13.8 ‰ (Table 7.1). The  $\delta^{18}\text{O}$  values for three of the four low-weight ( $\leq 1$  mg) glass samples are lower than most of the other glass samples (Fig 7.2). One other glass sample that weighed less than 1.5 mg (UPenn. 58-4-61b, 1.22 g), also has a low  $\delta^{18}\text{O}$  value, 12.3 ‰. The one faience sample that weighed less than 1.5 mg (UPenn. 73-5-276, 1 mg) has low  $\delta^{18}\text{O}$ , 12.9 ‰, relative to most other faience samples. These results may suggest that samples of low weight yielded low oxygen isotope ratios. However, experience at the Wisconsin SIL has demonstrated that analyses of samples of less than 1.5 mg show no statistically significant difference from those of greater weight (Fig 3, Valley et al., 1995).

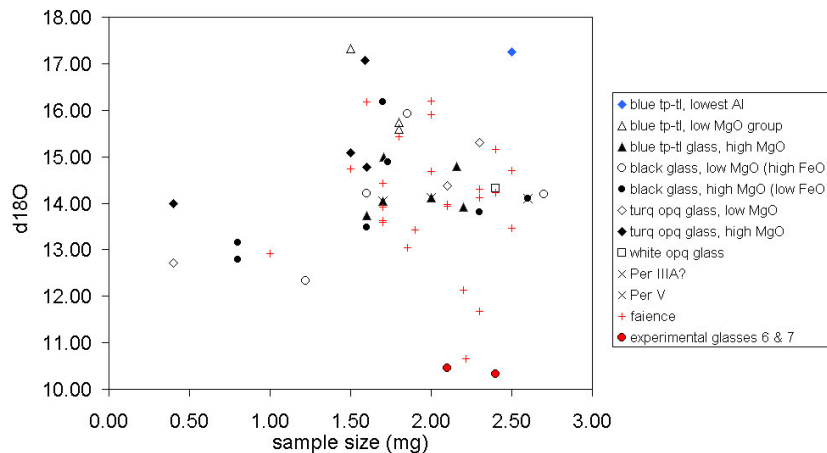


Fig 7.2.  $\delta^{18}\text{O}$  ratios as a function of sample weight.

The  $\delta^{18}\text{O}$  ratios do not seem to be affected by  $\text{CO}_2$  yield. The amount of oxygen evolved from a sample is measured by the instrument, once the oxygen has been converted to  $\text{CO}_2$ , as  $\mu\text{mols CO}_2$ . The proportion of  $\mu\text{mols CO}_2$  to sample weight, the  $\text{CO}_2$  yield, is a measurement of the amount of oxygen evolved from a sample from laser heating. If oxygen fractionation occurs during lasing, then samples that evolve less oxygen (low  $\text{CO}_2$  yield) would contain a greater proportion of the lighter oxygen isotope and have low  $\delta^{18}\text{O}$  values. This not true for the Hasanlu data, indicating that no fractionation of oxygen occurred during lasing of these archaeological samples (Fig 7.3).

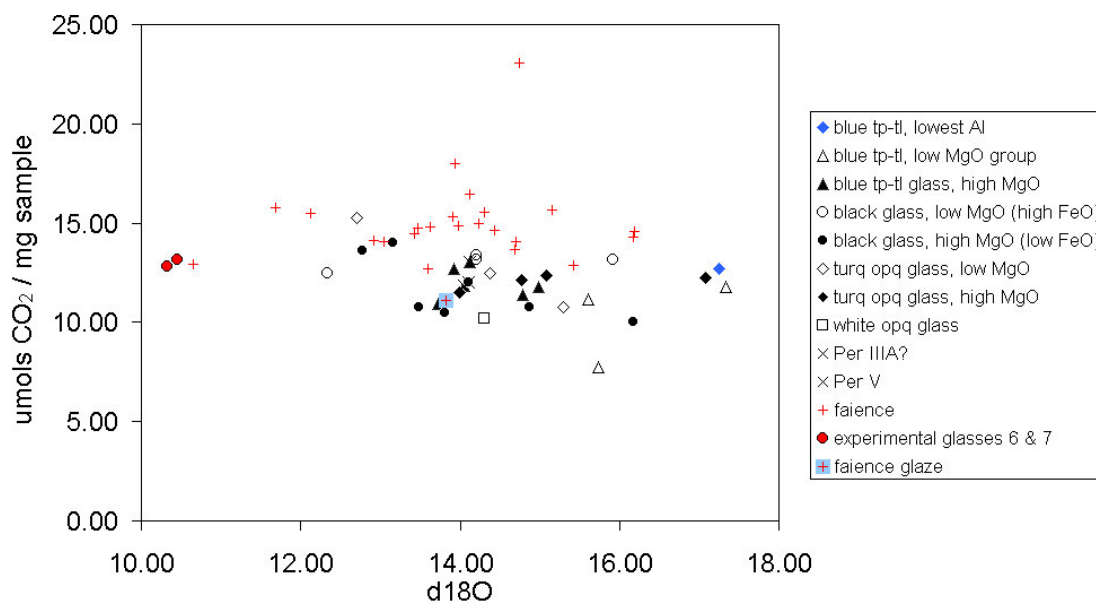


Fig 7.3. Relationship between  $\delta^{18}\text{O}$  and oxygen evolved, represented by  $\text{CO}_2$  yield ( $\mu\text{mols CO}_2 / \text{mg sample}$ ).

## DISCUSSION

### Contribution of Plant Ash to $\delta^{18}\text{O}$ Value of Manufactured Glass

Burning plants to concentrate sodium requires that a low enough temperature be maintained during ashing so that sodium is not volatilized. In the early 1970's, R. H. Brill documented glassmaking in a traditional workshop in Herat, Afghanistan (Brill, 1972b). In this glassmaking industry, craftsmen who supply sodium-rich plant ash to

glassmakers and soapmakers carry out ashing of plants in a covered hole dug into the ground. Whole plants are broken down and placed into the hole. A slow-burning, smoky fire is started on the plants and the hole is covered loosely with dirt and other material. Combustion occurs via reaction with oxygen, mainly from the atmosphere, which suggests that atmospheric oxygen becomes part of the raw material added to glassmaking batches. Organic phases combust yielding CO, CO<sub>2</sub>, and H<sub>2</sub>O. Alkali and alkaline earth elements exist as basic oxides in tree wood (Blander, 1998). Ashes of the salt-rich desert plants used in manufacturing ancient glasses typically contain mostly Na<sub>2</sub>CO<sub>3</sub>, with smaller amounts of CaCO<sub>3</sub>, MgCO<sub>3</sub>, KCl and K<sub>2</sub>SO<sub>4</sub> along with other chlorides, sulfates, sulfites, and phosphates (Turner, 1956). X-ray diffraction analysis of the ash used in experimental glass #7 (1330) shows the presence of Na<sub>2</sub>CO<sub>3</sub>, Na<sub>3</sub>H(CO<sub>3</sub>)<sub>2</sub>·2(H<sub>2</sub>O)<sub>2</sub>, Na<sub>2</sub>Ca(CO<sub>3</sub>)<sub>2</sub>, MgO, MgCO<sub>3</sub>, KHCO<sub>3</sub>, CaO<sub>4</sub>, and NaCl.

In basic glassmaking procedures, batch materials consisting of plant ash and quartz are mixed together and then heated in a furnace. At temperatures less than 600 C, the initial reactions are solid state reactions, mainly dissociation of carbonate phases and slow reaction between SiO<sub>2</sub> and Na<sub>2</sub>CO<sub>3</sub>. Solid state reactions continue at greater rates as batch temperature increases until about 800-900 C is reached. Melting of SiO<sub>2</sub> + Na<sub>2</sub>O starts in the range of 800 C to 900 C, depending on the batch composition. With increasing temperature, the range of melt compositions expands and incorporates CaO and MgO. Sulfate and chloride form a melt that is immiscible in silicate melts and may rise to the surface of the silica-rich melt to form a layer of *gall*. The CO<sub>2</sub> from dissociation of carbonate phases is only slightly soluble in the silica-rich melt and most of the CO<sub>2</sub> escapes from the melt as a gas. The high temperatures at which these processes take place suggests that no fractionation of oxygen occurs during firing of the batch materials (Faure, 1986).

For experimental glasses #6 and #7, theoretical oxygen isotope compositions of the plant ashes were calculated from the  $\delta^{18}\text{O}$  values measured from quartz (11.3 ‰) and glass (#6: 10.3 ‰; #7: 10.5 ‰). It was assumed that no oxygen isotope fractionation took place during glassmaking, and that dissociation of the carbonates was complete before melting began. It was also assumed that no oxygen fractionation occurred after the silicate melt formed, a possibility suggested by slow oxygen diffusion rates in rhyolitic and soda-lime-silica melts (Table 1, Cole and Ohmoto, 1986). Using a linear mass balance mixing model (Phillips and Koch, 2002), theoretical  $\delta^{18}\text{O}$  values for the two plant ashes were calculated:

$$\delta^{18}\text{O}_{\text{glass}} = f_{\text{quartz}} (\delta^{18}\text{O}_{\text{quartz}}) + f_{\text{plant ash}} (\delta^{18}\text{O}_{\text{plant ash}}),$$

where “f” is the molar fraction of oxygen in the samples of quartz and plant ash used to make the experimental glasses. Chemical compositions of the plant ashes are reported in Brill (1999, Table XXIV C).  $\text{CO}_2$  reported in the plant ash was not included in the oxygen mole fraction calculations because of the assumption of complete carbonate dissociation before melting. Additionally, the mole sum of oxygen in the quartz and ash (without  $\text{CO}_2$ ) used in the experiments more closely matched the molar quantity of oxygen in each glass. Given the  $\delta^{18}\text{O}$  values of experimental glasses #6 and #7 and the two splits from the sample of Spruce Pine quartz used to make these experimental glasses, the plant ash  $\delta^{18}\text{O}$  for glasses #6 and #7 was about 7.0 ‰ and 7.5 ‰, respectively. These  $\delta^{18}\text{O}$  results calculated for the plant ashes are about 15 ‰ lower than atmospheric  $\delta^{18}\text{O}$  values (Ehleringer and Cerling, 2002), suggesting that the oxygen in the plant ashes did not come from atmospheric oxygen added during combustion. Calculations were carried out to test the sensitivity of the  $\delta^{18}\text{O}$  of the

finished glass to changes in the proportions of the raw materials used. Fig 7.4 shows that for glass made with different proportions of the same quartz and plant ash used to make glass #6, the glass will closely reflect the  $\delta^{18}\text{O}$  of the silica, which may be pure quartz, sand or other  $\text{SiO}_2$ -bearing material. The figure demonstrates that this does not hold true if the  $\delta^{18}\text{O}$  of the plant ash is greatly different from that of the silica source. Laboratory analysis of the plant ashes should be carried out to resolve the relationships between  $\delta^{18}\text{O}$  in this raw material and the finished glass.

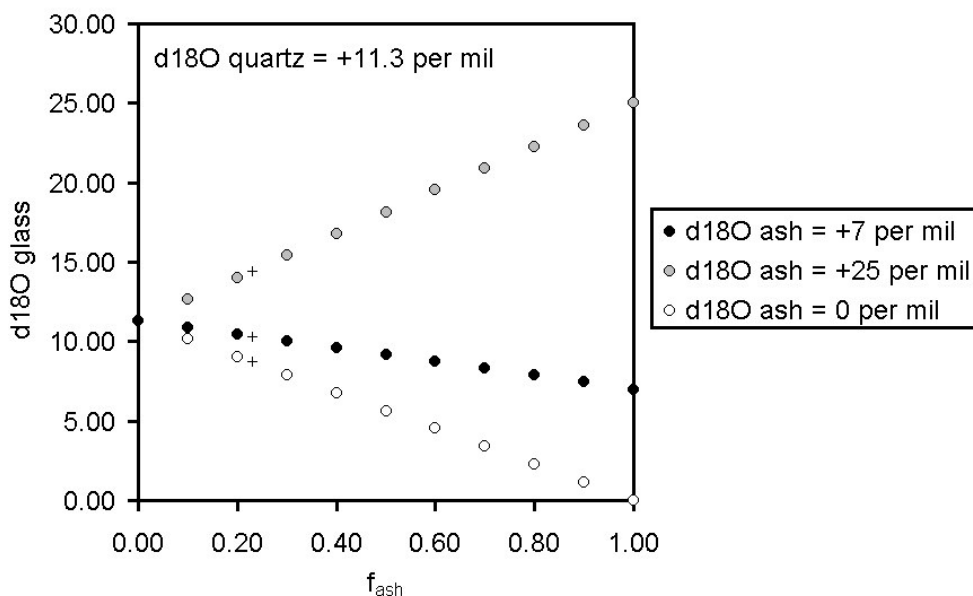


Fig 7.4. Calculated  $\delta^{18}\text{O}$  of glasses made with the same quartz but different plant ash as used for experimental glass #6. Black dots represent glass made with the same quartz and same plant ash as experimental glass #6. Crosses represent glasses made with the same proportions of plant ash and quartz as used for experimental glass #6.

### Effects of Weathering on Oxygen Isotope Compositions of Archaeological Glass

Weathered areas are present in most of the archaeological vitreous samples from Hasanlu, and even careful sampling using light microscopy cannot guarantee bulk samples completely free of weathered glass. The affect of weathering on the oxygen isotope analyses must be addressed because of the bulk samples used in the oxygen

isotope analyses. High alkali glasses usually weather initially by exchange of  $\text{Na}^+$  with  $\text{H}^+$  (or possibly  $\text{H}_3\text{O}^+$ ) from water (White, 1983; Newton, 1989). Subsequently, the silica network breaks down in hydrolysis reactions and a silica gel is formed, allowing water molecules to move freely in and out of the open network. This type of weathering can change the bulk oxygen isotope composition of the now-weathered glass. The top of the mound of Hasanlu is about 25 m above the valley floor, and all of the archaeological material described in this study was excavated from above the valley floor (Dyson, 1989a). Thus, the glasses would have been in contact only with meteoric water that had interacted with the soil of the mound. The climate around Hasanlu is dry with average annual precipitation around 300 mm, with rain occurring mostly in storms in the winter and spring. The average annual temperature is about 13 C, and ranges from about  $-5$  C to 33 C (Voigt, 1977).

For the Hasanlu vitreous materials, oxygen isotope ratios of the weathered areas may be a simple mix of original oxygen in the glass plus oxygen added from meteoric water. However, oxygen may have fractionated between meteoric water and glass. A 1.0245 fractionation factor between albitic glass and water may be used to calculate oxygen isotope composition of the weathered silicate glass (Taylor, 1968). The oxygen isotope ratio of regional meteoric water is probably around  $-11$  ‰, estimated from the average value of water from rivers that feed Lake Van in eastern Turkey, a region with similar climate to the Lake Urmia area (Faber, 1978). The  $\delta^{18}\text{O}$  of weathered glass from Hasanlu is calculated using a linear mass balance mixing model (Phillips and Koch, 2002):

$$\delta^{18}\text{O}_{\text{weathered glass}} = f_{\text{unweathered glass}} (\delta^{18}\text{O}_{\text{unweathered glass}}) + f_{\text{water}} (\delta^{18}\text{O}_{\text{water}}),$$

where “f” is the molar fraction of oxygen in unweathered glass and in the water of hydration. Assuming a simple mixing of glass and water, with no fractionation of oxygen, and an original  $\delta^{18}\text{O}$  value for unweathered glass of 14 ‰, a weathered glass that had 1 wt%  $\text{H}_2\text{O}$  added would have a  $\delta^{18}\text{O}$  ratio of 12.9 ‰, and a weathered glass with 20 wt%  $\text{H}_2\text{O}$  added would have a  $\delta^{18}\text{O}$  ratio of 1.9 ‰. Such large differences are not seen in the Hasanlu data. Assuming that fractionation of oxygen between water and glass took place, with -11 ‰ for water, the  $\delta^{18}\text{O}$  value of weathered glass would be about 13.7 ‰ (Fig 7, Taylor, 1968), suggesting that weathering did not cause large enough changes in the  $\delta^{18}\text{O}$  ratios to match the range of oxygen isotope values measured in the Hasanlu glasses presented here.

### **Possible Silica Sources for the Hasanlu Archaeological Samples**

The wide range in chemical compositions of the Hasanlu glasses (Tables 4.2, 5.1, and 8.1) are probably the result of the use of different proportions of the same batch materials or the use of different batch materials, including different host materials for colorants (Stapleton et al., Chapter 8). The oxygen isotope compositions of from 12.1 to 17.3 ‰ appear to echo this range in batch materials. All of the  $\delta^{18}\text{O}$  ratios of this study are shown in Fig 7.5. Most of the glass samples have  $\delta^{18}\text{O}$  ratios that fall between 13.5 ‰ and 16.2 ‰. Two blue transparent and one blue (turquoise) opaque glasses have heavier  $\delta^{18}\text{O}$  ratios, 17.1—17.3 ‰. Most of the faience samples have  $\delta^{18}\text{O}$  ratios of 13.4—16.2 ‰, similar to most of the glasses. Three faience samples have heavier  $\delta^{18}\text{O}$ , 18.1—18.9 ‰, and five are lighter, 10.7—13.1 ‰. The sample taken from the overfired, faience vessels (UPenn. 65-31-299a), has a  $\delta^{18}\text{O}$  of 16.2 ‰.

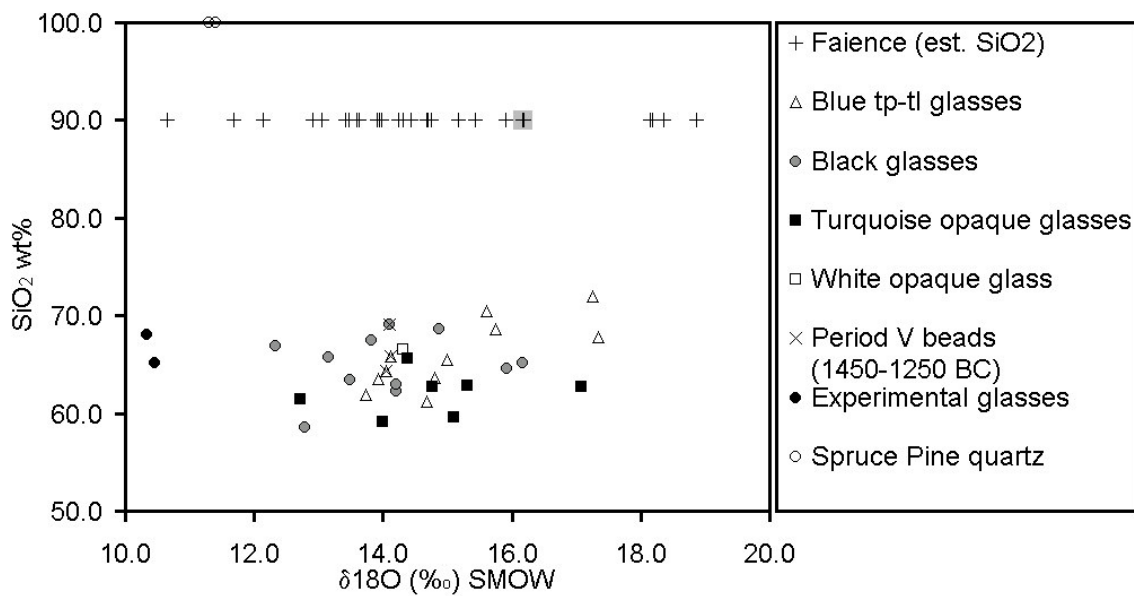


Fig 7.5. Oxygen isotope analyses for faience and glass samples. Black cross in gray box is sample from overfired faience vessels, which may represent locally-made objects. Bulk SiO<sub>2</sub> of faience is estimated from analyses of typical faience.

If one source of pure SiO<sub>2</sub> was used to make all of the Hasanlu glasses presented here, then the  $\delta^{18}\text{O}$  of this hypothetical SiO<sub>2</sub> would be about 50.9 ‰, calculated by fitting a line through all of the glass data and projecting to 100 wt% SiO<sub>2</sub> (Fig 7.6). If the glasses were a simple two-component mix of silica plus alkali, then the alkali would have had a  $\delta^{18}\text{O}$  of -51.8 ‰. A two-component batch is unlikely for the Hasanlu glasses because of the addition of coloring agents (Stapleton et al., Chapter 8), and the values calculated for one source of pure SiO<sub>2</sub> and one alkali source are probably unrealistic. Fitting a line through the experimental glasses #6 and #7 and Spruce Pine quartz, the plant ashes used in these experiments are calculated to have  $\delta^{18}\text{O}$  of about 8.1 ‰ and 8.8 ‰, respectively, shown as an average of 8.4 ‰ in Fig 7.6. These  $\delta^{18}\text{O}$  values are about 0.6–1.8 ‰ greater than those calculated for the plant ashes using molar fractions of oxygen in Spruce Pine quartz, experimental glasses #6 and #7.

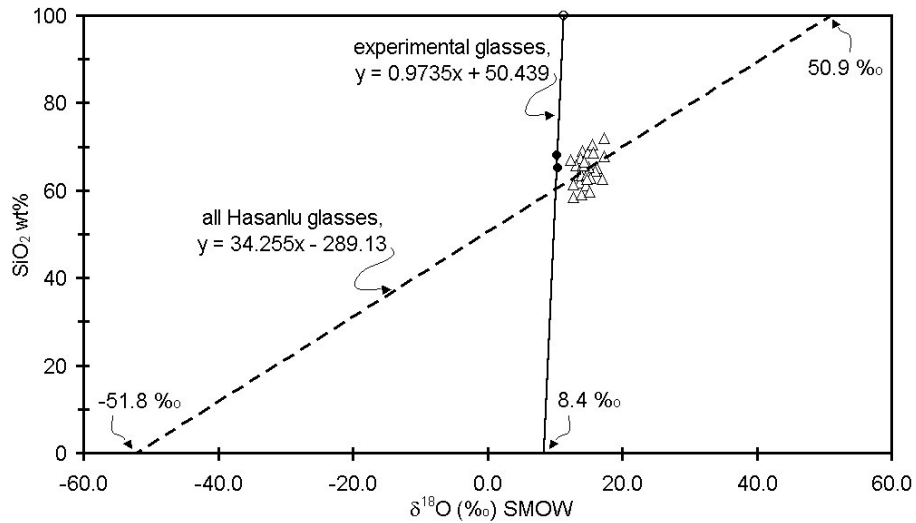


Fig 7.6. End member  $\delta^{18}\text{O}$  compositions calculated for the Hasanlu glasses, assuming one source of pure  $\text{SiO}_2$  was used to make the glasses. Dashed line drawn through the Hasanlu glass data is fitted using least squares regression analysis. Solid line is fitted through the experimental glasses #6 and #7 and the pure silica source used to make them (Spruce Pine quartz).

The  $\delta^{18}\text{O}$  results of experimental glasses #6 and #7 and the quartz used to make them suggest that the oxygen isotope composition of glass produced from plant ash and quartz should be closely related to that of the silica source, which is the major component in ancient glasses. The difference in  $\delta^{18}\text{O}$  between the quartz and the glasses is about 0.8—1.1 ‰. Natron-based glasses also seem to mostly reflect their silica source, but differ from it by about 3 ‰ (Brill et al., 1999). If the glasses and faience from Hasanlu closely reflect their silica source, then geologic silica deposits with  $\delta^{18}\text{O}$  values of around 12—16 ‰, assuming about 1 ‰ difference from the silica, can be sought as the silica source for most of the glass and faience samples. Biogenic deposits such as chert have very high  $\delta^{18}\text{O}$  values and may be ruled out as the main source of silica. Quartzite and arkose can have high  $\delta^{18}\text{O}$  values (Taylor et al., 1986), comparable to those of the Hasanlu vitreous materials. These rocks, however, were not likely to have been used in glassmaking because of the difficulty in mining hard quartzite, and because of the problems of melting a high aluminum arkose. Quartz

derived from rocks that have been hydrothermally altered by surface water interaction tend to have low  $\delta^{18}\text{O}$  ratios because of equilibration with low  $\delta^{18}\text{O}$  meteoric water and groundwater, which can have oxygen isotope ratios less than SMOW. Anorogenic granites, and the quartz in them, generally also have lower  $\delta^{18}\text{O}$  values, 6—9 ‰ (Sheppard 1986). Peraluminous, S-type granites usually have  $\delta^{18}\text{O}$  ratios larger than about 10 ‰ (Sheppard 1986), and are a possible quartz source for Hasanlu materials. Weathered sediments can have enriched  $\delta^{18}\text{O}$  from low-temperature, diagenetic alteration and overgrowths on detrital grains. The quartz in such sediments can have a wide range of  $\delta^{18}\text{O}$  depending on the original  $\delta^{18}\text{O}$  composition, extent of weathering,  $\delta^{18}\text{O}$  composition of the water of alteration, and the temperature at which alteration took place.

Inclusions in the glasses from Hasanlu include alkali feldspars, plagioclase, and quartz. The faience is comprised mostly of quartz but also contains trace amounts (less than 1%) of potassium feldspar and iron oxides. The inclusions in the glass and faience bodies suggest that the silica source came from a deposit that included felsic igneous rocks, consistent with the oxygen isotope values for most of the glasses from Hasanlu. It is suggested that the source of the quartz was a sand composed mainly of material weathered from an granitic rocks. The Ushnu-Solduz Valley in which Hasanlu sits is surrounded by Cenozoic limestone (Qom Formation), Permian and Cretaceous undifferentiated limestone and dolomite, Cretaceous ophiolitic deposits, post-Cretaceous intrusive granodiorites, and undifferentiated Precambrian metamorphic rocks. In Iran, the closest granite bodies are the Cambrian Doran Granite about 40 km southwest of Hasanlu, which is associated with undifferentiated Precambrian metamorphic rocks. No  $\delta^{18}\text{O}$  analyses of the granitic or other rocks from this area are known to this author.

## Using $\delta^{18}\text{O}$ to Identify Possible Glassmaking Batch Constituents of Some Hasanlu Glasses

Fourteen of the blue transparent to translucent glasses can be divided into two chemical groups based on MgO content, < 2 wt% and > 2 wt% MgO. Based on the chemical analyses, the glassmaking batch of four glasses in the low MgO group is posited to have contained quartz, altered feldspar or muscovite, as well as plant ash, as the major constituents (Stapleton et al., Chapter 8). The high MgO group appears to have been made with quartz and plant ash, but with no other major components. The colorant in both groups was probably added as crushed copper sulfide mineral, possibly roasted to a sulfate before addition to the batch. The  $\delta^{18}\text{O}$  ratios of blue tp-tl glasses from the low MgO and high MgO groups are different (Fig 7.7), corroborating the use of different mixes of batch materials for these groups. However, neither group has a constant  $\delta^{18}\text{O}$ :oxide weight% ratio for all samples analyzed, and the samples in either group do not show straight-line, simple mixing between two end members.

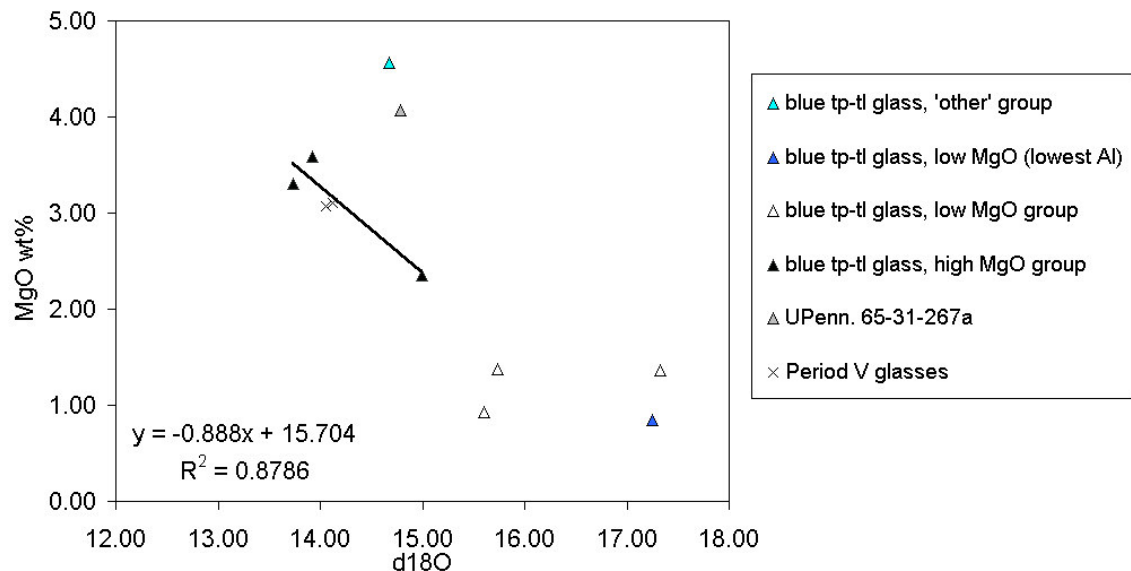


Fig 7.7. Blue tp-tl glasses fall into two broad groups based on MgO content. Sample with the lowest MgO also contains the lowest  $\text{Al}_2\text{O}_3$ , has a generally different chemistry than the remainder of the low MgO group, and is believed to have been made with different materials or different proportions of materials. Solid line is a least squares regression fitted through the 3 data points that represent the high MgO group.

The results from Fig 7.7 suggest that the glasses should be further subdivided and the identity of the batch materials reconsidered. Three blue tp-tl glasses in the high MgO group were examined as one subgroup that appears to have linear correlations between  $\delta^{18}\text{O}$  and  $\text{SiO}_2$  ( $R^2=0.90$ ),  $\text{Al}_2\text{O}_3$  ( $R^2=0.99$ ),  $\text{MgO}$  ( $R^2=0.88$ ), and  $\text{K}_2\text{O}$  ( $R^2=0.59$ ), but not between  $\text{SiO}_2$  and  $\text{Na}_2\text{O}$  (Figs 7.7 and 7.8). If it is assumed that sediment from a weathered granitic rock, composed of 70 wt%  $\text{SiO}_2$ , was used to make these three glasses then this weathered sediment would have had a  $\delta^{18}\text{O}$  of about 16.8‰. If this  $\delta^{18}\text{O}$  value is used in the regression lines for  $\text{Al}_2\text{O}_3$ ,  $\text{MgO}$ , and  $\text{K}_2\text{O}$  (Figs 7.7 and 7.8), the weathered material would have contained about 3.7 wt%  $\text{Al}_2\text{O}_3$ , 0.8 wt%  $\text{MgO}$ , and 0.7 wt%  $\text{K}_2\text{O}$ . The values calculated for these oxides are reasonable for sediment from weathered rock, but sediments produced by weathering can have a huge range in chemical composition and the values do not represent all weathered granitic rock.

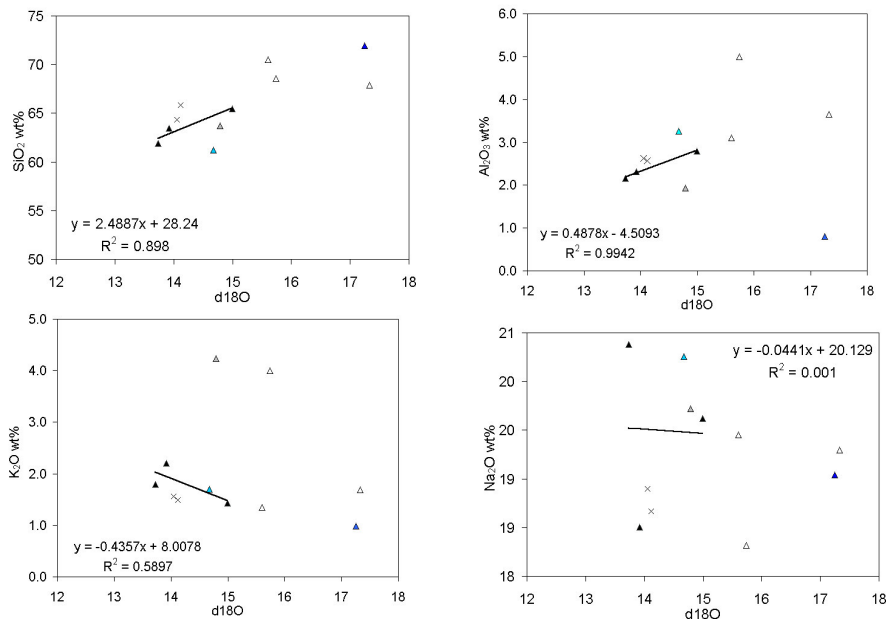


Fig 7.8. Correlations between  $\delta^{18}\text{O}$  and  $\text{SiO}_2$ ,  $\text{Al}_2\text{O}_3$ ,  $\text{K}_2\text{O}$ , and  $\text{Na}_2\text{O}$ , major oxides in granitic rocks. Symbols same as in Fig 7.7.

Many of the glasses from Hasanlu contain partly reacted batch materials and phases that crystallized from the glass melt, “devitrification” in glassmaking terms (Stapleton and Swanson, 2002a; Chapter 4). These heterogeneities may influence the bulk  $\delta^{18}\text{O}$  of the glass. Heterogeneities in glass have been shown to affect the oxygen isotope composition of manufactured glass. A failed Roman glass melt, currently *in situ* in a glassmaking tank furnace, has a range of  $\delta^{18}\text{O}$  values from 13.35 ‰ to 14.16 ‰ (Brill, 1999). The oxygen isotope differences correlate to differences in color and mineralogy in the glass, which was probably produced during experimentation by mixing plant ash and natron with local sand (Brill and Wosinski, 1965; Brill, 1967; Freestone and Gorin-Rosen, 1999).

#### **Comparison of Glasses from Hasanlu Period V**

In the high MgO group of blue transparent to translucent glasses, there are two samples from beads from the same excavation context and dated to about 1450-1250 BC, Period V. These two samples are chemically very similar and both contain rounded inclusions of spinel, which is not found in any of the other glasses. It seems likely that these two beads were made with glass from similar batch materials, perhaps in the same glassmaking workshop or even from the same glass melt. The two beads have the same  $\delta^{18}\text{O}$  ratio, 14.1 ‰, consistent with an origin of the glass from the same batch materials or same glass melt. Black glass from one other bead (UPenn. 73-5-350a) from Period V was analyzed and also yielded an oxygen isotope value of 14.1 ‰, the same as glass from the two blue Period V beads. These three analyses hint at homogeneity in the quartz source for Period V glasses, but more samples from this Period should be analyzed before any conclusions are drawn.

## CONCLUSIONS

Oxygen isotope analyses of vitreous materials from Hasanlu 11-9<sup>th</sup> c BC yield a wide range (12.3—17.3 ‰) of oxygen isotope ratios. The range is probably not an affect of weathering. At other archaeological sites, a wide variety of oxygen isotope compositions occurs when there are groups of glasses made with different raw materials. At Amarna in Egypt, copper-colored glasses, suggested to have been made with quartz and plant ash (Shortland and Tite, 2000) have oxygen isotope ratios of 15.12 ‰ to 16.0 ‰ (Brill, 1999), whereas glasses possibly made with quartz and natron have ratios of 16.89 ‰ and 17.46 ‰ (Brill, 1999, 2 cobalt blue glasses). Medieval glasses from the cathedral at Zerek Camii, Turkey probably made using plant ash have  $\delta^{18}\text{O}$  values of 12.18 ‰ to 12.87 ‰, and natron type glass yields 16.20 ‰. Brill (1999) also gives examples of Islamic glasses, three plant ash types and one natron type, the latter of which has higher  $\delta^{18}\text{O}$ , and of two stained glass windows from Rust, Austria that differ in chemical composition and in oxygen isotope composition. The wide range of oxygen isotope compositions of the vitreous artifacts from Period IVB (11-9<sup>th</sup> c BC) Hasanlu suggests that more than one source of silica was used to make these materials. Different silica sources could be the result of manufacture in different regions, with raw glasses or finished objects being traded into Hasanlu.

Glasses made in one region and in the same glassmaking industry appear to have a limited range in  $\delta^{18}\text{O}$  compositions, as indicated by the plant ash glasses mentioned above from Amarna and from Turkey. Oxygen isotope analyses of glasses from 4-9<sup>th</sup> c AD Roman glass manufacturing and recycling sites have a range of  $\delta^{18}\text{O}$  values smaller than that of the Hasanlu glasses. For example, at the site of Jalame, glasses have  $\delta^{18}\text{O}$  ratios of 14.07 ‰ to 15.17 ‰. These Roman glasses are chemically homogeneous and were manufactured from natron and sand. Chemical analyses,

archaeological evidence, and written documents indicate that the sand was probably derived from mature beach and river deposits along the eastern Mediterranean Sea, and that natron was mined from one area in Egypt, the Wadi Natrun (Brill, 1988a; Freestone et al., 2000). Recycled Roman glass was also used in the manufacturing process. The smaller range of  $\delta^{18}\text{O}$  values for Roman, natron-based glasses is probably an artifact of the limited sources of raw materials used in this industry. Roman glasses as a whole group, dating to about 1<sup>st</sup> c AD to 5<sup>th</sup> c AD, have  $\delta^{18}\text{O}$  of about 14-16 ‰ (Brill, 1999; I. C. Freestone, pers. comm.), a small range relative to that of the Hasanlu glasses. Glass manufacturing in ancient Rome was probably a centralized industry where the quality and trade of raw materials were well controlled, thus yielding a restricted range of oxygen isotope compositions. The  $\delta^{18}\text{O}$  spread for the Hasanlu glasses, 12.1-17.3 ‰, is not consistent with a tightly-controlled or centralized glassmaking industry.

Analyses of glasses from periods and regions comparable to Period IVB Hasanlu come from Assyria and Mitanni (Brill, 1999). From the site of 7<sup>th</sup> c BC Nimrud, then the capital of the Assyrian empire, four glasses with  $\delta^{18}\text{O}$  from 22.0 ‰ to 22.62 ‰ are reported (Brill, 1999). At Nuzi, a major city in the Mitanni empire, which ruled northern Mesopotamia in the 15<sup>th</sup>—mid-14<sup>th</sup> c BC, one sample from a cullet of dark blue glass yielded  $\delta^{18}\text{O}$  of 19.1 ‰. The  $\delta^{18}\text{O}$  values of the Hasanlu glasses are statistically different from Nimrud and Nuzi, as are the chemical compositions, suggesting that the glassmaking industries of these regions and periods did not develop out of the same glassmaking tradition, i.e. that the raw materials used and the way of making glass differed.

The effect of alkalies on the glass oxygen isotope composition depends on how large the difference is with the silica component and on the quantity added. In the experiments presented here, plant ash increased the  $\delta^{18}\text{O}$  ratio of the glass by about

1‰. Oxygen isotope results from archaeological glasses of natron-based compositions appear to show that natron can increase the  $\delta^{18}\text{O}$  ratio by a greater amount than plant ash. Thus, it appears that the oxygen isotope compositions of manufactured archaeological glass may be used to determine the sodium source if the silica source is known. The use of oxygen isotope ratios alone cannot resolve the silica sources. However, the main silicate raw material(s) used to manufacture an ancient glass may be inferred from oxygen isotope ratios if a large selection of artifacts are analyzed and the results compared to chemical, archaeological, and geological data.

## CHAPTER 8

### THE MANUFACTURE OF GLASSES AND GLAZES EXCAVATED FROM PERIOD IVB LEVEL (11<sup>TH</sup>—9<sup>TH</sup> C. B.C) AT HASANLU, IRAN

---

Colleen P. Stapleton, Samuel E. Swanson, and A. Mohamed Ghazi

To be submitted to *Journal of Archaeological Science*.

## INTRODUCTION

Interpretations of 2<sup>nd</sup> and early 1<sup>st</sup> millennium BC cuneiform glassmaking texts suggest that glass in the Near East was made with essentially pure quartz pebbles and plant ash mixed with colorants (Oppenheim et al., 1970). The plants are believed to be those that grow in dry climates or in saltwater marshes and can contain up to ten times more sodium than potassium, calcium, and magnesium. Chemical analyses of ancient glasses and replicate glassmaking experiments generally bear out these interpretations (Turner, 1956; Caley, 1962; Sayre and Smith, 1961; Brill, 1970a, 1988a; Henderson, 1985; Jackson et al., 1998). The cuneiform texts describe steps to make a number of “primary” or base glasses, coloring materials, and finished colored glasses. Complete interpretations of the texts are limited because the texts are fragmented and small parts and whole sections are missing. In addition, words that describe raw materials, materials produced in intermediate steps, finished products, and phrases that describe technical processes have not yet been fully understood. Oppenheim (1970) suggests that the texts also describe the manufacture of vitreous materials besides glass, including glaze and faience. The cuneiform texts are one of our most important sources of information about the technology involved in the ancient glassmaking industry.

The texts interpreted by Oppenheim (1970) were excavated from four different regions and periods: Kassite period Babylon, Hittite capital of Hattusa, 7<sup>th</sup> c BC library of Assurbanipal at Nineveh, and an un-provenanced text probably from the latter third of the 2<sup>nd</sup> millennium BC (Oppenheim, 1970). The texts appear to describe the raw materials and techniques of glassmaking in rather similar ways. However, it should be remembered that the texts record techniques practiced in specific regions and time periods and thus might not directly apply to glassmaking in other regions and periods in the Near East. In Europe, for example, some glasses dated to the late 2<sup>nd</sup> millennium BC, were made using the ashes of tress, “wood ash”, which contain greater potassium

and calcium than sodium (Wedepohl, 1997; Henderson, 1988; Hartmann et al., 1997). Oppenheim (1970) pointed out that variations in vocabulary between some of the cuneiform texts suggest that these records probably represent consolidation of more than one manufacturing tradition. In fact, there are some inconsistencies between the cuneiform written texts and the analytical data obtained from Near Eastern glasses dated to the 2<sup>nd</sup> and early 1<sup>st</sup> millennium BC. Glasses made with quartz and plant ash, as the main source of alkali, usually contain more than about 1.5 wt% each of K<sub>2</sub>O and MgO, yet some Near Eastern glasses of the 2<sup>nd</sup> and early 1<sup>st</sup> millennium BC contain significantly less of these oxides and thus fall outside of typical plant ash values. Low K<sub>2</sub>O and MgO glasses are usually considered to have been made with natron, a mineral source of sodium, that contains very little K<sub>2</sub>O and MgO. Low K<sub>2</sub>O and MgO glasses from the 2<sup>nd</sup> and early 1<sup>st</sup> millennium BC include dark blue, cobalt-colored glasses from Amarna, Egypt (Shortland and Tite, 2000; Lilyquist and Brill, 1993), and glasses from archaeological excavations from 11-9<sup>th</sup> c BC Hasanlu (Brill, 1999) and 7<sup>th</sup> c BC Nimrud (Brill, 1999). The K<sub>2</sub>O and MgO values of almost 80 Near Eastern glasses dated from 2<sup>nd</sup> millennium BC to the early 1<sup>st</sup> millennium BC are plotted in Fig 8.1, along with values typically assigned to plant ash- and natron-type glasses. The majority of glasses that have high MgO but low (lower than for typical plant ash glasses) K<sub>2</sub>O contents are cobalt blue glasses. The excavation sites of the cobalt glasses plotted in Fig 8.1 include 1400-1250 BC Mycenae, the c. 1300 BC Ulu Burun shipwreck, 7<sup>th</sup> c BC Nimrud, as well as mid-14<sup>th</sup> c BC Amarna in Egypt, and the data come from Brill (1999), Lilyquist and Brill (1993), and Shortland and Tite (2000). One cobalt blue from Hasanlu contains both low K<sub>2</sub>O and low MgO, appearing to be a natron-type glass (analysis 732, Table II D, Brill, 1999). All of the other eight low K<sub>2</sub>O and MgO glasses in Fig 8.1 are from Hasanlu (Brill, 1999; Stapleton and Swanson, 2002a, 2002b; Chapter 4, Chapter 5).

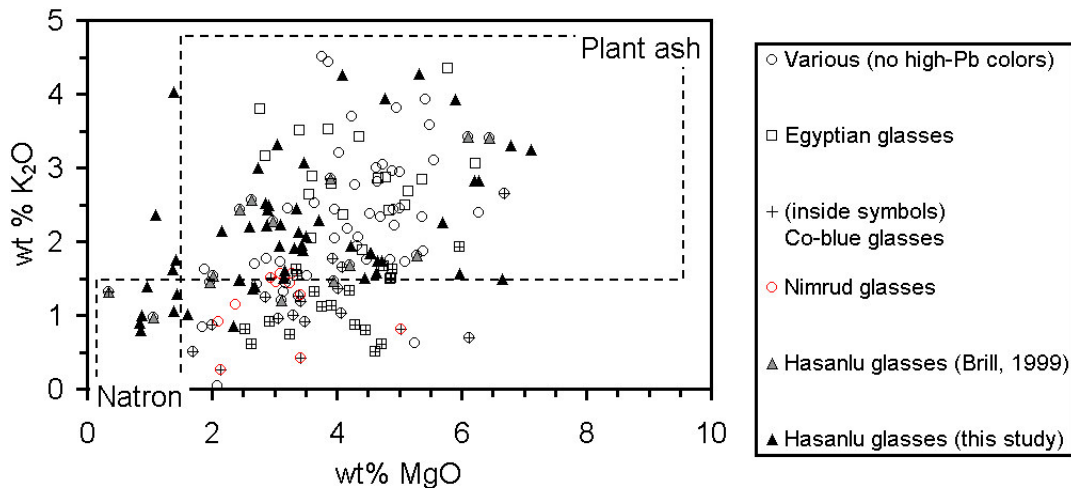


Fig 8.1.  $K_2O$  and  $MgO$  values of almost 80 Near Eastern glasses dated from 2<sup>nd</sup> millennium BC to the early 1<sup>st</sup> millennium BC. Dashed lines denote approximate compositions of glasses made with plant ash or natron (Lilyquist and Brill, 1993). Cobalt-colored blue glasses may have been made with natron and a  $MgO$ -rich colorant, making them fall outside of compositions normally associated with natron glasses.

The complex glassmaking practices described in the cuneiform texts may be an outcome of the technical adjustments that ancient glassmakers found necessary for manufacturing colored glasses. Most of the cobalt blue glasses in Fig 8.1 contain low  $K_2O$ , typical of natron glasses, but high  $MgO$ , typical of plant ash glasses. Magnesium- and cobalt-rich alum ore from the Western Oasis of Egypt was probably used to color many cobalt blue glasses of the mid-2<sup>nd</sup> millennium BC onwards, especially those from Egypt (Lucas, 1926; Kaczmarczyk, 1986). A recent study (Shortland and Tite, 2000) proposes that cobalt blue glasses from Amarna, Egypt were made using natron, rather than plant ash, and that the high  $MgO$  in those glasses is accounted for by use of Western Oasis cobalt ore added as colorant. This ore would have added up to about 4 wt%  $MgO$  but little  $K_2O$  to the final cobalt-colored glass (Shortland and Tite, 2000). Using plant ash in combination with the high  $MgO$  cobalt ore may have caused problems, perhaps devitrification or increased melt viscosity, that required changes in the chemical composition of the batch material. Natron was available and in common

use in dynastic Egypt as part of the mummification process (Nicholson and Henderson, 2002) and would have been a good source of sodium with low MgO. Other colored glasses also may have required adjustments in the glassmaking batch to accommodate the forms in which the colorant, or other raw material, was available. The Hasanlu glasses that deviate from typical plant ash compositions are not cobalt blue but are of the same colors as glasses plotted in the plant ash region of Figure 8.1. Differences in available raw materials from those described in the glassmaking texts may explain these Hasanlu compositions. The purpose of this paper is to use chemical analyses and microstructural studies to identify the materials used to make and color the c. 11-9<sup>th</sup> c BC glasses and glazes excavated from the site of Hasanlu (Period IVB) in northwestern Iran. This paper will describe some of the processes involved in manufacturing these Iron Age vitreous materials and compare them with the steps as detailed in the cuneiform glassmaking texts.

## METHODOLOGY

### **Archaeological Samples**

Thousands of glass artifacts were excavated from Period IVB (11<sup>th</sup>-9<sup>th</sup> c BC) at Hasanlu, southwest of Lake Urmia in northwestern Iran. Excavations at Hasanlu were carried out by the University of Pennsylvania under the direction of Robert H. Dyson from 1957-1977 (Dyson, 1989a). Period IVB, as identified by Dyson (1989a), is a destruction layer at Hasanlu deposited at the very end of the 9<sup>th</sup> century BC (Dyson and Muscarella, 1989). The mound of Hasanlu was not re-occupied until about 50-100 years later. Samples used in this paper come mainly from the Period IVB level, and four samples come from earlier Period V (1450-1250 BC; Dyson, 1989a).

The samples were obtained from the University of Pennsylvania (UPenn.) Museum of Archaeology and Anthropology in cooperation with Maude de Schauensee and Robert H. Dyson. Most of the glasses presented in this paper were sampled from

beads, both monochrome and polychrome. Colors sampled from the beads were blue transparent to translucent (tp-tl), blue opaque, black, white opaque, and yellow opaque. Nine samples of blue opaque (turquoise) glass were sampled from seven four-sided hollow tubes of unknown original use. Glazes were sampled from six ceramic vessels, one of which is decorated in Assyrian style with polychrome glazes. Glaze colors sampled were blue transparent, white opaque, and yellow opaque. Table 3.2 lists the glass and glaze samples analyzed, artifacts from which they were sampled, and their excavation location.

### **Electron Microprobe**

Electron microprobe analysis has been used for four decades in studies of archaeological materials (Herz and Garrison, 1998). This technique has proven useful because the very small samples can be characterized, and areas of corrosion or alteration can be identified and avoided during analysis (Stapleton and Swanson, 2002a; Chapter 4). Additionally, samples are not destroyed during analysis and can be analyzed using other techniques or stored for future investigations. Electron microprobe or SEM examination should be considered a necessary part of analytical projects that involve early glasses, because their microstructures are not homogeneous (Stapleton and Swanson, 2002a; Chapter 4). It may not be necessary to analyze each sample but a representative selection could be chosen to exhibit the microstructure, remnant batch inclusions, devitrification phases, crystalline colorants, and other micro-features that may be present.

Small (<1 mm<sup>3</sup>) fragments of sample were set into epoxy resin, dry-ground with 400 or 600 grit silicon carbide sandpaper until the fragments appeared on the ground surface, and then polished using diamond paste with a final polish using 0.25 um diamond paste (Stapleton and Swanson, 2002a; Chapter 4). No water was used during grinding or polishing, mainly because the small sample size did not require it, but also

because of the possibility of dissolving water soluble phases from the glass. Only alcohol was used to clean surfaces in between polishing. Polished samples were coated with carbon before being put into the electron microprobe. Major and minor element analyses were carried out on a JEOL 7300 microprobe with four wavelength dispersive spectrometers at the Department of Geology, University of Georgia (Athens, USA). Accelerating voltage was 15 kV, with a beam current of 2 nA as measured in a Faraday Cup, and a beam diameter of 20  $\mu\text{m}$  (0.02 mm). Calibration and analysis for each element was carried out for 20 seconds at peak and backgrounds levels. Synthetic  $\text{Na}_2\text{O-CaO-SiO}_2$  glasses were used as standards for  $\text{SiO}_2$  (SVRM-01),  $\text{Na}_2\text{O}$  (Corning B), and  $\text{PbO}$  (Corning C), and natural and synthetic mineral standards were used for the remaining elements. To minimize sodium loss and the apparent change in other major elements ( $\text{SiO}_2$ ) related to sodium loss, sodium and silicon were measured at the very beginning of each analysis, although the Si peak measurement lagged by about 20 seconds to 40 seconds because of the Si peak search. Calibration was performed before each run of analyses. Glass standards that are replicates of ancient glasses, including Corning A and Corning B (Rising, 1999), were regularly analyzed for each run. For each glass unknown, at least three randomly selected points were analyzed, and the average of these analyses are then used to represent the glass in comparative discussions and graphs. At least four points were analyzed for each glaze, including areas close to the ceramic body and within the body, where present. The purpose of analyses near and in the ceramic body was to identify interaction of the glaze with the body, which can introduce components like  $\text{Al}_2\text{O}_3$  and  $\text{FeO}$ . Analysis points in or near the ceramic body are not included in the average glaze compositions. Reproducibility, measured from repeat analyses on standard glass Corning B is better than about 2% relative for oxides present at greater than 10 wt%, and better than about 10% for the other oxides except  $\text{FeO}$ , which is around 40%. Detection limits are better than about

0.4 wt% for most oxides, except PbO which is about 1 wt%. Tin was sought in the blue tp-tl and blue opaque glasses or glazes but was not present above the detection limit of 0.3 wt% SnO<sub>2</sub>, although trace element analysis shows tin in some glasses (see “Laser ablation-Inductively Coupled Plasma-Mass Spectrometry”). Cobalt was sought in the blue opaque glasses, but was not present above the microprobe detection limit (0.4 wt% CoO). Microprobe results for glasses and glazes are presented in Tables 8.1 and 8.2, respectively, along with detection limits.

Table 8.1 Microprobe Analyses of Hasanlu Glasses

Object Museum Registration # (UPenn.)	n=	SiO <sub>2</sub>	TiO <sub>2</sub>	Al <sub>2</sub> O <sub>3</sub>	FeO	MnO	MgO	CaO	Na <sub>2</sub> O	K <sub>2</sub> O	P <sub>2</sub> O <sub>5</sub>	SO <sub>3</sub>	Cl	Sb <sub>2</sub> O <sub>5</sub>	CuO	PbO	Total
<i>DL (wt%)</i>		<i>0.09</i>	<i>0.20</i>	<i>0.09</i>	<i>0.40</i>	<i>0.34</i>	<i>0.10</i>	<i>0.08</i>	<i>0.18</i>	<i>0.08</i>	<i>0.30</i>	<i>0.36</i>	<i>0.07</i>	<i>0.31</i>	<i>0.45</i>	<i>0.97</i>	
<b>Blue transparent to translucent (tp-tl)</b>																	
61-5-89h2	10	59.01	0.21	4.95	0.53	bd	4.68	5.53	20.16	3.87	0.34	0.38	0.69	0.32	0.94	na	101.63
61-5-95a	3	64.33	0.27	2.49	1.35	0.34	3.42	7.41	18.11	2.02	0.30	bd	0.55	bd	1.39	na	101.97
61-5-95b	3	66.65	0.23	2.33	0.82	bd	3.35	6.35	18.20	2.11	bd	bd	0.78	bd	0.69	na	101.51
63-5-270a	6	61.24	0.31	3.27	1.68	bd	4.57	7.16	20.26	1.70	0.38	0.62	0.34	bd	1.33	na	102.84
63-5-276a	9	63.90	0.31	3.26	1.43	bd	2.81	8.24	17.43	2.17	0.45	0.43	0.45	bd	1.00	na	101.87
63-5-280a	8	67.87	0.23	3.65	0.56	0.61	1.36	2.60	19.30	1.69	0.40	0.42	0.82	bd	2.18	na	101.68
63-5-559a	4	65.05	0.37	4.41	0.86	bd	1.06	3.42	20.13	2.28	bd	0.61	0.37	0.55	4.81	na	103.91
63-5-559c	5	65.45	0.37	2.80	0.80	bd	2.36	5.75	19.62	1.44	0.37	0.47	0.58	bd	1.15	na	101.15
65-31-267a	5	63.71	0.23	1.93	1.18	bd	4.07	5.73	19.72	4.24	0.42	0.56	0.81	0.31	0.57	na	103.47
65-31-273a	5	61.89	0.21	2.17	0.92	bd	3.31	6.22	20.38	1.80	0.40	0.52	0.67	0.66	1.46	na	100.60
65-31-396d	5	68.60	bd	4.99	bd	0.56	1.37	1.97	18.32	4.00	0.36	0.41	0.54	bd	1.18	na	102.31
73-5-293b	5	65.85	0.27	2.57	1.52	bd	3.11	7.07	18.66	1.49	0.35	0.58	0.33	bd	1.33	na	103.12
73-5-350b	3	64.36	0.31	2.62	1.21	bd	3.07	6.87	18.90	1.56	0.51	0.49	0.40	bd	1.28	na	101.59
73-5-559d	5	64.25	0.25	2.41	1.09	0.37	3.01	6.20	19.71	1.89	0.41	0.43	0.68	bd	1.31	na	102.00
73-5-559e	4	70.49	bd	3.11	0.46	0.95	0.93	2.01	19.45	1.35	0.33	0.39	0.48	bd	0.83	bd	100.77
75-29-199a	4	71.95	bd	0.80	0.56	bd	0.85	4.67	19.04	0.98	0.29	0.59	0.27	2.55	1.08	na	103.63
75-29-307a	8	64.67	0.26	2.27	0.92	bd	3.40	5.93	17.92	2.29	0.49	0.53	0.39	0.30	1.76	bd	101.13
<b>Black</b>																	
58-4-61b	3	66.93	0.20	2.77	7.84	bd	1.28	1.83	19.96	1.53	0.39	bd	0.68	bd	bd	bd	103.40
61-5-89-1	3	67.23	bd	1.58	10.94	bd	1.26	2.11	18.03	0.97	0.30	bd	0.53	0.36	bd	na	103.30
61-5-89h3	6	64.61	0.23	2.53	10.99	0.33	2.40	1.98	18.03	1.23	0.47	0.36	0.38	bd	bd	bd	103.54
61-5-89i-3	3	70.52	0.25	1.11	8.01	bd	1.34	1.71	17.26	1.20	0.36	0.47	0.93	bd	bd	na	103.16
61-5-95a	8	58.61	0.41	4.27	1.08	bd	5.25	5.38	21.10	4.23	0.64	0.79	0.74	0.64	bd	bd	103.14
61-5-95c	5	63.39	0.27	2.33	0.91	bd	3.44	7.46	19.36	3.05	0.64	0.69	1.15	0.32	bd	1.43	104.44

Table 8.1 Continued

Reg. #	n=	SiO <sub>2</sub>	TiO <sub>2</sub>	Al <sub>2</sub> O <sub>3</sub>	FeO	MnO	MgO	CaO	Na <sub>2</sub> O	K <sub>2</sub> O	P <sub>2</sub> O <sub>5</sub>	SO <sub>3</sub>	Cl	Sb <sub>2</sub> O <sub>5</sub>	CuO	PbO	Total
61-5-95d	10	61.99	bd	2.98	0.41	bd	3.02	9.30	18.10	2.17	0.35	0.63	0.58	bd	bd	bd	99.99
63-5-269a	20	68.59	0.22	2.64	0.94	bd	3.56	6.25	20.78	2.04	0.35	0.96	0.98	bd	bd	bd	107.21
63-5-280a	10	57.34	0.32	5.10	2.28	bd	6.04	5.51	20.17	2.73	0.61	0.91	0.82	2.42	0.94	bd	105.19
65-31-247a	3	67.43	0.24	4.08	1.09	bd	2.65	6.31	19.41	2.26	0.38	0.44	1.05	0.33	bd	bd	105.66
65-31-273a	5	60.49	0.21	1.75	8.06	bd	2.60	5.00	18.10	2.19	0.40	0.82	0.72	bd	bd	na	100.34
65-31-396e	4	67.19	0.19	1.34	10.25	bd	1.47	2.69	17.91	0.93	bd	bd	0.62	bd	bd	bd	102.58
65-31-396f	4	65.70	0.20	2.00	13.04	bd	2.08	1.65	16.39	0.76	bd	bd	0.30	bd	bd	bd	102.12
65-31-396g	3	62.27	0.24	1.27	14.84	bd	0.70	3.98	15.10	0.76	0.36	bd	0.30	bd	bd	bd	99.82
65-31-396h	3	62.96	bd	1.35	15.15	bd	0.72	4.02	15.13	0.67	bd	bd	0.28	bd	bd	bd	100.28
65-31-397a	5	65.59	0.31	3.21	1.17	bd	3.03	6.79	17.67	3.30	0.42	0.42	0.47	0.37	bd	bd	102.76
65-31-728c	3	62.21	0.23	2.23	4.90	bd	4.27	5.96	19.86	1.45	0.77	0.42	0.40	0.30	bd	bd	103.00
73-5-305a	6	65.73	0.34	3.39	1.42	bd	3.34	6.72	19.48	1.92	0.34	0.42	0.49	1.28	bd	1.08	105.93
73-5-341a	5	68.38	0.25	2.68	6.29	bd	2.56	2.56	17.92	1.33	0.38	1.18	0.39	0.35	2.21	bd	106.49
73-5-350a	4	69.12	0.25	2.72	0.92	bd	2.18	5.74	18.87	2.16	0.63	bd	0.74	bd	bd	bd	103.33
73-5-559c	4	63.77	0.47	4.15	1.59	bd	2.38	5.55	19.77	1.44	0.71	0.53	0.70	bd	0.82	bd	101.87
73-5-559f	4	68.35	0.40	2.21	0.93	bd	2.89	5.12	18.20	2.48	0.51	0.42	0.64	bd	bd	bd	102.15
75-29-307a	5	65.19	0.32	2.01	0.72	bd	2.67	5.22	19.45	2.93	0.50	0.58	0.88	0.48	bd	bd	100.94
<b>Blue opaque (turquoise)</b>																	
61-5-54	4	64.36	bd	2.59	0.51	bd	4.39	4.89	18.76	1.79	0.36	0.66	0.29	2.44	3.51	bd	104.56
65-31-280	4	59.38	0.41	9.41	3.10	bd	2.74	4.08	18.06	2.42	bd	0.43	0.58	bd	0.85	bd	101.47
65-31-280	2	62.80	bd	2.58	0.54	bd	4.10	6.46	19.35	1.89	0.40	0.54	0.44	1.15	1.20	bd	101.43
65-31-282	1	59.81	bd	1.97	0.47	bd	6.43	6.99	20.13	1.44	bd	0.64	0.42	2.29	bd	bd	100.60
65-31-283	4	59.14	bd	1.36	0.56	bd	5.59	6.46	18.50	3.72	0.43	bd	0.66	3.91	1.78	bd	102.10
65-31-728e	3	65.68	bd	2.60	0.43	bd	4.44	5.08	18.17	1.81	0.46	0.69	0.26	2.16	3.21	bd	104.97
65-31-728f	4	61.43	bd	2.88	0.66	bd	4.49	5.65	19.06	1.65	0.29	0.47	0.27	1.83	2.22	bd	100.89
65-31-992	3	67.33	0.21	2.35	0.58	bd	4.57	5.22	17.51	1.55	0.23	0.58	0.32	1.75	2.03	bd	104.23
65-31-993	3	62.72	bd	2.13	0.59	bd	5.87	6.54	19.57	1.54	0.35	0.50	0.51	1.49	0.60	bd	102.40
73-5-781	3	62.68	bd	1.48	0.70	bd	5.58	6.89	19.36	2.23	0.40	0.53	0.37	1.63	1.01	na	102.86
73-5-782	3	59.66	bd	0.86	0.57	bd	6.40	6.18	18.11	3.11	0.52	0.41	0.42	2.72	2.00	bd	100.95
<b>Yellow opaque</b>																	
61-5-95a	7	60.63	0.31	2.19	0.95	bd	3.06	6.07	15.06	1.45	0.44	0.44	0.44	2.97	bd	8.61	102.63
61-5-95c	9	59.96	0.24	2.22	0.86	0.33	4.57	6.32	16.05	2.67	0.47	0.47	0.43	2.03	bd	7.17	103.79
63-5-280a	4	51.81	na	5.95	2.20	na	4.74	4.27	15.59	1.69	0.35	0.42	0.28	7.68	na	9.93	104.89
73-5-305a	5	53.14	0.30	2.69	1.50	na	3.44	6.83	12.39	1.32	bd	0.46	0.31	1.81	na	16.70	100.88
73-5-559d	5	59.36	na	4.54	1.40	na	3.24	5.38	15.15	1.69	0.45	0.43	0.57	1.04	na	9.10	102.35
73-5-559f	4	52.38	na	2.77	1.14	na	2.77	6.66	12.04	1.51	0.48	0.52	0.28	4.57	na	16.09	101.22
75-29-307a	7	57.34	na	3.01	1.46	na	5.03	6.10	15.99	2.15	0.60	0.46	0.41	2.34	na	8.83	103.70
<b>White opaque*</b>																	
63-5-276a	1	60.41	0.29	3.71	1.30	bd	4.04	8.09	20.28	1.87	bd	0.44	0.46	2.27	bd	na	103.15
63-5-280a	1	53.83	0.29	6.19	1.30	bd	4.88	3.21	22.19	1.62	0.51	bd	0.56	6.47	0.64	na	101.69
73-5-559e	4	66.58	0.21	3.26	0.79	bd	1.84	2.92	16.83	1.38	bd	0.53	0.27	7.38	bd	bd	101.99

Data are averages of n analyses.

DL: detection limit.

\* White glasses with n=1 are extensively weathered and only a small area was available for analysis.

Table 8.2 Microprobe Analyses of Glazes (Point Analyses and Averages) and Aluminum-Rich Inclusions in Glazes

Upenn.#, glaze color

Analysis # SiO<sub>2</sub> TiO<sub>2</sub> Al<sub>2</sub>O<sub>3</sub> FeO MnO MgO CaO Na<sub>2</sub>O K<sub>2</sub>O P<sub>2</sub>O<sub>5</sub> SO<sub>3</sub> Cl Sb<sub>2</sub>O<sub>5</sub> CuO PbO Total

**Glazes, Point Analyses and Averages**

**UPenn. 60-20-344, blue tp glaze**

21	70.58	bd	1.74	1.01	bd	1.34	2.29	16.24	3.49	bd	bd	0.95	bd	2.47	bd	100.11
22	70.96	bd	2.11	0.67	bd	1.21	1.92	15.38	3.43	bd	bd	0.99	bd	2.95	bd	99.61
23	71.06	bd	3.17	0.77	bd	1.18	1.82	13.49	3.88	bd	bd	0.77	bd	2.82	bd	98.97
24	70.43	bd	2.41	1.20	bd	1.21	1.95	13.74	3.89	bd	bd	0.79	bd	3.61	bd	99.22
<i>average</i>	<i>70.76</i>	<i>bd</i>	<i>2.36</i>	<i>0.91</i>	<i>bd</i>	<i>1.23</i>	<i>1.99</i>	<i>14.71</i>	<i>3.67</i>	<i>bd</i>	<i>bd</i>	<i>0.88</i>	<i>bd</i>	<i>2.96</i>	<i>bd</i>	<i>99.48</i>

**UPenn. 60-20-346, blue tp glaze**

26	63.71	bd	2.08	0.88	bd	1.60	6.08	13.56	4.06	0.66	0.35	0.67	bd	3.53	bd	97.17
27	68.63	bd	1.47	0.53	bd	1.18	5.02	12.20	4.12	0.54	bd	0.53	bd	2.35	bd	96.57
28	69.73	bd	1.51	1.04	bd	1.15	5.07	12.61	4.30	0.48	bd	0.78	bd	3.05	bd	99.73
29	68.79	bd	1.55	0.61	bd	1.17	5.96	11.64	4.07	0.30	bd	0.93	bd	3.03	bd	98.06
30	62.17	bd	2.57	0.85	bd	1.71	7.05	13.12	3.82	0.60	bd	0.88	0.31	3.62	bd	96.69
32	65.97	bd	1.22	0.51	bd	1.26	8.13	12.37	4.19	0.42	bd	0.63	bd	2.91	bd	97.62
33	69.49	bd	1.44	0.53	bd	1.18	6.13	11.70	4.05	0.48	bd	0.84	bd	3.49	bd	99.33
<i>average</i>	<i>66.93</i>	<i>bd</i>	<i>1.69</i>	<i>0.71</i>	<i>bd</i>	<i>1.32</i>	<i>6.21</i>	<i>12.46</i>	<i>4.09</i>	<i>0.50</i>	<i>0.35</i>	<i>0.75</i>	<i>0.31</i>	<i>3.14</i>	<i>bd</i>	<i>98.44</i>

**UPenn. 60-20-348, Assyrian style sherd, blue tp glaze inside**

21	66.58	bd	1.51	0.57	bd	2.74	5.82	13.23	2.13	bd	1.35	0.50	bd	3.73	bd	98.16
22	66.07	bd	2.23	0.60	bd	2.87	5.84	13.77	2.18	bd	bd	0.50	bd	3.28	bd	97.35
23	66.49	bd	1.46	0.46	bd	2.56	6.01	11.65	2.30	bd	0.47	0.34	bd	2.90	bd	94.64
25	68.40	bd	1.86	0.35	bd	2.71	6.63	11.80	2.29	bd	bd	0.40	bd	2.58	bd	97.03
26	67.92	bd	1.95	0.46	bd	2.55	5.33	13.40	2.24	bd	0.43	0.42	bd	3.97	bd	98.68
27	61.01	bd	1.74	0.60	bd	2.92	5.89	16.20	2.03	bd	3.91	0.87	bd	3.32	bd	98.49
28	66.08	bd	2.14	0.60	bd	3.09	5.71	13.96	2.28	0.43	0.64	0.58	bd	3.79	bd	99.29
	<i>66.08</i>	<i>bd</i>	<i>1.84</i>	<i>0.52</i>	<i>bd</i>	<i>2.78</i>	<i>5.89</i>	<i>13.43</i>	<i>2.21</i>	<i>0.43</i>	<i>1.36</i>	<i>0.52</i>	<i>bd</i>	<i>3.37</i>	<i>bd</i>	<i>98.42</i>

**UPenn. 60-20-348, Assyrian style sherd, blue tp glaze outside**

13	64.95	0.19	2.11	0.65	bd	3.16	7.40	8.97	5.44	bd	0.46	0.09	0.45	3.61	bd	97.48
14	65.91	bd	2.41	0.87	bd	3.33	7.34	8.30	5.44	0.30	0.50	0.29	bd	3.14	bd	97.83
15	65.76	bd	4.59	bd	bd	2.62	5.54	8.33	6.10	0.30	0.50	0.08	bd	3.04	bd	96.86
33	65.51	bd	2.04	0.73	bd	3.13	7.28	8.70	5.37	bd	0.51	0.11	0.30	2.90	bd	96.58
<i>average</i>	<i>65.53</i>	<i>0.19</i>	<i>2.79</i>	<i>0.75</i>	<i>bd</i>	<i>3.06</i>	<i>6.89</i>	<i>8.58</i>	<i>5.59</i>	<i>0.30</i>	<i>0.49</i>	<i>0.14</i>	<i>0.38</i>	<i>3.17</i>	<i>bd</i>	<i>97.85</i>

**UPenn. 60-20-348, Assyrian style sherd, yellow opaque glaze**

6	46.45	bd	1.60	1.92	bd	2.18	3.25	5.33	3.29	bd	0.40	0.13	2.36	0.53	27.92	95.35
8	47.55	bd	1.47	2.48	bd	2.14	2.97	5.46	3.59	0.28	bd	0.08	1.35	bd	27.32	94.68
9	46.37	bd	1.56	2.27	bd	1.81	3.15	5.52	3.45	bd	0.37	0.28	2.49	bd	25.00	92.27
10	48.75	bd	2.53	2.17	bd	1.93	3.97	5.81	4.06	bd	bd	0.48	1.07	bd	22.83	93.59
<i>average</i>	<i>47.28</i>	<i>bd</i>	<i>1.79</i>	<i>2.21</i>	<i>bd</i>	<i>2.01</i>	<i>3.33</i>	<i>5.53</i>	<i>3.60</i>	<i>0.28</i>	<i>0.38</i>	<i>0.24</i>	<i>1.82</i>	<i>0.53</i>	<i>25.77</i>	<i>94.77</i>

**UPenn. 60-20-348, Assyrian style sherd, white opaque glaze**

11	59.81	bd	4.00	0.96	bd	3.28	6.46	7.85	5.24	0.72	0.47	0.13	2.89	bd	4.89	96.69
12	59.84	bd	6.26	0.57	bd	2.00	4.09	7.50	6.35	bd	bd	0.13	2.95	bd	4.02	93.71
13	63.11	bd	1.57	0.43	bd	3.66	7.48	7.97	5.33	0.48	0.58	0.37	3.04	bd	3.51	97.53
14	63.88	bd	1.03	0.49	bd	3.55	6.81	8.26	5.65	0.36	1.52	0.54	2.24	bd	2.52	96.85
15	64.04	bd	1.45	0.63	0.38	6.40	10.77	6.41	4.30	bd	bd	0.31	1.81	bd	1.11	97.60
20	59.14	bd	0.75	0.30	0.41	12.68	19.35	2.60	1.97	bd	bd	0.22	1.23	bd	bd	98.65
21	63.17	bd	5.76	1.01	bd	2.89	4.68	8.22	6.57	bd	bd	0.25	2.32	bd	2.13	96.99
<i>average</i>	<i>61.86</i>	<i>bd</i>	<i>2.97</i>	<i>0.63</i>	<i>0.39</i>	<i>4.92</i>	<i>8.52</i>	<i>6.97</i>	<i>5.06</i>	<i>0.52</i>	<i>0.86</i>	<i>0.28</i>	<i>2.35</i>	<i>bd</i>	<i>3.03</i>	<i>98.36</i>

Table 8.2 Continued

Upenn.#, glaze color	Analysis #	SiO <sub>2</sub>	TiO <sub>2</sub>	Al <sub>2</sub> O <sub>3</sub>	FeO	MnO	MgO	CaO	Na <sub>2</sub> O	K <sub>2</sub> O	P <sub>2</sub> O <sub>5</sub>	SO <sub>3</sub>	Cl	Sb <sub>2</sub> O <sub>5</sub>	CuO	PbO	Total
<b>UPenn. 60-20-349, blue tp glaze</b>																	
	31	68.14	bd	1.09	bd	bd	0.87	2.74	14.94	3.19	bd	bd	1.19	bd	5.05	bd	97.22
	32	68.39	bd	3.49	0.41	bd	0.77	2.18	14.47	3.36	0.31	bd	0.98	bd	4.57	bd	98.92
	33	65.68	bd	1.32	0.59	bd	0.90	3.34	15.17	3.26	0.42	2.38	2.05	2.00	3.76	bd	100.87
	34	65.60	bd	1.10	0.46	bd	1.03	3.00	15.65	3.10	0.61	2.28	2.26	bd	4.63	bd	99.71
	35	68.40	bd	1.52	0.46	bd	0.94	2.78	14.74	3.35	bd	0.47	0.98	bd	5.27	bd	98.92
	38	70.20	bd	1.34	0.43	bd	0.93	2.73	14.93	3.15	0.55	0.59	1.13	bd	5.03	bd	101.03
	<i>average</i>	<i>67.74</i>	<i>bd</i>	<i>1.64</i>	<i>0.47</i>	<i>bd</i>	<i>0.91</i>	<i>2.80</i>	<i>14.98</i>	<i>3.24</i>	<i>0.47</i>	<i>1.43</i>	<i>1.43</i>	<i>2.00</i>	<i>4.72</i>	<i>bd</i>	<i>101.82</i>
<b>UPenn. 63-5-54, blue tp glaze</b>																	
	44	62.99	bd	1.92	0.50	0.34	1.57	4.59	17.50	3.15	0.60	bd	1.26	bd	4.89	bd	99.31
	45	64.72	bd	1.90	0.58	bd	1.54	4.19	16.93	3.44	0.66	0.35	1.04	bd	5.23	bd	100.59
	46	64.67	bd	2.04	0.74	bd	1.59	4.37	16.89	3.21	0.42	bd	1.17	bd	4.72	bd	99.82
	<i>average</i>	<i>64.13</i>	<i>bd</i>	<i>1.95</i>	<i>0.61</i>	<i>0.34</i>	<i>1.57</i>	<i>4.38</i>	<i>17.11</i>	<i>3.27</i>	<i>0.56</i>	<i>0.35</i>	<i>1.16</i>	<i>bd</i>	<i>4.95</i>	<i>bd</i>	<i>100.36</i>
<b>UPenn. 93-4-154, blue tp glaze</b>																	
	51	63.88	bd	2.91	0.52	bd	1.38	3.66	15.59	3.24	0.37	0.42	0.94	bd	5.43	bd	98.34
	52	67.70	bd	2.58	bd	bd	1.38	3.12	14.97	3.52	0.80	bd	1.34	bd	4.10	bd	99.51
	53	67.89	bd	2.55	0.54	bd	1.20	3.70	13.85	3.55	0.43	bd	1.37	bd	4.15	bd	99.24
	<i>average</i>	<i>66.49</i>	<i>bd</i>	<i>2.68</i>	<i>0.53</i>	<i>bd</i>	<i>1.32</i>	<i>3.49</i>	<i>14.80</i>	<i>3.44</i>	<i>0.53</i>	<i>0.42</i>	<i>1.22</i>	<i>bd</i>	<i>4.56</i>	<i>bd</i>	<i>99.49</i>
<b>Aluminum-Rich Inclusions in Glazes</b>																	
<b>UPenn. 60-20-348, Assyrian style sherd, blue tp glaze inside</b>																	
	29	65.41	bd	9.75	0.60	bd	1.80	2.78	10.81	3.15	bd	bd	0.32	bd	2.42	bd	97.04
	30	42.75	bd	27.07	bd	bd	1.06	1.05	14.06	1.01	bd	4.60	3.52	bd	0.70	bd	95.81
<b>UPenn. 60-20-348, Assyrian style sherd, blue tp glaze outside</b>																	
	16	51.15	0.60	2.76	2.61	bd	16.19	20.39	2.33	0.37	bd	bd	0.19	bd	1.74	bd	98.34
	17	43.91	bd	25.69	1.58	bd	0.92	1.87	15.61	3.12	bd	3.24	2.77	bd	0.12	bd	98.84
	18	49.32	bd	26.87	2.18	bd	0.14	0.79	14.11	4.53	bd	0.72	0.46	bd	0.33	bd	99.44
	19	61.05	0.62	12.98	1.57	bd	0.87	2.30	5.75	8.36	bd	bd	0.16	bd	2.02	bd	95.69
<b>UPenn. 60-20-348, Assyrian style sherd, white opaque</b>																	
	16	23.18	0.30	8.91	3.96	bd	4.83	14.21	0.82	0.64	bd	1.45	0.24	bd	bd	bd	58.54
	19	27.20	bd	1.15	bd	bd	1.45	18.26	3.96	2.36	bd	bd	0.11	44.34	bd	1.93	100.75
	17	55.72	bd	1.64	0.70	bd	10.26	17.45	3.81	2.42	bd	0.85	0.23	1.21	bd	1.99	96.27
	18	63.45	bd	7.30	0.72	bd	2.26	3.38	5.89	6.38	bd	bd	0.13	2.44	bd	4.32	96.28
<b>UPenn. 60-20-349, blue tp glaze</b>																	
	36	64.98	bd	10.93	0.60	bd	0.47	1.24	10.82	4.77	0.31	bd	0.71	bd	2.24	bd	97.08

### Laser Ablation-Inductively Coupled Plasma-Mass Spectrometry (LA-ICP-MS)

The small samples available for analysis in the present study required that loss of sample during preparation and analysis be kept to a minimum. It was decided to conduct trace element analyses on the polished samples used for electron microprobe analyses by using laser sampling for inductively-coupled plasma mass spectrometry

(LA-ICP-MS; Stapleton et al., submitted; Chapter 6). Although laser-sampling it is not currently widely applied to ancient manufactured glass analysis, solution-based sample introduction ICP-MS has been successfully used to analyze trace elements in a number of studies on manufactured glasses (Heyworth et al. 1989; McCray et al. 1995; Lambert et al. 1996; Hartmann et al., 1997; Rising, 1999). The micro-sampling ability of the LA-ICP-MS technique seems well-suited to the analysis of ancient glasses, given the homogeneity of the glasses on the order of 10-100  $\mu\text{m}$ .

Saitowitz et al. (1996) first used laser ablation ICP-MS on manufactured glass to determine the concentration of REEs of Islamic glasses from South Africa. More recently, laser ablation sampling of manufactured glasses has been carried out by Gratuze et al. (2000) and Shortland (2002). National Bureau of Standards (NBS) glasses 610 and 612 have been used as the calibration standards in these studies. These NBS glasses are synthetic glasses with major element matrices that are different from those of typical ancient manufactured glasses in that they contain higher  $\text{Al}_2\text{O}_3$  and  $\text{SiO}_2$  and lower alkalis. For analysis of the Hasanlu glasses and glazes, modern replicates of ancient glasses produced by Corning Glass Works (Brill, 1966, 1972a) and the University of York, UK (Freestone, pers. comm.) that are used as standards for major and minor element analyses in museum laboratories were chosen as calibration standards for the trace element analyses. The trace elements in the Corning standards were first reported in an analytical round-robin exercise by Brill (1966, 1972a) and have been regularly analyzed by Rising (1999), but they are not commonly used for trace element standardization. The application of the Corning and York glasses in trace element analysis is still in the experimental stage and comparisons of these standards with the NBS glasses and other certified standards should be carried out to determine the relative accuracy of the reported trace element concentrations in these standards.

LA-ICP-MS analysis was carried out at the Geology Department of Georgia State University (Atlanta, USA) on a New Wave-Merchantek 213 nm Nd-YAG laser and a Finnigan MAT Element 2 ICP-MS equipped with a fast field regulator. Laser parameters were set at 20 Hz rep rate (laser pulses/second), 25  $\mu\text{m}/\text{second}$  raster speed, 100  $\mu\text{m}$  raster spacing, 100  $\mu\text{m}$  laser spot diameter. The laser fluence was between about 1.2 and 1.5  $\text{J}/\text{cm}^2$ . Flux in laser energy during an analysis will affect the volume of material ablated and, in turn, the measured concentrations of isotopes. To account for this flux, an internal standard is measured during analysis and compared to its known concentration. Calcium was chosen for the sensitivity of the ICP-MS instrument and because it was measured in all of the Hasanlu glasses and glazes during microprobe analysis. The counts acquired for each isotope were normalized to the calcium counts acquired at the same time. This normalized value was then standardized to the known calcium concentration. This procedure was carried out on both the standards, using the reported calcium reported by Rising (1999), and unknowns, using calcium measured from microprobe analyses.

Synthetic ancient glasses Corning A, Corning B, and York 76-C-145 were used as calibration standards by calculating calibration curves from concentration against counts measured. The recent re-evaluations of the Corning glasses reported in Rising (1999) are used here as the calibration values. Glass York 76-C-145 was used only as the calibration standard for arsenic because this element is not reported by Rising (1999). Corning D and York glasses 76-C-145, 76-C-147, 76-C-150, 77-C-33 were tried as calibration standards for other elements, but did not yield good calibration curves and may be inhomogeneous in trace elements or calcium. The analyses took place on two separate days. On the second day of analysis, a gas blank was measured at the beginning of the run and used as the blank for both days. Corning B was analyzed at the beginning of each run, and in between sample changes during the second day of

analysis to check for instrumental drift. All analyses reported here are corrected to the gas blank. The isotopes analyzed, As, Sn, Zn, Pb, Ag, Sr, and Ba (Table 8.3), were chosen to help determine the sources of metal colorants and the presence of feldspar in batch materials.

Table 8.3 LA-ICP-MS Analyses of Glasses and Glazes from Hasanlu (wt% isotope)

Museum Registration # (UPenn.)	Zn66	As75	Sr88	Ag109	Sn118	Ba137	Pb208
<b>Blue transparent-translucent (tp-tl) glasses</b>							
65-31-396d	0.0054	0.0016	0.0142	0.0001	0.0140	0.0861	0.0126
73-5-559a	0.0006	0.1076	0.0115	bd	0.0139	0.0471	0.0573
73-5-559e	bd	0.0115	0.0069	bd	0.0142	0.0358	0.0148
65-31-267a	0.0100	0.0052	0.0239	bd	0.0184	0.0357	0.0299
61-5-95a	bd	0.0005	0.0236	bd	0.0141	0.0290	0.0677
65-31-273a	bd	0.0009	0.0280	bd	0.0139	0.0304	0.0211
<b>Black glasses</b>							
65-31-396e	0.0063	0.0008	0.0129	bd	0.0140	0.0401	0.0148
65-31-396f	bd	0.0122	0.0069	bd	0.0139	0.0254	0.0121
65-31-396g	0.0608	0.0369	0.0133	bd	0.0140	0.0282	0.0129
61-5-95a	bd	0.0006	0.0305	bd	0.0142	0.0355	0.1354
65-31-397a	0.0002	0.0007	0.0277	bd	0.0139	0.0351	0.0313
65-31-728c	bd	0.1590	0.0389	bd	0.0141	0.0344	0.0309
<b>Blue opaque (turquoise) glasses</b>							
65-31-728e	bd	0.4251	0.0221	0.0004	0.0420	0.0334	0.0418
65-31-728f	bd	0.5383	0.0266	0.0006	0.0393	0.0365	0.0514
65-31-992	bd	0.3455	0.0286	0.0004	0.0142	0.0345	0.0414
65-31-283	bd	0.1390	0.0303	bd	0.0142	0.0724	0.0444
65-31-993	bd	0.2134	0.0372	bd	0.0141	0.0337	0.0356
73-5-781	bd	0.0060	0.0419	bd	0.0173	0.0333	0.0167
<b>Blue transparent-translucent Glazes</b>							
60-20-346	bd	0.0079	0.0288	bd	0.1528	0.0374	0.0193
63-5-64	0.0366	0.0061	0.0310	0.0005	0.1416	0.0374	0.0876

## RESULTS

Results of major element analyses on the glasses and glazes are presented in Tables 8.1 and 8.2, and trace element analyses in Table 8.3. Analytical results on some glasses and glazes are published in Stapleton and Swanson (Chapter 4, 2002a; Chapter 5, 2002b) and Stapleton et al. (submitted; Chapter 6). The glasses contain about 52-72 wt% SiO<sub>2</sub>, 12-22 wt% Na<sub>2</sub>O, 0.7-4.2 wt% K<sub>2</sub>O, 0.7-6.4 wt% MgO, 1.7-9.3 wt% CaO. Aluminum occurs at around 0.8-6 wt% Al<sub>2</sub>O<sub>3</sub> and iron at between 0.4 wt% and 15 wt% FeO. Most glasses contain P<sub>2</sub>O<sub>5</sub>, SO<sub>3</sub>, and Cl at less than 1 wt% each. Antimony occurs in the blue opaque, yellow opaque, and white opaque glasses at around 1—8 wt% Sb<sub>2</sub>O<sub>5</sub>, mostly in the crystalline colorants. The antimony and lead reported in some of the blue tp-tl and black glasses occurs in discrete phases that are not homogeneously distributed in these samples, and the Sb<sub>2</sub>O<sub>5</sub> and PbO values listed in Table 8.1 may not be representative of an entire glass sample. Copper in the black glasses is also inhomogeneously distributed. The yellow opaque glasses contain around 7 wt% to 17 wt% PbO, partly in the crystalline colorant and partly in the glass matrix. In the blue opaque and blue tp-tl glasses, copper occurs at around 0.6-4.8 wt% CuO. Cobalt was not detected in the blue opaque glasses. Tin was not detected in the blue opaque or blue tp-tl glasses. Neither cobalt nor tin were analyzed in any of the other glasses.

The glazes contain about 50-70 wt% SiO<sub>2</sub>, 5.5-15 wt% Na<sub>2</sub>O, 2.2-5.6 wt% K<sub>2</sub>O, 1-5 wt% MgO, 2-8.5 wt% CaO. Aluminum occurs at around 1.2-3.2 wt% Al<sub>2</sub>O<sub>3</sub> and iron around 0.5-2.2 wt% FeO. Phosphorus and sulfur are present at less 1 wt% each of P<sub>2</sub>O<sub>5</sub> and SO<sub>3</sub>, except for two blue glazes that contain about 1.2 wt% SO<sub>3</sub>. Chlorine varies from 0.1 wt% to 1.4 wt% Cl. The blue transparent glazes contain about 3-5 wt% CuO. The yellow glaze contains almost 30 wt% PbO and 2 wt% Sb<sub>2</sub>O<sub>5</sub>. The white opaque glaze contains about 3 wt% PbO and 2.5 wt% Sb<sub>2</sub>O<sub>5</sub>. Occasional, small, <5 um, crystals of calcium antimonate or tin-oxide occur in the blue glazes, which are reflected in the

Sb<sub>2</sub>O<sub>5</sub> content of three of the blue glazes. Details of the blue glazes on the bridge-spouted vessels are discussed in Stapleton et al. (submitted; Chapter 6). The colorants were identified using chemical analysis and modern glass color chemistry theory (Bamford, 1977; Weyl, 1951). All of the blue tp-tl and blue opaque glasses and glazes are colored by Cu<sup>2+</sup> dissolved in the glass matrix. The blue opaque glasses are opacified by crystalline Ca<sub>2</sub>Sb<sub>2</sub>O<sub>7</sub>. White glasses and glazes are colored and opacified by Ca<sub>2</sub>Sb<sub>2</sub>O<sub>7</sub>. Yellow opaque glasses and glazes are colored and opacified by Pb<sub>2</sub>Sb<sub>2</sub>O<sub>7</sub>. Black glasses are colored and opacified by sub-micron-sized, spherical inclusions of Fe<sub>x</sub>Cu<sub>y</sub>S. Some of the sulfide inclusions also contain antimony and/or lead.

## DISCUSSION

### **Alkali Content in Fresh vs. Corroded/Weathered Glass**

Analyses of high alkali glass must be examined with some caution because of the ease with which these glasses react with water (Newton, 1989). Corrosion and weathering can change the alkali content of glass, first and primarily by exchange of water for sodium and subsequently by breakdown of the silica network in the glass. Many of the glasses plotted in Fig 8.1 were analyzed by bulk chemical techniques which can include some small areas of corroded glass, invisible to the unaided eye. Using the imaging capabilities of the electron microprobe, corroded or otherwise altered areas of glass can be avoided during chemical analysis. Microprobe analyses of corroded areas of Hasanlu glasses, normalized to Na<sub>2</sub>O, show that K<sub>2</sub>O is usually greater than in fresh glass by up to 300%, and that MgO is usually lower by at least 30% (Fig 8.2). Corroded glasses from Hasanlu generally yield microprobe analysis totals that are up to 20 wt% less than fresh glass (Fig 8.3). Analysis of synthetic glasses made with between 0 wt% H<sub>2</sub>O and 10 wt% H<sub>2</sub>O (Swanson, 1977, 1979) yield analysis totals that are consistent with their water contents (Fig 8.4). Thus analysis totals of around 100 wt% for Hasanlu

glasses from this study are of fresh, uncorroded material, and the lower analytical totals represent weathering (hydration) in the Hasanlu glass.

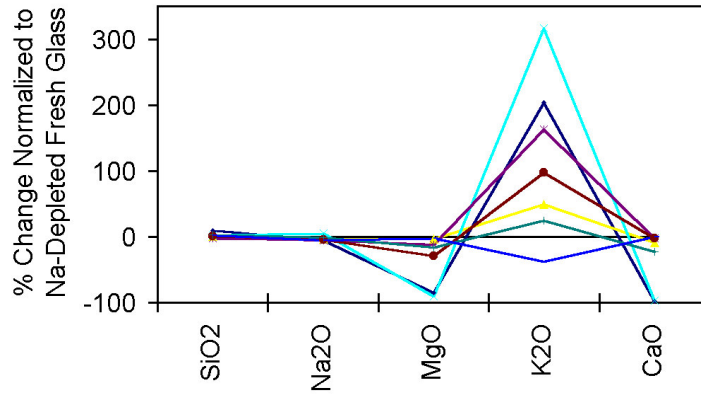


Fig 8.2. Major oxides of weathered glasses normalized to Na<sub>2</sub>O in those glasses.

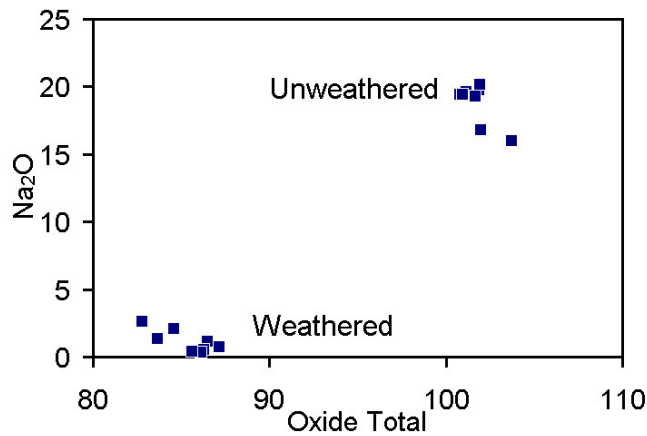


Fig 8.3. Analytical totals of microprobe analyses of weathered and unweathered glasses from Hasanlu.

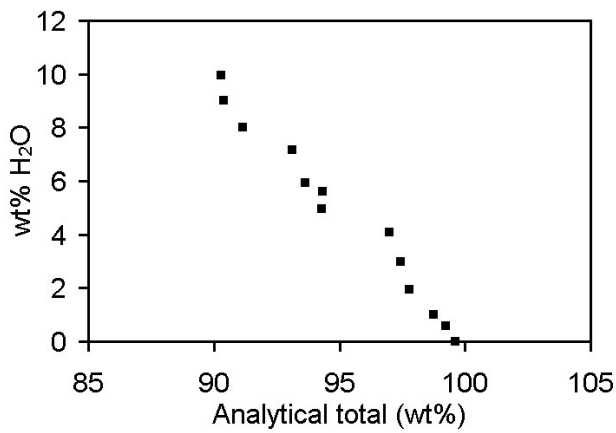


Fig 8.4. Experimental glasses containing between 0-9.96 wt% H<sub>2</sub>O (Swanson, 1977, 1979). Decreasing totals reflect glasses with increasingly greater water content.

## **Raw and synthesized materials used in Hasanlu glasses**

The variations in the chemical compositions of glasses from Hasanlu are the result of the glassmaking process and not the result of weathering. Inclusions of partly reacted batch materials remain in a number of glasses and are used to identify some of the original glassmaking batch materials. Using simple bivariate plots, bulk compositions of glass can be shown to be mixtures of two or more materials. If original compositions of the raw materials are known or can be realistically estimated, then proportions of the original materials can be calculated. This has been shown to work well with uncolored glasses made with a natron-sand mix and with a natron-sand-plant ash mix (Brill and Wosinski, 1965; Brill, 1967; Freestone and Gorin-Rosen, 1999). Interpretation of raw materials used in intentionally-colored glasses like those from Hasanlu are complicated by the addition of components that come in with the colorant and possibly by additional steps used in manufacturing these colored glasses. The additional components and steps can add elements that normally enter with the main glassmaking ingredients, including Si, Al, Na, K, Mg, and Ca, changing the ratios from those of the initial raw materials. This seems to be the case for the Hasanlu glasses. Most of the glasses from Hasanlu do not have straight line mixing relationships in bivariate plots of the major glassmaking oxides. In the following discussion, examples that more clearly show the presence of specific phases in glassmaking batches are used to infer the presence of these phases in other glasses.

### *Plant Ash*

Round inclusions rich in sulfur and containing sodium, potassium, and sometimes chlorine occur in many of the Hasanlu glasses and glazes (Fig 8.5, Table 8.4). The sulfur-rich inclusions are 10-50  $\mu\text{m}$  in diameter in all of the glasses except the blue opaques (turquoise), where they are on the order of 5  $\mu\text{m}$  in diameter (when present). Glass surrounding and in contact with the inclusions is not corroded, indicating

that the inclusions were not deposited during weathering of the glass. It is apparent from the spherical shape of the inclusions that they existed as immiscible liquids in the melt that formed the glass. Immiscible phases are normally allowed to float to the top of a glassmaking melt, and are then removed from the melt to make a more clear, inclusion-free glass. The terms gall, scum, salt cake, or sandiver are used by glassmakers to describe immiscible phases that form in glassmaking melts. Gall is usually composed mainly of alkali sulfates with smaller amounts of alkali chlorides (Turner, 1956). The cuneiform glassmaking texts make two references to scum that forms on top of glasses made during intermediate steps but do not specifically state to remove it (Oppenheim, 1970).

Table 8.4. Microprobe Analyses of Alkali Sulfate Inclusions in Hasanlu Glasses

UPenn. # (glass color)	Na <sub>2</sub> O	K <sub>2</sub> O	SO <sub>3</sub>	Cl
65-31-273a (blue tp-tl)	40.5	2.9	14.3	0.6
73-5-559e (white opq)	44.5	1.1	29	0.3
75-29-307a (yellow opq)	40.7	5.1	30	0.4

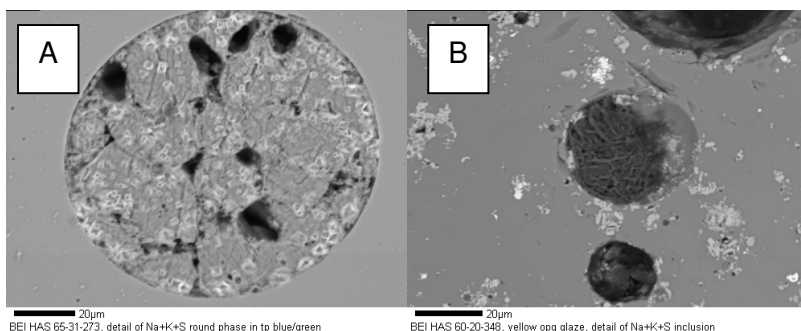


Fig 8.5. Rounded inclusions rich in Na, K, S, and Cl. Back scattered electron images (BSI). Scales bars are 20 µm. A) Mid-grey, largest, blocky crystals inside inclusion contain Na, K, and S. Small, white to grey cubic crystals contain Na and Cl and are probably halite (NaCl). Blue tp-tl glass from bead, UPenn 65-31-273. B) Two phases exist in the round inclusion in the center of the image. The dark phase contains mostly Na and S, and the interstitial, lighter phase contains mostly K and S. Yellow opaque glaze on Assyrian-style vessel, UPenn. 60-20-348.

Analyses of the alkali- and sulfur-bearing inclusions were carried out using electron microprobe (Table 8.4). These analyses are considered to be semi-quantitative because severe degradation of the inclusions under the electron beam. The compositions, however, are consistent with alkali sulfate and chloride minerals similar to thenardite ( $\text{Na}_2\text{SO}_4$ ), apthitalite ( $(\text{K}, \text{Na})_3\text{Na}(\text{SO}_4)_2$ ), and halite ( $\text{NaCl}$ ). Alkali sulfate phases are extremely soluble in water. The use of alcohol (acetone or methanol) during sample preparation preserved these inclusions. Other phases that appear to have been part of immiscible liquids include K-Ca-phosphate, Ca-sulfate, and Mg-Si-S-bearing phases, but are not common in the glasses. The sulfate phases are not likely to have been added to the glasses as sulfides grains because the textures after reaction of sulfide with the silicate glass melt would have been significantly different (Larocque et al., 2000).

The sulfate inclusions occur in all the colors of glasses discussed in this paper, including those that have low (<1.5 wt%)  $\text{K}_2\text{O}$  and  $\text{MgO}$ . These inclusions must thus have entered the glass in one of the main glassmaking materials, rather than with any particular colorant. Plant ashes usually contain sodium sulfate and potassium sulfate phases, which can occur on the order of 10 wt% in ashes of salt-tolerant desert plants (Brill, 1970a). Sources of glassmaking quartz, the other main ingredient in early glasses, do not normally contain sulfate as high as that found in plant ashes. It is suggested that all of the glasses from Hasanlu analyzed in this paper were made using plant ash. Glasses with low  $\text{K}_2\text{O}$  and  $\text{MgO}$  are mainly black and blue tp-tl glasses and were probably made with a smaller proportion of plant ash (see discussion of blue tp-tl in "Potassium Feldspar" and black in "Polymetallic sulfides"). The difference in the size of alkali sulfate inclusions that occur in the blue opaque glasses could have been caused by crushing the glass and washing it in water. A second way to remove the inclusions would have been to allow them to rise to the surface of the melt, where they could have

been scraped off. The phases produced during ashing and the chemical composition of plant ash are notoriously variable, being affected by many factors including season of plant harvest, part of plant ashed, parent soil composition, climate, and ashing technique (Sanderson and Hunter, 1981; Smedley et al., 2001). Variation in the amount of sulfate present in the Hasanlu glasses may be explained partly by variations in ashing. Some differences in absolute levels of  $K_2O$  and  $MgO$  in the glasses may also be attributed to inhomogeneous ash compositions.

### *Quartz*

The major source of silica in ancient and modern glasses is the mineral quartz, which exists in a wide variety of geologic settings. The most common source of pure quartz pebbles is hydrothermal veins. The use of this type of quartz would contribute silicon and oxygen to a glass, with only trace amounts (less than about 0.01 wt%) of other elements. Another common source of quartz is in sand, which is typically composed mainly of quartz and lesser amounts of accessory minerals including aluminum-rich feldspars and clays, and iron oxides. If sand is used to make glass, significant amounts of  $Al_2O_3$  and  $FeO$  can be contributed by the accessory minerals, as in early Roman glasses which contain 2-3 wt%  $Al_2O_3$  and 0.5 wt%  $FeO$  (Henderson, 1991; Stapleton, submitted). Proportionally smaller amounts of other elements that make up feldspars and clays may also enter the glass. Low-iron batch materials are preferred for making white opaque glass because of the color which small amounts of iron can impart (Weyl, 1951), and low-iron quartz sources are typically chosen to make this color of glass. If all of the iron in the white and blue opaque glasses is assumed to have entered with the quartz, then the quartz source would have contained about 0.5-2 wt%  $FeO$ , significantly greater than normally occurs in hydrothermal vein quartz.

If all of the aluminum entered the glasses in a sand, then a positive correlation should exist between  $SiO_2$  and  $Al_2O_3$ . There are, however, no clear positive correlations

between these two oxides, in either the entire group of analyzed glasses and glazes (Fig 8.6) or in most analyses grouped by glass or glaze color. One group of blue tp-tl glasses with high MgO (> 2 wt%) and multiple analyses of a blue glaze (UPenn. 60-20-344) show generally higher Al<sub>2</sub>O<sub>3</sub> with higher SiO<sub>2</sub>. No positive correlations appear to exist between SiO<sub>2</sub> and the other major oxides that are not colorants, Na<sub>2</sub>O, K<sub>2</sub>O, and CaO. Analyses in some glazes and one blue opaque glass show that they contain aluminum-bearing inclusions with compositions close to those of feldspars and aluminum-rich areas that are probably melted or partly-melted feldspars, but there is no mixing line between the aluminum-rich phases and pure quartz (Fig 8.7).

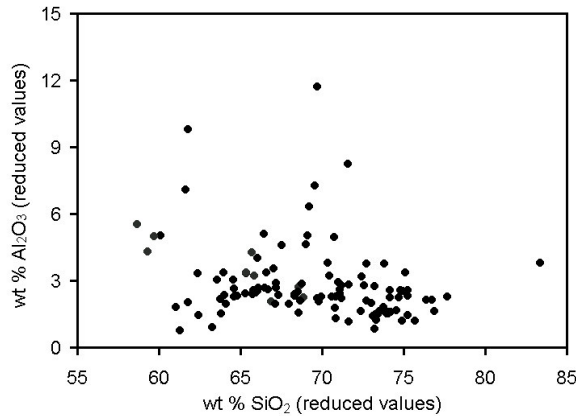


Fig 8.6. SiO<sub>2</sub> and Al<sub>2</sub>O<sub>3</sub> in the glasses and glazes from Hasanlu. No correlation exists between these components, which are consider to enter the glasses in quartz-rich sand. Reduced values are from bulk compositions recalculated to include only SiO<sub>2</sub>, Al<sub>2</sub>O<sub>3</sub>, MgO, CaO, Na<sub>2</sub>O, K<sub>2</sub>O, oxides associated with the major glassmaking batch materials.

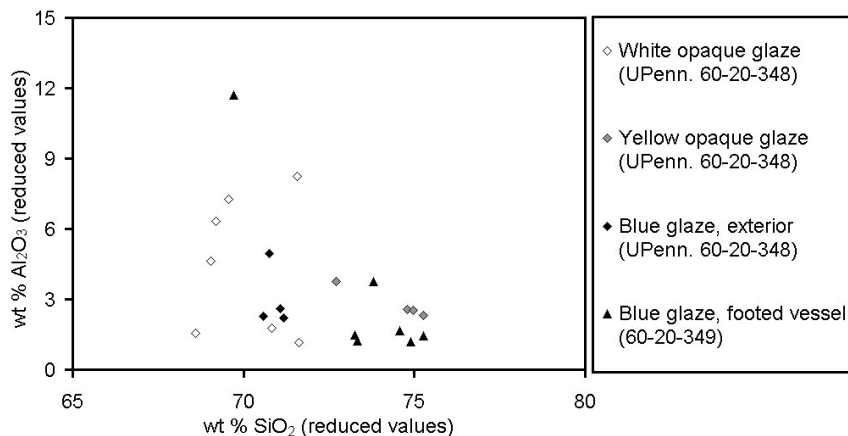


Fig 8.7. Multiple analyses on glazes show Al<sub>2</sub>O<sub>3</sub>-rich areas. For definition of “reduced values”, see Fig 8.6.

Relationships between  $\text{SiO}_2$  and  $\text{Al}_2\text{O}_3$ ,  $\text{Na}_2\text{O}$ ,  $\text{K}_2\text{O}$ , and  $\text{CaO}$  in some samples point more clearly to the presence of feldspars in the batch materials. Plots of  $\text{Na}_2\text{O}$ ,  $\text{K}_2\text{O}$  and  $\text{Al}_2\text{O}_3$  (Fig 8.8) and of  $\text{Na}_2\text{O}$ ,  $\text{CaO}$ , and  $\text{Al}_2\text{O}_3$  (Fig 8.9) suggest that the proportions of these oxides in the yellow opaque glasses (bulk compositions) and the white opaque and yellow opaque glazes (multiple analyses on each sample) on an Assyrian-style vessel were partly controlled by the presence of alkali feldspars and not plagioclase. The batch for the yellow opaque glaze on the Assyrian-style vessel might have contained both alkali feldspar and plagioclase feldspar because the proportions of  $\text{K}_2\text{O}$ ,  $\text{Na}_2\text{O}$ , and  $\text{CaO}$  suggest affinities with both feldspars. Blue glaze on a footed vessel appears to have contained muscovite (perhaps altered potassium feldspar?) in the batch material. Grains of quartz, sodium-rich alkali feldspar, and plagioclase feldspar also occur in blue tp-tl and yellow opaque glasses. The inclusions are not common and do not occur in all samples of these colors. The inclusions are rounded to sub-angular and range in size from about 50  $\mu\text{m}$  to 0.5 mm in largest dimension, consistent in size and shape with derivation from sand (Stapleton and Swanson, 2002a).

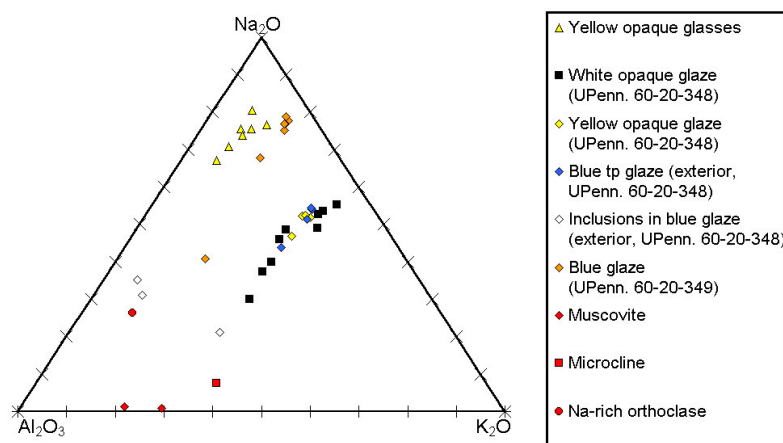


Fig 8.8.  $\text{Na}_2\text{O}$ ,  $\text{K}_2\text{O}$ , and  $\text{Al}_2\text{O}_3$  (wt%) proportions in white opaque, yellow opaque, and blue tp glazes (each point is one analysis) on an Assyrian-style vessel (UPenn. 60-20-348) show evidence of mixing of potassium feldspar with low  $\text{Al}_2\text{O}_3$  material. Blue glaze on another vessel and yellow opaque glasses (averages of multiple analyses) show mixing of sodium-rich alkali feldspar with low  $\text{Al}_2\text{O}_3$  material. Mineral data from Deer et al. (1966).

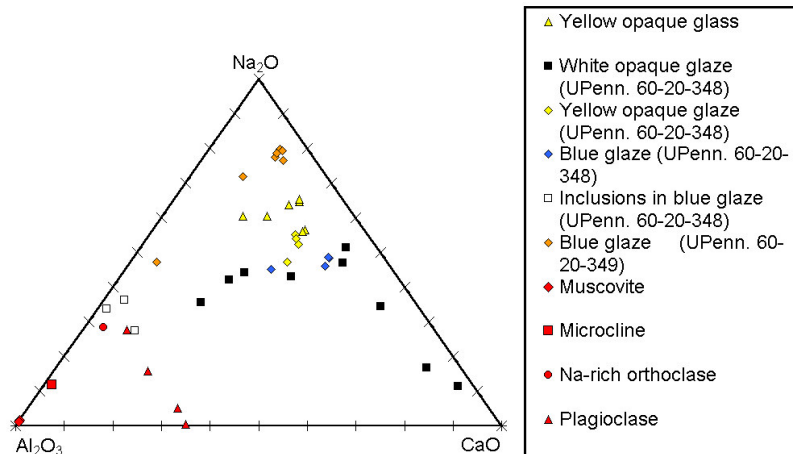


Fig 8.9. Same data as Fig 8.8.  $\text{Na}_2\text{O}$ ,  $\text{CaO}$ , and  $\text{Al}_2\text{O}_3$  (wt%) proportions in glazes and glasses do not show addition of plagioclase feldspar.

The source of  $\text{SiO}_2$  in the Hasanlu glasses and glazes is suspected to be a sand, based mainly on the iron content of the white opaque and blue opaque colors and on the physical evidence for the presence of quartz and feldspar in some of the samples, and on the proportions of feldspar-forming oxides in some of the samples. The presence of feldspars and aluminum-rich phases but the lack of clear positive  $\text{SiO}_2$ - $\text{Al}_2\text{O}_3$  correlations in most of the bulk compositions may indicate that the glasses and glazes were made with different sources of sand. The wide range in oxygen isotope compositions is consistent with origin of quartz from a variety of sources (Stapleton et al., Chapter 7). The cuneiform glassmaking texts call for addition of a quartz-bearing raw material in multiple steps during the manufacture of many of the glasses they describe. Additionally, the texts state that multiple batch materials, each made with different proportions of a quartz-bearing raw material, are required to be mixed together to produce certain colored glasses. These multiple steps would obscure the ratios of  $\text{SiO}_2$  to  $\text{Al}_2\text{O}_3$ ,  $\text{Na}_2\text{O}$ ,  $\text{K}_2\text{O}$ , and  $\text{CaO}$  in the original quartz-bearing raw material(s). The chemical relations in the Hasanlu glasses and glazes may also be the result of multiple mixing steps similar to those describe in the cuneiform glassmaking texts.

### *Potassium Feldspar*

A group of low MgO blue tp-tl glasses that have a negative  $\text{SiO}_2\text{-Al}_2\text{O}_3$  correlation, also exhibit a positive  $\text{K}_2\text{O}$  and  $\text{Al}_2\text{O}_3$  correlation (Fig 8.10). In addition, Ba and Sr are correlated with  $\text{K}_2\text{O}$  and  $\text{Al}_2\text{O}_3$  (Fig 8.11). The associations between K, Al, Sr, and Ba in this group of low MgO blue tp-tl glass suggest that these elements entered the glass in the same material, an aluminum- and potassium- bearing mineral. In the low MgO blue glasses, the wt%  $\text{K}_2\text{O}:\text{Al}_2\text{O}_3$  ratio ranges from 0.4 to 0.8, consistent with derivation of potassium from either muscovite, a potassium-rich mica, or potassium feldspar, but not a clay mineral such as illite. Ratios of  $\text{K}_2\text{O}:\text{Al}_2\text{O}_3$  less than about 0.6 are lower than expected for potassium feldspar. Feldspars commonly alter to potassium-rich micas during weathering and hydrothermal alteration, and the range in  $\text{K}_2\text{O}:\text{Al}_2\text{O}_3$  in the low MgO blue tp-tl glasses may represent partially altered potassium feldspar. The  $\text{K}_2\text{O}:\text{Al}_2\text{O}_3$  ratio may have been affected by addition of  $\text{Al}_2\text{O}_3$  during the glassmaking process. Aluminum can enter a glass melt through several routes including from the sand used as the silica source or from clay crucibles used in high temperature processes, both of which would decrease the  $\text{K}_2\text{O}:\text{Al}_2\text{O}_3$  ratio from that of a potassium feldspar. Aluminum may also be added to glass melt through coloring agent mixtures, as appears to be the case for the black glasses (Fig 5.2, Stapleton and Swanson, 2002b), but there is no correlation between aluminum and the copper colorant in these blue glasses. Assuming that all of the  $\text{Al}_2\text{O}_3$  in the blue tp-tl glasses came in with a potassium feldspar, the proportion of potassium feldspar in the batch would have been around 10-30 % by weight.

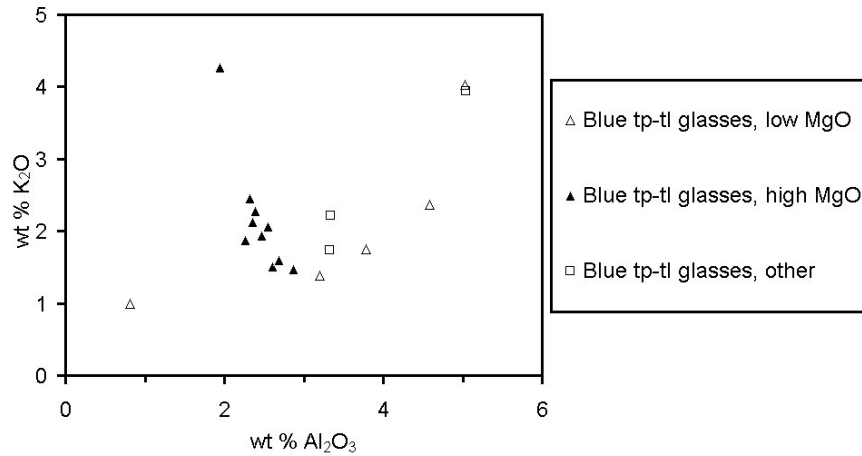


Fig 8.10. Blue tp-tl glasses can be divided into three groups based on major element chemistry, “low MgO”, “high MgO”, “other” (Fig. 5.2). “Low MgO” blue tp-tl glasses show positive correlation between Al<sub>2</sub>O<sub>3</sub> and K<sub>2</sub>O.

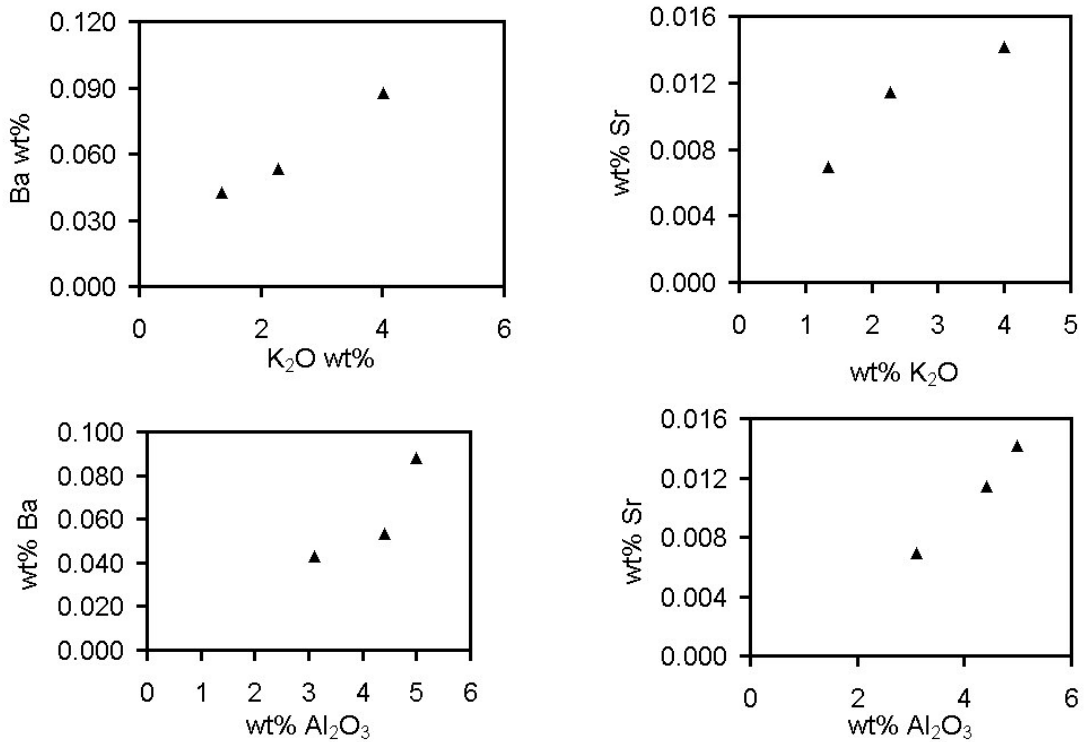


Fig 8.11. Low MgO blue tp-tl glasses. Positive correlations between Ba, Sr and K, and Ba, Sr, and Al<sub>2</sub>O<sub>3</sub> in the low MgO blue tp-tl glasses, but not in other glasses, suggest that potassium feldspar was a large component of the batch material.

Along with the low MgO blue tp-tl glasses, a group of three other samples of blue tp-tl glasses (“Other” group, Fig 8.10), a blue glaze on a bridge-spouted vessel (UPenn. 60-20-346), and the yellow opaque glasses show generally higher  $\text{Al}_2\text{O}_3$  with lower  $\text{SiO}_2$  (Fig 8.12). The negative  $\text{SiO}_2$ - $\text{Al}_2\text{O}_3$  correlations suggest that the majority of these two components were added in separate batch ingredients. The proportions of  $\text{Al}_2\text{O}_3$ ,  $\text{Na}_2\text{O}$ ,  $\text{K}_2\text{O}$ , and  $\text{CaO}$  presented in Figs 8.8 and 8.9 suggest that the  $\text{Al}_2\text{O}_3$  probably came from feldspar. The amount of  $\text{SiO}_2$  contributed from the proportion of feldspar apparently present in the batches, based on total  $\text{Al}_2\text{O}_3$  content, would not be great enough to account for the high  $\text{SiO}_2$  of the bulk compositions, but probably came from quartz. These glasses may have been made in fewer steps than detailed by the cuneiform glassmaking texts, and perhaps were single step mixes of plant ash, sand, feldspar, and colorant. Fewer mixing and melting steps are also suggested by colorant-related inclusions, as discussed below in “Copper Minerals” and “Lead Antimonate”.

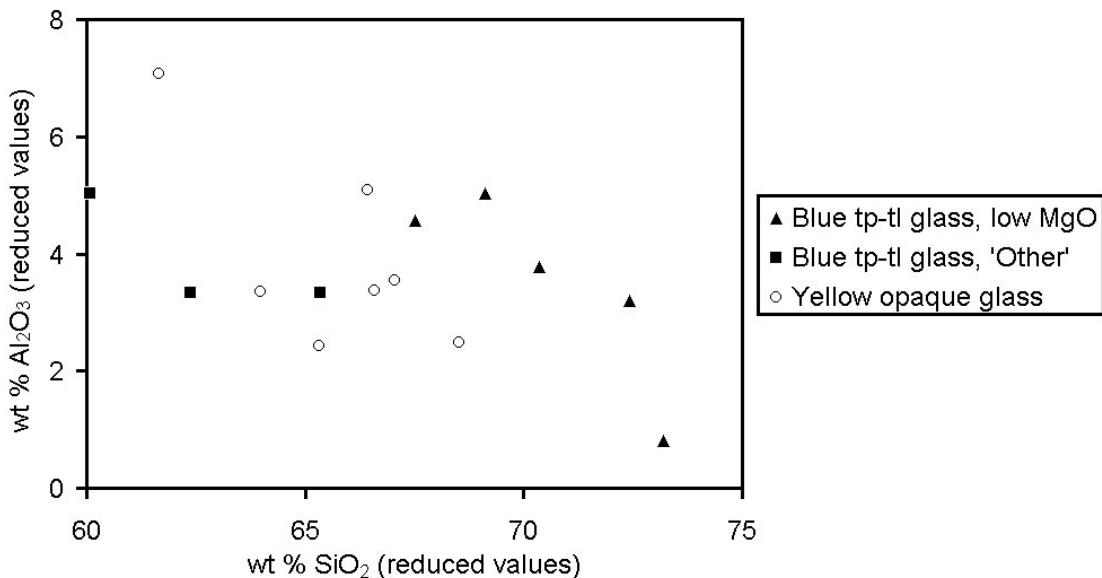


Fig 8.12. The yellow opaque glasses and some blue tp-tl glasses and exhibit generally lower  $\text{Al}_2\text{O}_3$  with higher  $\text{SiO}_2$ . Data shown here have been recalculated to include only  $\text{SiO}_2$ ,  $\text{Al}_2\text{O}_3$ ,  $\text{MgO}$ ,  $\text{CaO}$ ,  $\text{Na}_2\text{O}$ , and  $\text{K}_2\text{O}$  and then normalized to 100 wt% (reduced values) because of the presence of >10 wt% coloring oxides in the yellow opaque glasses.

### *Dolomite*

There is strong evidence that a calcium-magnesium carbonate mineral or rock was intentionally used in the vitreous materials excavated from Hasanlu. Calcium is an important component of alkali-silica glasses because it stabilizes the atomic structure of sodium-rich glasses so that they are not soluble in water. Calcium is also a component of the white antimonate compound that colors and opacifies many glasses. A white opaque glaze on a vessel (UPenn. 60-20-348) decorated in imitation of Assyrian style has an inhomogeneous microstructure dominated by three phases, one of which is crystalline  $\text{Ca}_2\text{Sb}_2\text{O}_7$  which colors and opacifies the glaze (Fig 8.13). The other two phases, represented by "A" and "B" in Fig 8.13, are amorphous and distinguished from each other mainly by CaO and MgO content (Table 8.5). Phase "A" in Fig 8.13 contains about five times less CaO and MgO and greater  $\text{SiO}_2$ ,  $\text{Al}_2\text{O}_3$ ,  $\text{Na}_2\text{O}$ ,  $\text{K}_2\text{O}$ ,  $\text{PbO}$ , and  $\text{Sb}_2\text{O}_5$  than phase "B". Phase "B" is interstitial to "A", contains vesicles on the order of about 1  $\mu\text{m}$  diameter and most of the  $\text{Ca}_2\text{Sb}_2\text{O}_7$  crystals. Element maps of Ca and Mg (Fig 8.14) show that these elements are concentrated in phase "B". Multiple analyses of different areas in phase "B" show a positive correlation between CaO and MgO, indicating that these components entered the glass together. The ratio of CaO:MgO in phase "B" is the same as that of the mineral dolomite,  $\text{CaMg}(\text{CO}_3)_2$ , strongly suggesting that dolomite was a major component of this phase. The vesicles present in this area were probably made as the dolomite decomposed to yield  $\text{CO}_2$  gas upon heating.

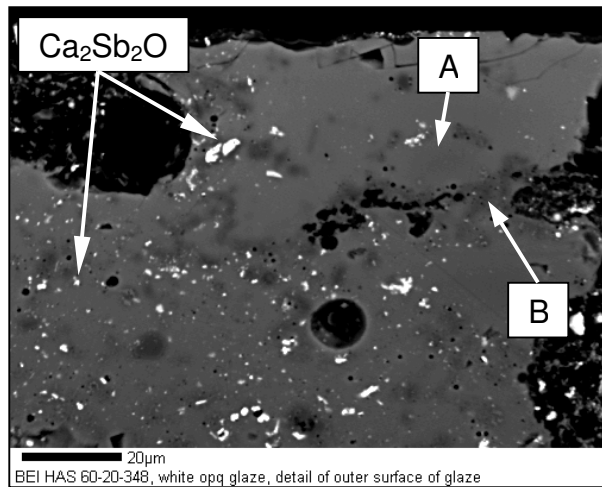


Table 8.5

	A	B
SiO <sub>2</sub>	63.5	55.7
Al <sub>2</sub> O <sub>3</sub>	7.3	1.6
MgO	2.3	10.3
CaO	3.4	17.5
Na <sub>2</sub> O	5.9	3.8
K <sub>2</sub> O	6.4	2.4
PbO	4.3	2.0
Sb <sub>2</sub> O <sub>5</sub>	2.4	1.2
SO <sub>3</sub>	<0.4	0.9
Cl	0.1	0.2

Fig. 8.13. White opaque glaze on Assyrian style vessel (UPenn. 60-20-348) is composed of a phase that has angular borders (“A”), appearing to have been added as fragments, and an interstitial phase (“B”) rich in Ca-Mg which contains most of the Ca<sub>2</sub>Sb<sub>2</sub>O<sub>7</sub> crystals. BSI. Scale bar is 20 um.

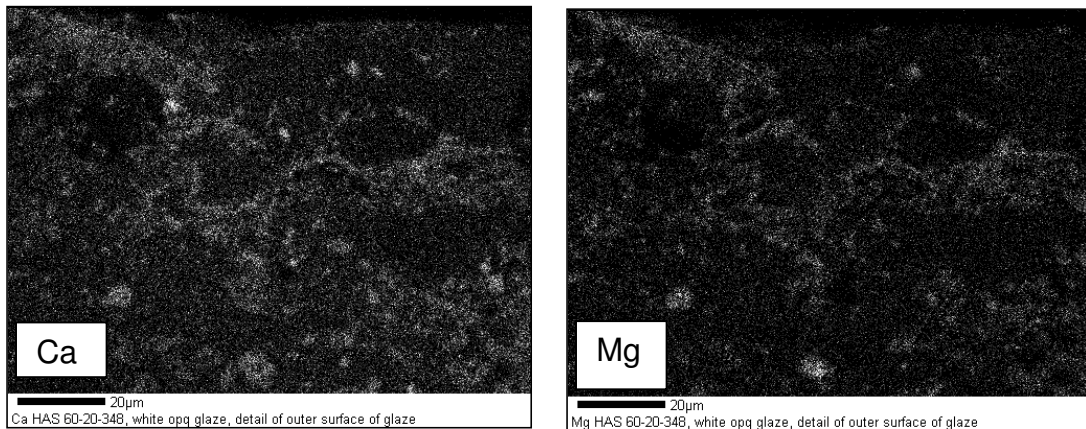


Fig 8.14. Elemental maps of Ca and Mg distribution in area of white opaque glaze shown in Fig 8.13. Scale bars are 20 um.

Most of the white opaque glasses from Hasanlu are heavily weathered. Analyses of apparently unweathered areas of white opaque glasses are available from only three samples. There is no remnant dolomite in these white glasses, but two have CaO:MgO ratios similar to those of the white glaze and of dolomite (Fig 8.15), suggesting that dolomite was part of the batch material. The lower absolute levels of

CaO and MgO in the white glasses compared to the dolomite-rich area of the glaze indicates that a smaller proportion of dolomite was used in the glassmaking materials.

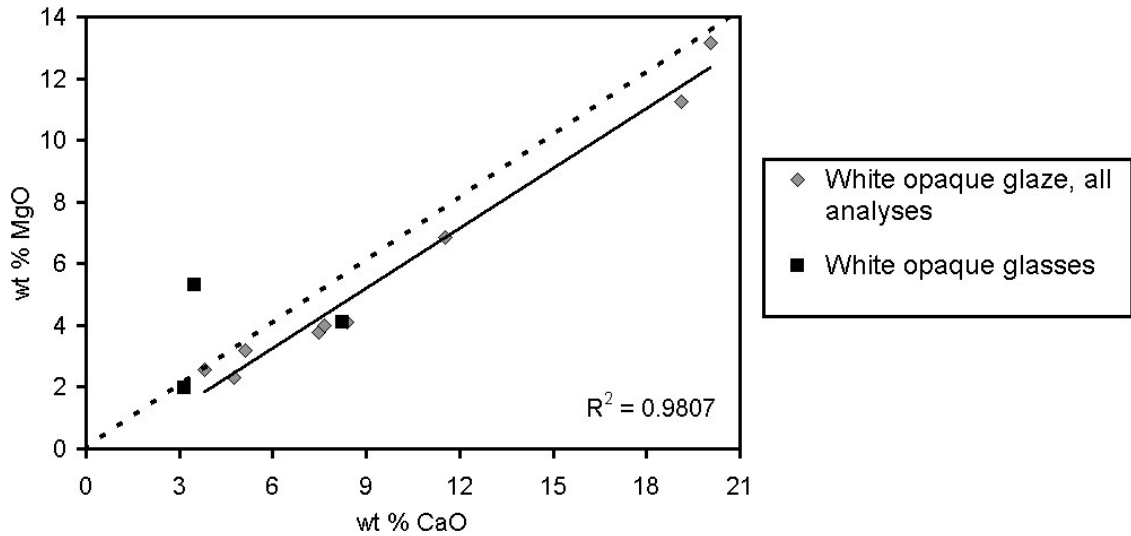


Fig 8.15. White opaque glaze and glasses. Solid line is regression line fitted to analyses of high and low MgO areas of white opaque glaze in Fig 8.13 (UPenn. 60-20-348). Dolomite CaO:MgO ratio represented by dashed line.

The blue opaque glasses have a generally positive correlation between CaO and MgO and can be divided into two groups based on the levels of these oxides (Fig 8.16). The glasses in the low MgO group have CaO:MgO ratios similar to dolomite. A plot of K<sub>2</sub>O and MgO shows the negative mixing relationship expected in the low MgO glasses from mixing dolomite with plant ash that contained about 2.5 wt% K<sub>2</sub>O and 2.7 wt% MgO. The CaO:MgO ratios in the group of the high MgO blue opaques are different from dolomite. The higher K<sub>2</sub>O and MgO in these glasses is consistent with the presence of greater proportions of plant ash in these batches than for the low MgO blue opaques. A greater proportion of plant ash, which is rich in MgO, would have increased the total amount of MgO in a glass batch that was already rich in MgO from containing dolomite. Neither CaO nor MgO have positive correlations with SiO<sub>2</sub> in the white glaze

or in the blue opaque and two white opaque glasses (Fig 8.17), indicating that dolomite was not a major constituent of the sand used to make these glasses and glaze. The dolomite was probably intentionally added to the glassmaking batch materials in a separate phase from the quartz, as it was for the white opaque glaze which is seen as phase “B” in Fig 8.13.

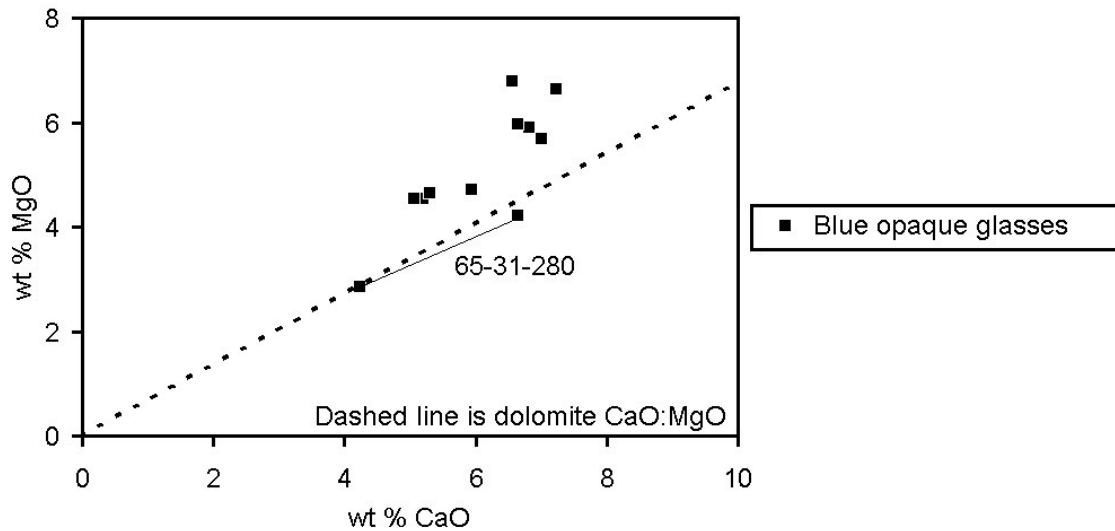


Fig 8.16. Blue opaque glasses can be divided into low MgO group (< 5 wt% MgO) and high MgO group. The low MgO group shows CaO:MgO close to dolomite. Two different areas in sample UPenn. 65-31-280 have CaO:MgO ratios similar to dolomite. The high MgO group show increasing MgO for the same CaO level, which may be from addition of a greater proportion of Mg-rich plant ash to the batch.

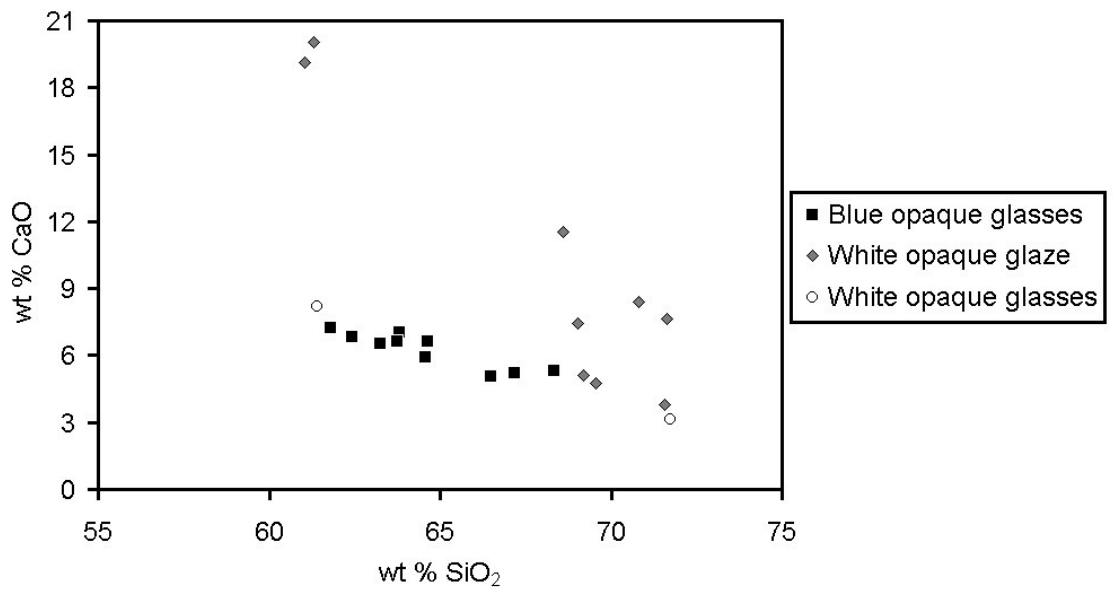
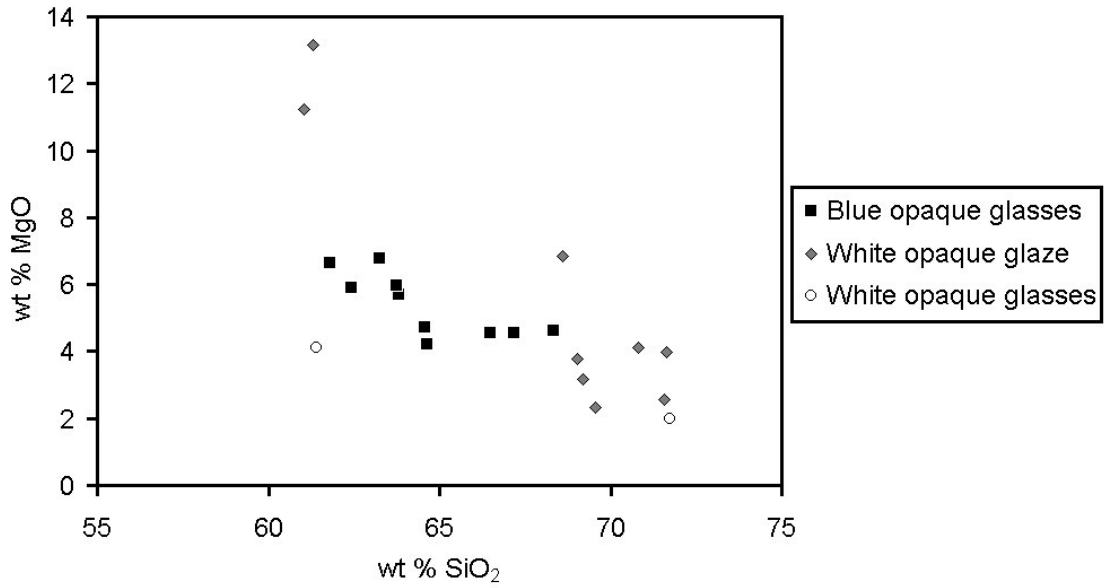


Fig 8.17. MgO and CaO do not have positive correlations with SiO<sub>2</sub> in the blue opaque glasses, white opaque glasses, white opaque glazes, suggesting that dolomite was not part of the batch material for these samples.

### *Synthesized Calcium Antimonate ( $Ca_2Sb_2O_7$ ) in White and Blue Opaques*

The calcium antimonate crystals that color and opacify the white opaque glaze appear to have been produced in two amorphous phases (“A” and “B”, Fig 8.13), both of which themselves are mixes of several phases. Phase “A” is composed of angular particles up to about 40  $\mu\text{m}$  diameter. Phase “B” is interstitial to “A” and does not appear to occur in areas more than 10  $\mu\text{m}$  wide. The two phases are represented by analyses listed in Table 8.5. Sodium values in these two analyses may be low because the analyses were carried out using electron beams with diameters smaller than the 20  $\mu\text{m}$  diameter optimized for this study. Phase “A” contains higher  $\text{SiO}_2$ ,  $\text{Al}_2\text{O}_3$ ,  $\text{Na}_2\text{O}$ ,  $\text{K}_2\text{O}$ ,  $\text{PbO}$ , and  $\text{Sb}_2\text{O}_5$ . It has already been established in a previous section that  $\text{K}_2\text{O}$  and  $\text{Al}_2\text{O}_3$  in the white glaze was added mainly from potassium feldspar (see “Quartz” and “Potassium feldspar” above). The amount of  $\text{SiO}_2$  in phase “A” is too high to be accounted for by the potassium feldspar alone and quartz also must have been present. Sodium was probably added mainly in plant ash, since a sodium-bearing feldspar does not appear to have been part of the batch (Figs 8.8 and 8.9). Plant ash also would have added  $\text{MgO}$ ,  $\text{CaO}$ , and additional  $\text{K}_2\text{O}$ . Lead and antimony in phase “A” are dissolved in the glass matrix, but their original batch material is unknown. Small,  $<2$   $\mu\text{m}$ , crystals of  $Ca_2Sb_2O_7$  occur in phase “A”. The occurrence of these crystals in “A” appears to be rare, although it is difficult to determine the boundaries between “A” and “B” when the particle sizes of “A” are small.

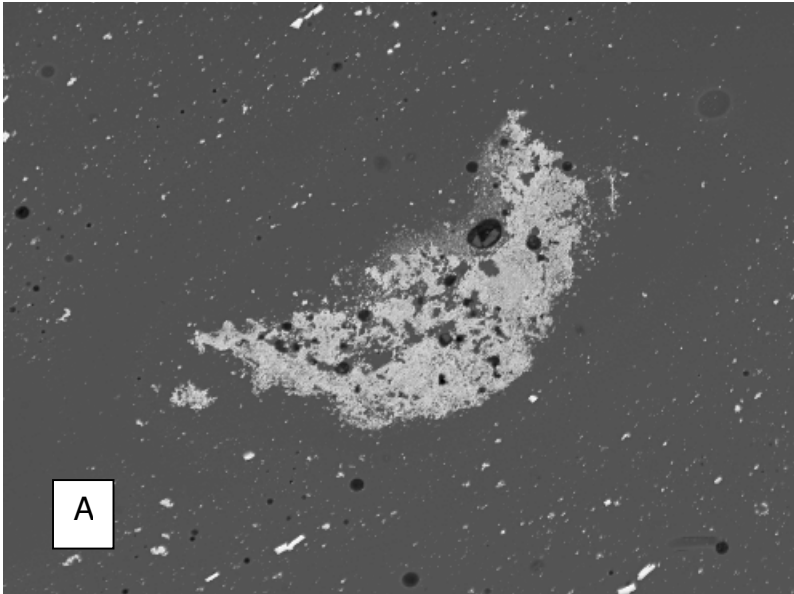
Phase “B” in the white opaque glaze was made with dolomite (see “Dolomite” above), which composed about half of the batch of “B” by weight. The remainder was made up of mainly  $\text{SiO}_2$ , probably as quartz sand. The high  $\text{K}_2\text{O}$ :  $\text{Al}_2\text{O}_3$  ratio and low  $\text{Al}_2\text{O}_3$  in phase “B” indicate that feldspar was not a main component in the batch for “B”. It is possible that a small amount of plant ash was added and would account for  $\text{Na}_2\text{O}$ ,  $\text{K}_2\text{O}$ ,  $\text{CaO}$ , and  $\text{MgO}$ . Lead and antimony occur in phase “B” at about half the amount as

in phase “A”. The molar Sb:S ratio of “B” in Figure 8.13 is the same as that for the mineral stibnite ( $\text{Sb}_2\text{S}_3$ ). No  $\text{Ca}_2\text{Sb}_2\text{O}_7$  crystals or other crystalline material was seen in the area analyzed for phase “B”. Thus, the batch material for phase “B” was probably a mix of stibnite, dolomite, quartz, plant ash, and an unknown lead material. The largest  $\text{Ca}_2\text{Sb}_2\text{O}_7$  crystals in the white opaque glaze occur in or near phase “B” mainly as individual crystals up to about 10  $\mu\text{m}$  long. Small aggregates of less than about 10  $\mu\text{m}$  also occur in “B”, but are not common.

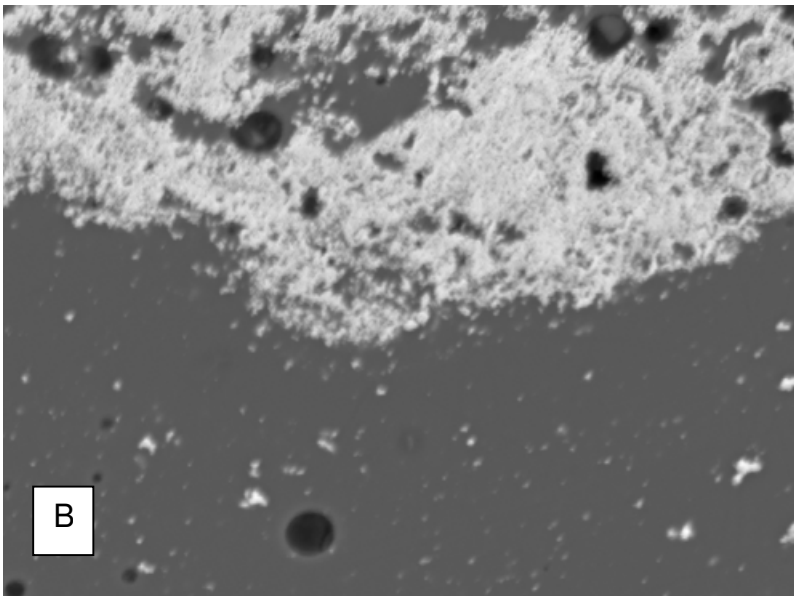
The molar  $\text{CaO}:\text{Sb}_2\text{O}_5$  ratio and the phase in which antimony is added to a batch probably affects the formation and crystal habit of  $\text{Ca}_2\text{Sb}_2\text{O}_7$ . Aggregates of  $\text{Ca}_2\text{Sb}_2\text{O}_7$  crystals of about 20  $\mu\text{m}$  and larger are common in glasses colored or opacified by calcium antimonate (Mass et al. 2002, Shortland, 2002). In experimental reproductions of white opaque and blue opaque glasses that contain  $\text{Ca}_2\text{Sb}_2\text{O}_7$ , Shortland (2002) produced glasses with large aggregates of around 40  $\mu\text{m}$  diameter of  $\text{Ca}_2\text{Sb}_2\text{O}_7$  crystals. These experiments were carried out using laboratory grade reagents, with  $\text{Sb}_2\text{O}_5$  mixed into unfired batch materials (oxides) and into pre-made glass that had been crushed to a powder. In these experiments, a molar  $\text{CaO}:\text{Sb}_2\text{O}_5$  ratio of greater than about 16 was needed to produce enough  $\text{Ca}_2\text{Sb}_2\text{O}_7$  to make the glasses opaque. In phase “B” of the white glaze from Hasanlu, the molar  $\text{CaO}:\text{Sb}_2\text{O}_5$  ratio is about 84, whereas it is less than 1 in phase “A” and probably accounts for the rare occurrence of  $\text{Ca}_2\text{Sb}_2\text{O}_7$  crystals in that phase. The well-formed  $\text{Ca}_2\text{Sb}_2\text{O}_7$  crystals seen in phase “B” and the lack of large aggregates of crystals are possibly the result of adding antimony in a phase different from Shortland’s (2002) experimental glasses, where apparently solid antimony pentoxide was used. There are aggregates of  $\text{Ca}_2\text{Sb}_2\text{O}_7$  crystals in the white opaque glasses, but these were not examined in detail.

The  $\text{Ca}_2\text{Sb}_2\text{O}_7$  crystals in blue opaque glasses act to opacify the glass and enhance the blue color given by copper. Many of the blue opaque glasses contain

irregular-shaped aggregates, up to about 0.1 mm by 0.1 mm, of  $\text{Ca}_2\text{Sb}_2\text{O}_7$  crystals. Some of the aggregates contain sulfur-rich areas (Fig 8.18) or inclusions of Na-K-sulfates (Fig 8.19). The association of these phases in aggregates with  $\text{Ca}_2\text{Sb}_2\text{O}_7$  crystals suggests that sulfide ore, perhaps stibnite, and plant ash were mixed in some step during manufacture of  $\text{Ca}_2\text{Sb}_2\text{O}_7$ . In one aggregate, the alkali sulfate (now degraded) appears to exhibit crystal faces, as opposed to the spherical form exhibited by immiscible alkali sulfate liquids in silicate (glassmaking) melts (Fig 8.5). The alkali sulfate crystals in the aggregate probably formed in a solid-state reaction where no silicate melt existed. This reaction regime suggests formation during a step that occurred prior to the batch melting that formed the glass. A mix of plant ash, calcium (perhaps as dolomite), and antimony ore may have been prepared first by heating the mix at temperatures less than 900 C, around which alkali silicates melt, to make  $\text{Ca}_2\text{Sb}_2\text{O}_7$  crystals. This mix would then be added to either a "primary" base glass that was colored blue or to a mix of raw glassmaking batch materials and melted.

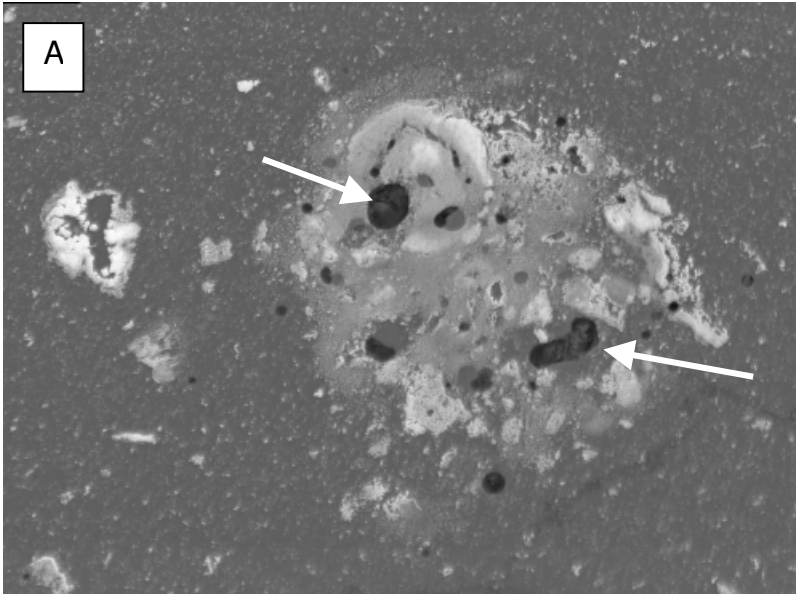


50 $\mu$ m  
BEI HAS 65\_31\_728f, detail of largest bright inclusion visible in BSI of sample



10 $\mu$ m  
BEI HAS 65\_31\_728f, detail of largest bright inclusion visible in BSI of sample

Fig 8.18. A) Aggregate of  $\text{Ca}_2\text{Sb}_2\text{O}_7$  crystals. BSI. Scale bar is 50  $\mu\text{m}$ . B) Detail of aggregate in A. Largest mid-grey area inside aggregate (top, center) is sulfur-rich glass containing about 2 wt%  $\text{SO}_3$ . Note small crystals apparently sloughing off large aggregate, showing that small  $\text{Ca}_2\text{Sb}_2\text{O}_7$  crystals may not be crystallization products directly from glass.



BEI HAS 65-31-283, turquoise, detail of largest bright BSI inclusion



BEI HAS 65-31-283, turquoise, detail of largest bright BSI inclusion

Fig 8.19. A) Aggregate of  $\text{Ca}_2\text{Sb}_2\text{O}_7$  crystals with associated Na-K-S inclusions noted by arrows. B) Detail of A that shows apparent crystal faces on one Na-K-S inclusion.

## Copper Sulfide Minerals

The copper used to color the blue glasses and glazes could have come from common geologic ores or minerals, metal alloys, or slags from copper smelting and melting operations. Elements associated with copper in these potential sources; arsenic, tin, zinc, lead, and iron, carry over into the glass with the copper and can be used to infer the source material. There is no obvious correlation of arsenic, tin, zinc, or lead with copper in the blue tp-tl glasses, indicating that copper alloy was not the copper source for these glasses. The blue tp-tl glasses contain generally more iron than the blue opaque glasses and blue glazes (Fig 8.20). Most slags that form as products of copper smelting contain significantly less copper than iron, with Cu:Fe usually less than 1 (Hauptman et al., 1988, Tylcote, 1976, Table 17; Lupu, 1969), precluding copper smelting slags as a source of copper for the blue tp-tl glasses. In these blue glasses, the molar ratio of Cu:Fe is about 0.4 to 5, with most analyses between 0.7 and 1.7. In the common copper ore minerals chalcopyrite ( $\text{CuFeS}$ ) and bornite ( $\text{Cu}_5\text{FeS}$ ), the molar Cu:Fe ratios are 1 and 5, respectively. Roasting sulfide minerals to drive off the sulfur will not change their Cu:Fe ratios. The Cu:Fe ratio of the glasses suggest that the copper in the blue tp-tl glasses was added to the glassmaking batch material as raw or roasted copper sulfide ore minerals.

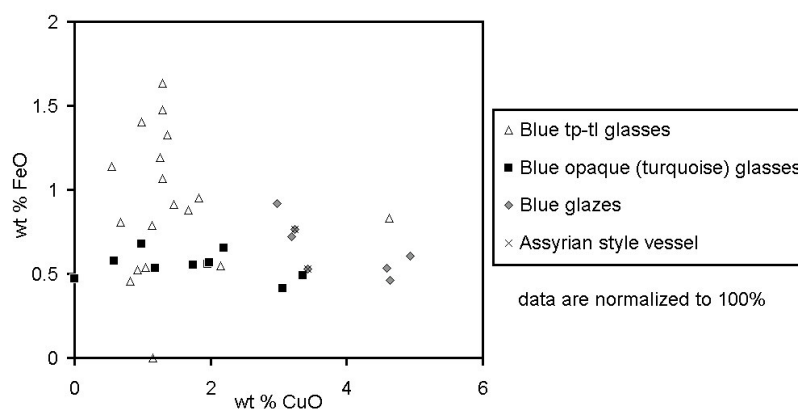


Fig 8.20. Iron is higher in the blue tp-tl glasses than in other copper-colored glasses or glazes.

## *Copper Alloys*

Two bronze artifacts from Period IVB Hasanlu have been analyzed (de Schauensee, 1988). The blue transparent glazes on the two bridge-spouted vessels have Cu:Sn and Cu:As ratios that are comparable to those of the bronze artifacts and the copper used to color these glazes is suggested to have been derived from bronze of similar composition (Chapter 6; Stapleton et al., submitted).

The FeO content of the blue opaque glasses is constant and does not vary with CuO (Fig 8.20). Because of its abundance in the Earth's crust and its chemical affinity with copper, iron is one of the most common contaminants in copper ores and minerals. The lack of variation between copper and iron suggests that raw ore or mineral was not used as the phase in which copper was added to the glassmaking batch material for the blue opaque glasses. If the colorant was a copper ore or slag, it had an unusual Cu-Sb-Sn composition. Instead, the low FeO level suggests that a more pure form of copper was used, perhaps from manufactured copper metal or copper alloy.

In the blue opaque glasses, As and Cu are positively correlated (Fig 8.21), indicating that they entered the glass batch in the same raw material. The ratio of weight% Cu:As in these glasses is about 1:0.01 to 1:0.4. The two bronze artefacts from Period IV Hasanlu have Cu:As ratios of 1:0.001 and 1:0.003 (de Schauensee, 1988), much lower than those of the blue opaque glasses. The wt% Cu:Sn ratios of these glasses are also significantly lower than those of the two analyzed bronze artifacts. Bronze metals of the type excavated from the IVB levels at Hasanlu were not likely to have been the source of copper for the blue opaque glasses. Other early 1<sup>st</sup> millennium BC arsenic-bearing copper artifacts from another Iranian site also have lower Cu:As and Cu:Sn ratios (Thornton et al., 2002). The two blue opaque glasses with the highest arsenic content also contain the highest amounts of copper, tin, and antimony, which were elements commonly alloyed with copper. Manufactured copper metal alloys from

the early 1<sup>st</sup> millennium BC have a wide range of compositions and thus it is not possible to confidently dismiss alloyed copper as the source of the copper added to the glassmaking batch materials of the opaque blue glasses.

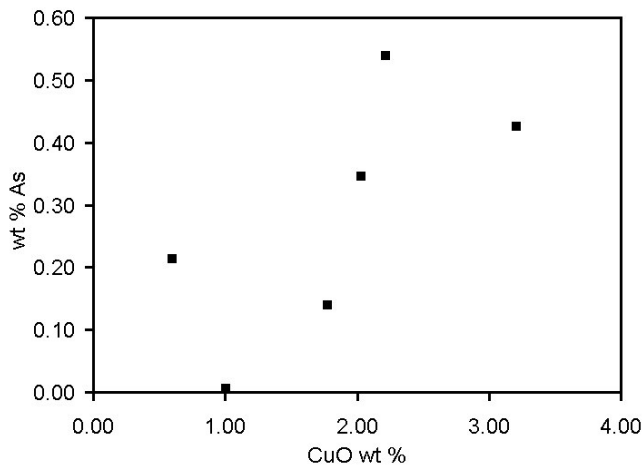


Fig 8.21. Blue opaque glasses. CuO and As are positively correlated.

#### *Polymetallic Sulfides ( $Fe_xCu_yS$ ) in Glassy Host Material*

Most of the black glasses from Hasanlu are colored by small (< 1  $\mu$ m diameter) droplets of sulfide, mostly of iron and copper but some also containing lead and antimony (Chapter 4; Stapleton and Swanson, 2002a). The spherical shape of these sulfide inclusions indicate that they were immiscible sulfide liquids in the silicate glass melt. The presence of sulfur and copper in the inclusions indicates that a sulfidic copper ore, rather than an iron ore, was the ultimate source for metals in the inclusions. Black glasses that contain very high iron, greater than about 5 wt% FeO, show a positive correlation between iron and arsenic (Fig 8.22), suggesting that an Fe-As mineral, possibly arsenopyrite ( $FeAsS$ ), was also part of the ore body. The inclusions were probably not added as crushed iron sulfide minerals because they do not have textures that preserve the original mineral texture and shape (Larocque et al., 2000).

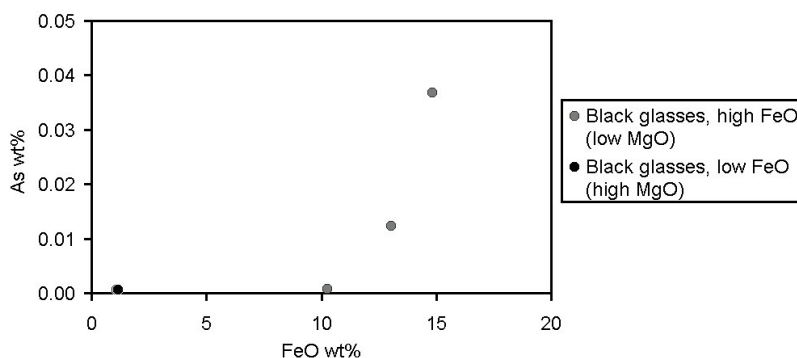


Fig 8.22. High iron black glasses have a positive FeO and As correlation.

In the sulfide droplets, the dominance of iron in association with copper, antimony, and lead suggests that these elements were brought together during a process to remove impurities from a copper ore, either during smelting or refining. Two phases are possible sources for the sulfide droplets: matte or iron-rich inclusions. Matte is the sulfur-rich phase that can form clumps during smelting of sulfidic copper ores (Bachmann, 1982; Craddock, 1995). However, matte is composed mostly of monosulfide phases that are relict, partially reacted ore minerals (Bachmann, 1982) and this precludes matte as the source of the sulfide droplets found in the black glasses.

Ancient copper smelted from sulfidic ores contained interstitial, iron-rich impurities some of which appear to have been intergrowths of mostly iron sulfide with lesser copper sulfide and some smaller (< 1µm) inclusions such as lead sulfide (Figs 159 and 161b-c, Roman, 1990). These iron-rich impurities were removed during a secondary, refining process by adding quartz-bearing sand, which did not have to be pure, to smelted copper (Tylecote, 1976; Tylecote and Boydell 1978; Craddock, 1995). The whole mass was heated until the interstitial iron reacted with the sand and formed a melt that contained fayalite ( $\text{Fe}_2\text{SiO}_4$ ). The slag produced also would have contained sulfides of iron, copper, and lead, along with other elements present as an impurities in the sand. The black glasses fall into two chemical groups based on their iron contents

(Fig 8.23). The high FeO group contains about 5 wt% FeO to 15 wt% FeO. This high FeO group has a generally negative correlation between SiO<sub>2</sub> and FeO, and shows a possible mixing line between fayalite (Fe<sub>2</sub>SiO<sub>4</sub>) and a SiO<sub>2</sub>-rich phase (Fig 8.23). This would be consistent with the presence of a fayalite-rich slag, derived from refining copper, in a glassmaking batch that also contained sand. The low FeO group contains up to about 2 wt% FeO. Iron and aluminum are positively correlated in the low iron group, indicating that these two elements were added to the glassmaking batch in the same phase. The sand chosen to remove iron impurities from copper does not need to be specially prepared or especially clean and may contain many impurities including aluminum. The black glasses appear to have been colored by the addition of copper refining slag that contained fayalite and iron-rich sulfide droplets.

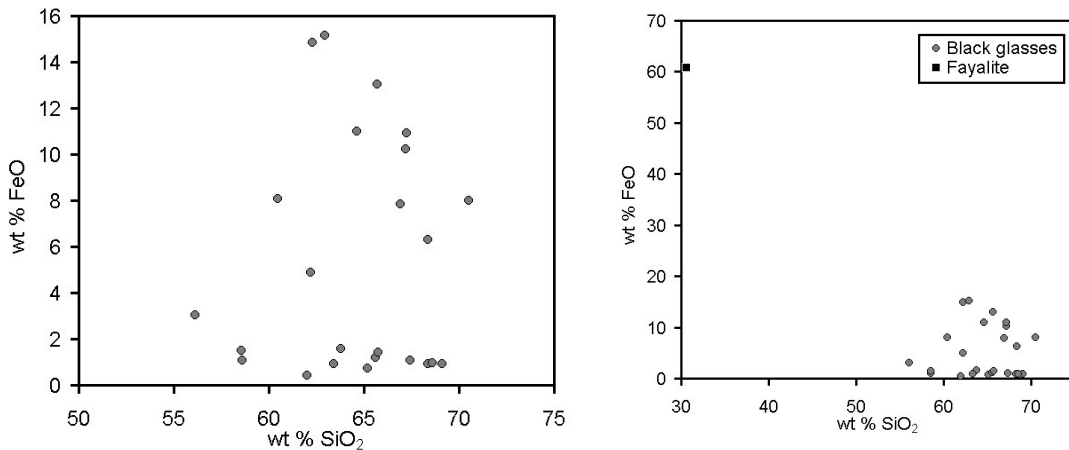


Fig 8.23. Black glasses can be divided into low iron (< 4 wt% FeO) and high iron. The negative correlation between SiO<sub>2</sub> and FeO in the high iron group may be from addition of fayalite (Fe<sub>2</sub>SiO<sub>4</sub>).

If all of the FeO in the high iron black glasses entered as fayalite, then approximately 30-45 wt% of these glasses was composed of fayalite. If these high iron glasses are recalculated without the fayalite component and normalized to 100%, K<sub>2</sub>O and MgO recalculate to around 1.2-1.5 wt% each, similar to plant ash glasses. Low iron black glasses contain high K<sub>2</sub>O and MgO, consistent with the use of plant ash (Fig 8.24).

The effect of high levels of iron colorant and associated  $\text{SiO}_2$  on the apparent levels of other components in the high iron glasses emphasizes the problems inherent in using absolute levels of  $\text{K}_2\text{O}$  and  $\text{MgO}$  to determine whether natron or plant ash was used to make a glass.

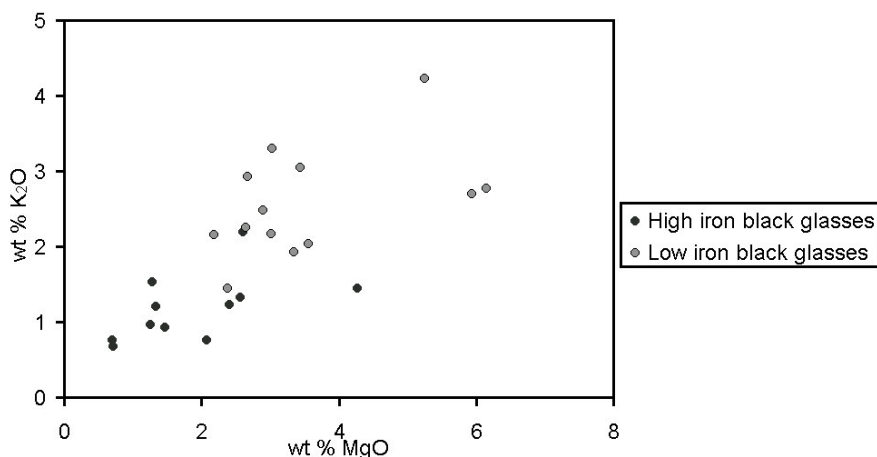


Fig 8.24. MgO and  $\text{K}_2\text{O}$  in black glasses.

#### *Lead Antimonate ( $\text{Pb}_2\text{Sb}_2\text{O}_7$ )*

The yellow opaque glasses and glaze are highly heterogeneous (Fig 8.25), containing not only a lead antimonate phase, but also calcium antimonate and sodium antimonate crystals. There are many large, rounded alkali sulfate inclusions, evidence of the use of plant ash as the sodium source (Fig 8.25). In one yellow opaque glass (UPenn. 73-5-559d), a rounded, strontium-rich, sulfur-bearing grain is associated with calcite and a lead-rich inclusion (Fig 8.26). The surrounding glass contains about 4 times more  $\text{Al}_2\text{O}_3$  than the main area of glass. This glass and associated inclusions probably represent partially reacted lead ore mixed with feldspar. No antimony was detected in the crystalline phases and occurs at less than 0.5 wt%  $\text{Sb}_2\text{O}_5$  in the surrounding aluminum-rich, glassy area. Alkali feldspar has been shown to have been part of the glassmaking batch (see section "Alkali feldspar"), and  $\text{PbO}$  and  $\text{K}_2\text{O}$  have a negative relationship in all of the yellow opaque glasses (Fig 8.27), suggesting that these

components were added to the batches in separate ingredients. Antimony was probably also added as a separate ingredient. The inhomogeneity in these glasses suggests that they did not undergo significant processing during manufacture. In contrast to glasses that contain  $\text{Ca}_2\text{Sb}_2\text{O}_7$  crystals, which appear to have been made in a step prior to addition to the glassmaking batch, the  $\text{Pb}_2\text{Sb}_2\text{O}_7$  crystals appear to have been made by mixing plant ash, quartz sand, feldspar, lead ore, and an antimony-bearing phase.

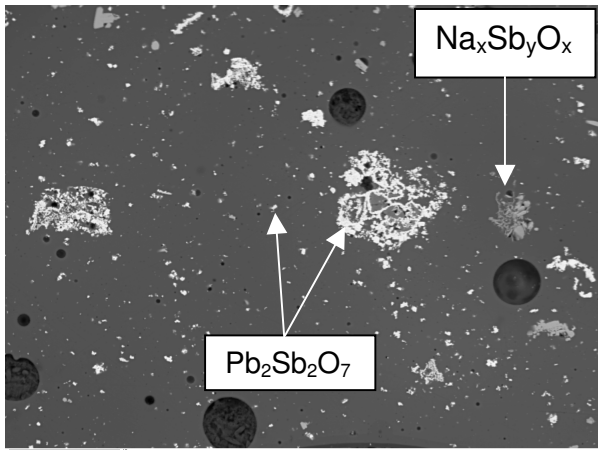


Fig 8.25. Yellow opaque glaze on Assyrian style vessel (UPenn. 60-20-348) with  $\text{Pb}_2\text{Sb}_2\text{O}_7$ . Round, dark inclusions are alkali sulfates formed from immiscible liquids. BSI. Scale bar is 40  $\mu\text{m}$ .

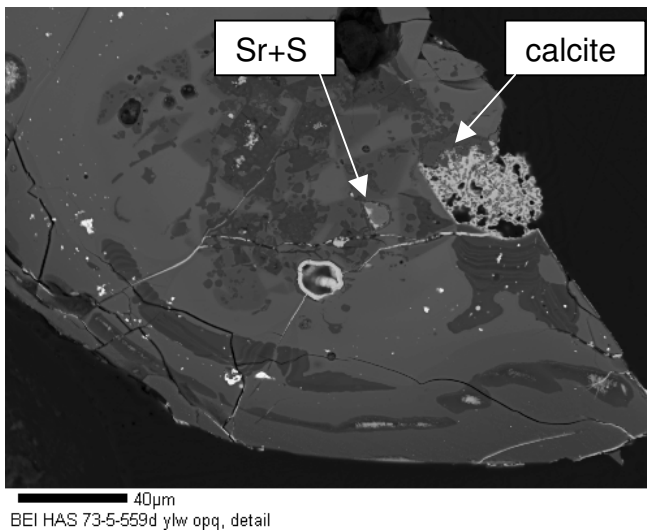


Fig 8.26. Yellow opaque glass (UPenn. 73-5-559d) showing original batch material. Glass is partly weathered (dark gray) and has lead-rich phosphate deposited in fractures and weathered glass. BSI. Scale bar is 40  $\mu\text{m}$ .

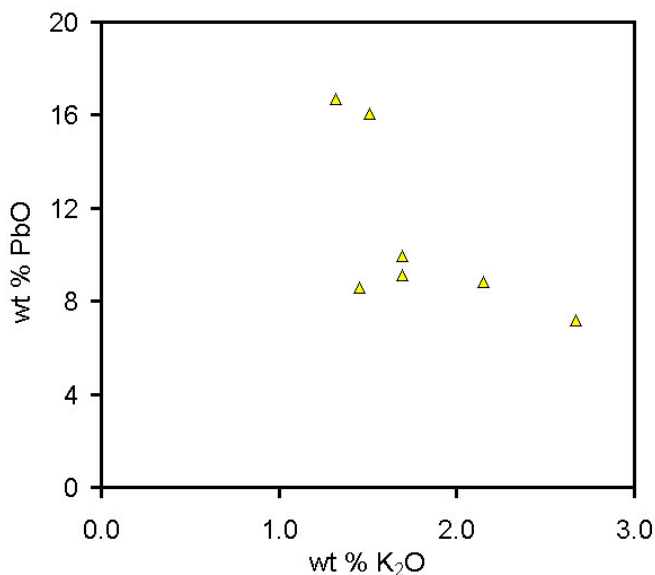


Fig 8.27. Yellow opaque glasses do not have a positive correlation between K<sub>2</sub>O and PbO.

### Comparison to the Cuneiform Glassmaking Texts

Oppenheim (1970) identified products as “primary glass” that are used as a base glass to which colorants and opacifiers are added to make a secondary glass.

Oppenheim suggests that some primary glasses were batch material that had been sintered but not completely melted to form a full glass. Many parts of the texts state the use of repeated heating, grinding, and washing intermediate material with water.

Pouring into water or sprinkling water onto melt or hot glass is required in between some sintering steps or at the end of production of a glass. Oppenheim (1970) suggests that this procedure was used to facilitate grinding the glass in between sintering or melting steps so that a more finely made glass could be obtained. The manufacturing procedures for some glasses are described several times, but the steps required are not always the same in each description. For some glasses, like tuzuku and dusu, the texts use terms for raw materials, colorants, and primary glasses that have not been previously used or described in the texts or have not be successfully translated by

modern scholars. In some cases, the term used to name the resulting material is not understood.

The manufacturing steps described for the Hasanlu glasses represent examples of glassmaking technology as it was practiced in some factories or workshops in the early 1<sup>st</sup> millennium BC. The steps may not apply to all of the Hasanlu glasses because not all of the glasses exhibit all of the same characteristics. The steps tentatively suggested for making blue tp-tl, blue opaque, white opaque, and yellow opaque glasses from Hasanlu are compared in the following discussion with some of the descriptions for manufacturing glass in the cuneiform glassmaking texts. Some raw materials identified from the Hasanlu glasses are compared with terms in the cuneiform texts.

#### *Blue transparent glass*

The blue tp-tl glasses from Hasanlu could have been made by following the directions for making tersitu-preparation or tersitu-glass as described and translated in the cuneiform glassmaking texts translated by Oppenheim and interpreted by Oppenheim and Brill in Oppenheim et al. (1970). First, a base glass called zuku-glass is made by mixing finely ground quartz-stone and plant ashes. This mix is fired until it glows red, then cooled and ground finely again. There is no description of what this first firing does to the mix. The finely ground 1<sup>st</sup>-fired mix is fired a second time until it glow golden-yellow and then is poured onto a fired brick, indicating that it is now molten glass. This glass has had no colorant added to it. The next step is to heat an ingredient called “slow copper” until it glows red, then “throw” ground zuku-glass onto the heated “slow copper”. Apparently, the zuku-glass will absorb some of the copper but some of the copper will settle under the glass, in which case the mix should be stirred until all of the copper mixes with the zuku-glass. Tersitu-preparation and tersitu-glass are used as a base glass for making other high-temperature materials that are meant to be imitations of precious stones like lapis lazuli, “green” lapis lazuli (which may be turquoise), and red

lapis lazuli, although they are not meant to be exact enough to fool anyone. The term “slow copper” would refer to the copper sulfide ore. In the cuneiform text directions, “slow copper” was first heated before being mixed with anything else, which, if it was a copper sulfide mineral, would oxidize the mineral and cause the formation of copper sulfates and metallic copper which would make it easier for oxidized copper, as  $\text{Cu}^{2+}$ , to enter the glass and give the blue color.

#### *White opaque glass*

Another glass described in the texts is busu-glass (Oppenheim, 1970). Busu-glass does not need to be processed further in order to be used to make objects, but it can be used in the batch of other glasses to make them opaque. Ashes, quartz, anzahhu-glass, and “white stuff” are mixed together and placed in a cold kiln and heated until sintered. Then the mass is put into a crucible and heated, after which it is poured into water. The manufacture of anzahhu-glass is not described in the glassmaking texts, but Oppenheim (1970) points out that it probably contains antimony, based on the use of a similar term in cuneiform medical texts. “White stuff” is stated in the texts to come from the sea and is translated as shell or roasted coral. Heated shell or coral forms lime,  $\text{CaO}$ , and was probably the source of  $\text{CaO}$  in the busu-glass batch used to make the crystalline  $\text{Ca}_2\text{Sb}_2\text{O}_7$  opacifier. The combination of batch components for busu-glass is similar to that suggested for the white opaque glaze, including the use of two pre-formed phases “A” and “B”. Phase “A” contains antimony in a glass matrix and may be equivalent to anzahhu-glass. Phase “B” was made with dolomite, which appears to have been used for the calcium that it contains in order to make  $\text{Ca}_2\text{Sb}_2\text{O}_7$  crystals. “White stuff” in the glassmaking texts may have been a term that referred to more closely to lime ( $\text{CaO}$ ) than to its uncalcined sources, sea shell or coral. Lime can be derived by roasting (calcined) from any calcium-bearing carbonate, including limestone or dolomite.

### *Blue opaque glass*

In parts of the glassmaking texts, tersitu glass is mixed with other primary glasses to make opaque glasses. Zaginduru glass was produced to imitate “green lapis lazuli”, which may have referred to the mineral turquoise (Oppenheim, 1970). Zaginduru may be the color equivalent of the blue opaque (turquoise) glasses from Hasanlu. To make zaginduru glass, the glassmaking texts require mixing together tersitu-preparation with busu-glass, washed anzahhu-glass, plant ashes, and “white stuff”. In this recipe, anzahhu-glass had to be washed before being used in the zaginduru-glass, indicating that it contained water-soluble impurities. The Hasanlu blue opaque glasses appear to have been made with some of the same batch materials, including copper-bearing tersitu-preparation, plant ashes, and “white stuff” (dolomite). The lack of large alkali sulfate inclusions in the glass matrix of the blue opaque glasses is consistent with a washing step, related in the zaginduru recipe by washed anzahhu-glass. The two zaginduru glass batch materials that contain antimony, busu-glass and anzahhu-glass, could have been used to make many of the Hasanlu glasses, but it is not clear if they could account for the large  $\text{Ca}_2\text{Sb}_2\text{O}_7$  aggregates, thought to have been pre-made by mixing plant ash, antimony sulfide ore and possibly lime, that occur in some glasses. The blue opaque glasses that contain these inclusions may have been made by procedures or raw materials other than those listed for zaginduru glass.

### *Yellow opaque glass*

A primary glass called dusu appears to have been made in a variety of colors, although only the term for the color red seems to have been translated with confidence. Confusingly, Oppenheim (1970) lists “yellow glass” in a glossary as one interpretation for dusu, but does not mention yellow in his discussions. The ingredients for one type of dusu could have been used to make yellow opaque glass similar to those from Hasanlu. The recipe requires quartz, plant ash, anzahhu-glass, “white stuff”, tuzku-glass, and

antimony to be mixed together (Oppenheim, 1970). Tuzku is believed to contain lead because it appears only in recipes for yellow opaque and red opaque glasses, which are the only glasses in which lead is found up to around 30 wt% PbO (Henderson and Warren, 1983; Freestone, 1987; Brill, 1988b). Yellow glasses are colored and opacified by crystalline  $\text{Pb}_2\text{Sb}_2\text{O}_7$ . The steps for making this particular color of dusu are not described at all except to mix the ingredients together. In fact, the manufacturing procedure suggested for the yellow opaque glasses from Hasanlu in which sand, plant ash, lead ore, and an antimony-bearing phase are mixed together and melted, is consistent with the dusu-glass recipe from the glassmaking texts.

## CONCLUSIONS

The glasses and glazes from Hasanlu clearly demonstrate that the main raw materials used in 1<sup>st</sup> millennium BC glassmaking were broader than simply plant ash and pure quartz. Plant ash appears to have been the main source of sodium in the Hasanlu glasses, even those that contain less than 1.5 wt% each of  $\text{K}_2\text{O}$  and  $\text{MgO}$ . The low levels of these oxides are probably the result of using lower proportions of plant ash, as shown by black glasses that contain high levels of colorant, 5-15 wt%  $\text{FeO}$ . Quartz-rich sand appears to have been used for most of the Hasanlu glasses. Alkali feldspar made up about 10-30 wt% of the batch materials for one group of blue tp-tl glasses and all of the yellow opaque glasses, probably added as a separate ingredient from the quartz. Dolomite composed significant portions of the blue opaque and white opaque glasses, most of it as part of the coloring and opacifying agent, which contained  $\text{Ca}_2\text{Sb}_2\text{O}_7$  crystals. The proportions and compositions of batch materials used in the manufacture of the glasses from Hasanlu were varied, depending on the color of glass produced. The chemical compositions appear to confirm the use of multiple steps to prepare colorants and to manufacture glasses.

The colorant technology used in the Hasanlu glasses plainly shows the advanced state of glassmaking in the early 1<sup>st</sup> millennium BC Near East. Both copper ore and copper alloys were used to color the blue glasses and glazes, indicating that the glassmakers were aware of the actual agent, copper, that imparted the blue color and knew how to manipulate different materials that contained that agent. In other words, the glassmakers knew that it was copper, and not a particular mineral or a particular alloy that was the necessary ingredient for coloring. Similarly, for the blue opaque and white opaque glasses, the glassmakers understood that lime could be obtained from dolomite, as well as sea shell or coral as the cuneiform glassmaking texts state. The occurrence of black glasses, as different from dark blue or dark purple, is rare in the 2<sup>nd</sup> and 1<sup>st</sup> millenniums BC. The black glasses from Hasanlu appear to have been colored by addition of iron-rich slag derived from refining of smelted copper. It would have been necessary for the glassmakers to control the redox conditions of the melt to ensure the survival or development of the sulfide droplets that made the glasses appear black.

This study of glasses from Hasanlu shows that early 1<sup>st</sup> millennium BC glassmakers understood the interaction of materials they used. The variety of batch materials used in the Hasanlu glasses, the different copper agents for example, indicate that not all of the raw materials were uniform throughout the glassmaking industry. The apparently complicated and confusing directions in the cuneiform texts probably partly reflect the diversity of raw materials used in geographically separate glassmaking workshops.

## CHAPTER 9

### CONCLUSIONS AND RECOMMENDATIONS FOR FUTURE RESEARCH

Ancient, alkali-rich glasses are often heterogeneous as a result of weathering and incomplete melting of batch and colorant materials. These heterogeneities must be avoided in chemical analysis of glass because they are not representative of the glass as a whole. Avoiding these heterogeneities is a difficult task if bulk analytical techniques are used. This research has demonstrated that it is necessary to image the microstructure of ancient glasses in order to characterize the extent of weathering and to identify heterogeneities. Electron microprobe analysis (EMPA) can be used in routine analysis to image samples and to avoid weathered areas during analysis, something that bulk analytical techniques cannot perform. Identification of inhomogeneities using EMPA can aid in determining glass batch materials and manufacturing steps. In addition, EMPA is well-suited to the minimal sampling desired for archaeological glass and is essentially non-destructive. Samples used in EMPA can subsequently be examined using other micro-analytical techniques to obtain additional important information such as trace element data using laser ablation inductively coupled mass spectrometry (LA-ICP-MS). EMPA should be seen as an essential first step in the analytical investigations of small, ancient glass fragments.

The 1.5 wt% values of  $K_2O$  and  $MgO$  that are used to classify ancient glasses as either “plant ash” (>1.5 wt%) or “natron” (<1.5 wt%) and quoted in this dissertation are based on analyses of experimental glasses made using plant ash or natron (for example, see Sayre and Smith, 1961; Brill, 1988a), and of analyses of ancient glasses documented in contemporaneous texts as having been made using plant ash or natron (for example, see Oppenheim et al., 1970; Lilyquist and Brill, 1993; Freestone et al., 2000). The 1.5 wt% values have not been chosen based on statistical analysis of data and are used as guidelines for classification. Some researchers use the phrases “plant ash-type” and “natron-type” to denote that a glass has a chemical composition

consistent with the named alkali source. Historical and archaeological data are used to corroborate classification of glasses as being made of plant ash or natron.

This commonly-used classification system can be applied with caution to the glasses excavated from Hasanlu. All of these glasses are suggested here to have been made using plant ash based on the presence of gall (alkali sulfate, Fig 8.5) thought to be from plant ash, bulk chemical compositions, historical documents, and archaeological evidence. Plant ashes can contain sulfate on the order of 10 wt% (Brill, 1970a), which commonly form alkali sulfate inclusions in glass melts made using plant ashes (Turner, 1956). It is possible that sulfate inclusions may form in a glass made with evaporite minerals, such as natron, if the evaporite material contains sulfate phases. Sulfate phases are found with some natron (Brill, 1999). For example, the Beypazari trona deposit of the Hirka Formation in central Turkey contains Ca- and Mg- sulfate phases but no alkali sulfate minerals except for a mixed Mg-Na sulfate, bloedite (Helvacı, 1998). In these deposits,  $\text{Na}_2\text{SO}_4$  is below detection (< 25 ppm),  $\text{K}_2\text{O}$  and  $\text{MgO}$  occur at less than 300 ppm, and  $\text{Na}_2\text{O}$  is greater than 30 wt%. It seems unlikely that natron of the type from the Beypazari deposit was used to make glasses from Hasanlu. However, other natron deposits with sulfate phases cannot be ruled out. Bulk chemical compositions of the Hasanlu glasses, recalculated to remove colorants, yields high  $\text{K}_2\text{O}$  and  $\text{MgO}$  values, consistent with a plant ash alkali source. Colorants must be “removed” from the glass by recalculating the bulk compositions to exclude the colorant components. In the case of the black glasses from Hasanlu, this requires subtraction of both  $\text{FeO}$  and  $\text{SiO}_2$  because fayalite was a major part of the coloring phase added to the glass batch (Fig 8.23). This calculation makes the black glasses that plot in the “natron” field in Fig 8.1 more closely resemble plant ash glasses. Historical documents, cuneiform glassmaking texts, from 7<sup>th</sup> century BC Near East state that plant ash should be used to make glass (Oppenheim et al., 1970). The documents were probably copied

from earlier, 13<sup>th</sup> c BC texts (Oppenheim et al., 1970) and thus represent a long-standing industrial complex that used plant ash to make glass. Natron has not been identified in these texts. A written account by the Roman author Pliny in the 1<sup>st</sup> c AD is the first reference to the use of natron as an alkali source for glassmaking. Thus, the mineralogical and chemical data of the Hasanlu glasses combined with the historical and archaeological evidence strongly indicates that the alkali source used to make the glasses from Hasanlu was plant ash.

However, if the low K<sub>2</sub>O and MgO glasses were made with natron, then these glasses could have been imports into Hasanlu, based on their small numbers. Natron glass was probably being made in Egypt at this time. On the other hand, glassmakers in or near Hasanlu may have changed from plant ash to natron as the alkali source for the low K<sub>2</sub>O and MgO glasses. Political and economic changes marked the end of the transition between the late Bronze and early Iron Ages, around the 13<sup>th</sup> to 12<sup>th</sup> century BC, for the dominant eastern Mediterranean civilizations in Egypt, Mesopotamia, and Anatolia. The immediate cause of these changes may have been attacks from groups outside of these main political entities. The spread of the mineral-based glass technology in the Iron Age may have been related to migration of skilled glassmakers during this period of unrest. Additionally, known resources of plant alkalies may have become scarce, forcing glassmakers to search for appropriate substitutes. Changes in the alkali from a plant to a mineral source could have affected glass recipe preparations, melting temperatures and conditions, or quality of the finished glass. Revisions to the known glassmaking technology probably would have accompanied a change from plant to mineral alkali. Based on the small number of low K<sub>2</sub>O and MgO glasses found at Hasanlu, this author does not believe these glasses were made using natron.

The glasses from Period IVB Hasanlu (11<sup>th</sup> to 9<sup>th</sup> c BC) have a wide range of chemical compositions. Major, minor, and trace element data obtained from microprobe

and LA-ICP-MS analysis indicate that the glasses from Hasanlu were made using different combinations of quartz sand, plant ash, and alkali feldspar as the main ingredients, and dolomite, copper ore, copper alloy metal, slag from copper refining, antimony ore, and lead ore as parts of the colorants. For some glasses, positive correlations between some oxides suggest simple glassmaking procedures involving one or two steps of mixing and melting batch materials. However, most glasses do not show simple correlations in oxides and are probably the result of mixing batch materials in multiple steps, including separate steps for processing colorants. The preparation of the materials used in manufacturing, for example of the  $\text{Ca}_2\text{Sb}_2\text{O}_7$  and copper colorants, demonstrate that the craftsmen had a well-developed technical knowledge of the properties of materials and of their interaction during firing. The glassmaking industry appears to have interacted with other pyrotechnological industries. Glassmakers shared technical information about the use of raw materials and colorants with potters, metallurgists, and miners.

The oxygen isotope compositions of the glasses from Hasanlu exhibit a large range in values, consistent with the complicated, multi-step, manufacturing procedures suggested by the major, minor, and trace element chemistry. The large range may also be the result of the use of quartz from several different geologic deposits which would suggest that the glasses were made in more than one factory or in several different regions, and then brought into Hasanlu.

The glasses from Hasanlu are different in major element composition from those of other 2<sup>nd</sup> millennium BC and early 1<sup>st</sup> millennium BC glasses from the Near East including those from Nuzi, Amarna, Nimrud (Fig 9.1). The glasses from Hasanlu are also different from glasses from a number of other Near Eastern, Mesopotamian, and Egyptian sites including 23<sup>rd</sup> c Tell Brak, 15<sup>th</sup>-13<sup>th</sup> c BC Tell Al Rimah, 13<sup>th</sup> c BC Ulu Burun shipwreck, 13<sup>th</sup>-11<sup>th</sup> c BC Timna, 8<sup>th</sup> c BC Altin Tepe, 5<sup>th</sup> c BC Persepolis, and 14<sup>th</sup>

c BC Egypt (see data in Brill, 1999, and Vandiver, 1982, 1983b). The sites that these comparative data come from are not contemporaneous with Hasanlu IVB and some of the sites are represented by only one sample of glass, but there are no data sets that exactly match temporally or geographically with Hasanlu of this period. The location of manufacture of the Hasanlu glasses is still not certain. However, the chemical differences between the glasses from Hasanlu and other Near Eastern, Mesopotamian, and Egyptian glasses suggest that the glasses from Hasanlu were made either near Hasanlu or imported into Hasanlu from an as yet unidentified region. Either scenario suggests that by the early 1<sup>st</sup> millennium BC, the knowledge of glassmaking appears to have extended beyond the boundaries of Mesopotamia and Egypt and outside of the centers of the dominant political powers of the period.

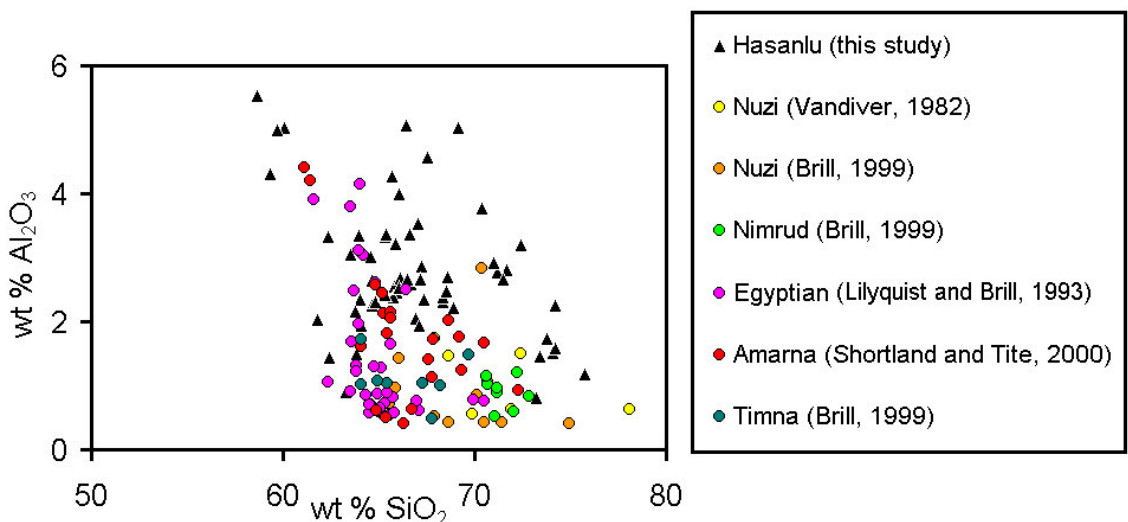


Fig 9.1. Comparison of SiO<sub>2</sub> and Al<sub>2</sub>O<sub>3</sub> in glasses from Hasanlu (this study) and other Near Eastern and Egyptian sites. The Hasanlu glasses have higher Al<sub>2</sub>O<sub>3</sub> than most other Near Eastern glasses. The glasses with >2wt% Al<sub>2</sub>O<sub>3</sub> from Egypt, Amarna, and Timna are cobalt blue glasses in which the Al<sub>2</sub>O<sub>3</sub> is associated with the cobalt colorant.

#### Future research

Trace element analyses should be carried out on the remainder of the Hasanlu glasses to corroborate the limited data obtained by LA-ICP-MS. In conjunction with these trace element analyses, additional analysis of the Corning and York glass

standards by LA-ICP-MS could be carried out and compared with certified standards such as NBS 610 and NBS 612. To determine variability in the copper and lead ore(s) used, lead isotope analysis could be carried out on the blue tp-tl and yellow opaque glasses from Hasanlu.

The experimental glasses produced in this study (#6 and #7) and by Brill (1970a) demonstrated that it is relatively easy to make a good quality glass from quartz and plant ash, the two main glassmaking materials listed in the cuneiform texts (Oppenheim, 1970). To establish a clearer understanding of the complexities suggested by the Hasanlu glass data and the cuneiform texts, more detailed glassmaking experiments should be carried out. Experimental reproductions using sodium-rich plant ash and quartz-rich sand could be used to try to replicate the microstructure and chemistry of the Hasanlu glasses. Multiple mixing and melting steps could be carried out to determine changes in oxygen isotope composition at different steps and in the final glass. Ash produced under different conditions could be analyzed for differences in chemistry, phases present, and oxygen isotope composition and then compared to glasses produced with the same ashes. These replicate glasses could also be used to further study the mechanisms of hydration of high-alkali glasses and the affects of weathering on the oxygen isotope composition of ancient glasses.

For further understanding of the glass industry in this region, it would be helpful to carry out more detailed studies of the microstructure of glass from nearby Dinkha Tepe, about 20 km west of Hasanlu (McGovern et al., 1991). Analysis of oxygen isotope ratios of glasses from Dinkha Tepe and from Nuzi to compare with the Hasanlu data may also be useful. In addition, it is necessary to identify glass and glassy materials from surrounding regions, including from Iran, Syria (Alalakh, pers. com. Aslihan Yener), Western Asia, and the Indus Valley, and to continue analytical studies of these materials.

## REFERENCES CITED

Armstrong, J. (1984) ZAF and  $\alpha$ -Factor Correction Procedures for the Quantitative Analysis of Individual Microparticles. In (K. F. J. Heinrich, Ed.) *Microbeam Analysis*, p. 208.

Bachmann, H.-G. (1982) *The Identification of Slags from Archaeological Sites*. Institute of Archaeology Occasional Publication 6. London: Institute of Archaeology.

Bamford, C. R. (1977) *Colour generation and control in glass*. Glass Science and Technology 2. Amsterdam: Elsevier Scientific Publishing Company.

Barag, D. (1970) Mesopotamian Core-Formed Glass Vessels (1500-500 BC). In (A. L. Oppenheim, R. H. Brill, D. Barag, and A. von Saldern, Eds.) *Glass and Glassmaking in Ancient Mesopotamia*. Corning, NY: Corning Museum of Glass, pp. 131-199.

Bedal, L.-A., Fleming, S., de Schauensee, M., and Hancock, R. (1995) Second millennium B.C. pottery at Hasanlu Tepe and Dinkha Tepe: INAA and petrographic studies. In (P. B. Vandiver, J. R. Druzik, J. L. G. Madrid, I. C. Freestone, and G. S. Wheeler, Eds.) *Materials Issues in Art and Archaeology IV Materials Research Society Symposium Proceedings 352*, pp. 453-467.

Beale, T. W. (1973) Early trade in highland Iran: a view from a source area. *World Archaeology* 5 (2), pp. 133-148.

Bimson, M. and Freestone, I. C. (1987) *Early Vitreous Materials* (eds.). British Museum Occasional Paper 56. London: British Museum Press.

- Blander, M. (1998) *Acid-base reactions leading to fouling and corrosive ionic liquids in the combustion of biomass*. Abstract presented at EUCHEM.
- Brill, R. H. (1966) Interlaboratory comparison experiments on the analysis of ancient glass. *Comptes rendus, VIIe Congres International du Verre, Bruxelles, 28 juin-3 juillet 1965, Section B*, pp. 226.1-226.4
- Brill, R. H. (1967) A Great glass slab from ancient Galilee. *Archaeology* 20 (20), pp. 88-95.
- Brill, R. H. (1970a) The chemical interpretation of the texts. In (A. L. Oppenheim, R. H. Brill, D. Barag, and A. von Saldern, Eds.) *Glass and Glassmaking in Ancient Mesopotamia*. Corning, NY: Corning Museum of Glass, pp. 105–128.
- Brill, R. H. (1970b) Lead and oxygen isotopes in ancient objects. In *The Impact of the Natural Sciences on Archaeology*. London: The British Academy, pp. 143-164.
- Brill, R. H. (1972a) A Chemical-analytical round-robin on four synthetic ancient glasses. *International Congress on Glass, Versailles, Sept.-Oct., 1971, Artistic and Historical Communications*, 93-110. L'Institut du Verre, Versailles.
- Brill, R. H. (1972b) *The Glassmakers of Herat*. Video. Corning, NY: Corning Museum of Glass.
- Brill, R. H. (1988a) Scientific investigations. In (Ed. G. D. Weinberg) *Excavations at Jalame: Site of a Glass Factory in Late Roman Palestine*, pp. 257-294.

Brill, R. H. (1988b) A Red opaque glass from Sardis and some thoughts on red opaques in general. *Journal of Glass Studies* 30, pp. 16-27.

Brill, R. H. (1999) *Chemical Analyses of Early Glasses, Volumes 1 & 2*. Corning, NY: Corning Museum of Glass.

Brill, R. H. and Moll, S. (1963) The electron-beam probe microanalysis of ancient glass. In (Eds. F. R. Matson and G. E. Rindone) *Advances in Glass Technology, Part 2. History papers and discussions of technical papers of the VI International Congress on Glass*. New York: Plenum Press, pp. 293–302.

Brill, R. H. and Wosinski, J. F. (1965) A Huge slab of glass in the ancient necropolis of Beth She'arim. *Comptes rendus, VIIe Congres International du Verre, Bruxelles, 28 juin-3 juillet 1965, Section B*, pp. 219.1-219.11

Brill, R. H., Clayton, R. H., Mayeda, T. K., and Stapleton, C. P. (1999) Oxygen Isotope Analyses of Ancient Glasses. In (Ed. R. H. Brill) *Chemical Analyses of Early Glasses, Volume 1*. Corning, New York: The Corning Museum of Glass, pp. 301-322.

Caley, E. R. (1962) *Analyses of Ancient Glasses 1790–1957*. Corning, NY: Corning Museum of Glass.

Cole, D. R. and Ohmoto, H. (1986) Kinetics of Isotope Exchange at Elevated Temperatures and Pressures, in (Eds. J. W. Valley, H. P. Taylor, Jr., and J. R. O'Neil) *Stable Isotopes: High Temperature Geological Processes*. Reviews in Mineralogy, Vol. 16 Washington, DC: Mineralogical Society of America, pp. 41-90.

Craddock, P. T. (1995) *Early Metal Mining and Production*. Washington, D. C.: Smithsonian Institution Press.

Curtis, J. (1995) Introduction, in (Curtis, J., Ed.) *Early Mesopotamia and Iran: Contact and Conflict, 3500-1600 B.C.* London: British Museum Press.

Deer, W. A., Howie, R. A., and Zussman, J. (1966) *An Introduction to the Rock-Forming Minerals*. Harlow, UK: Longman.

Dyson, R. H. (1965) Problems of protohistoric Iran as seen from Hasanlu. *Journal of Near Eastern Studies* 24, pp. 193-217.

Dyson, R. H. (1977) Architecture of the Iron I period at Hasanlu in western Iran and its implications for theories of migration on the Iranian plateau, in *Le Plateau Iranien et L'Asie Centrale des Origines a la Conquete Islamique, Colloques Internationaux du CNRS 567*. Paris: CNRS, pp. 155-169.

Dyson, R. H. (1989a) Rediscovering Hasanlu. *Expedition* 31 (2-3), pp. 3-11.

Dyson, R. H. (1989b) The Iron Age architecture at Hasanlu: an essay. *Expedition* 31 (2-3), pp. 107-127.

Dyson, R. H. and Muscarella, O. W. (1989) Constructing the chronology and historical implications of Hasanlu IV. *Iraq* 27, pp. 1-27.

Dyson, R. H. and Voigt, M. M. (1989) *Expedition* 31 (2-3).

Dyson, R. H. and Voigt, M. M. (2003) A Temple at Hasanlu. In (Eds. N. F. Miller and K. Abdi) *Yeki bud, yeki nabud: Essays on the Archaeology of Iran in Honor of William M. Sumner*. Monography Series 48. Los Angeles: The Cotsen Institute of Archaeology, pp. 219-236.

Ehleringer and Cerling (2002) Stable Isotopes in Biological and Ecological Dimensions of Global Environmental Change. In (H. A. Mooney and J. G. Canadel) *Volume 2: The Earth System*, Encyclopedia of Environmental Change (T. Munn, Ed.). Chichester: J. Wiley and Sons, Ltd., pp. 544-550.

Elsenheimer, D. and Valley, J. W. (1993) Submillimeter scale zonation of  $\delta^{18}\text{O}$  in quartz and feldspar, Isle of Sky, Scotland. *Geochimica et Cosmochimica Acta* 57, pp. 3669-3676.

Faber, E. (1978)  $^{18}\text{O}/^{16}\text{O}$  and D/H analyses on waters from Lake Van area. In (E. T. Degens, F. Kurtman) *The Geology of Lake Van*. Number 169. Ankara: Maden Tetkik ve Arama Enstituesue Yayinlarindan, pp. 45-49.

Faure, G. (1986) Principles of Isotope Geology. New York: J. Wiley and Sons.

Freestone, I. C. (1987) Composition and microstructure of early opaque red glass. In (M. Bimson and I. C. Freestone, Eds.) *Early Vitreous Materials*. British Museum Occasional Paper 56. London: British Museum Press, pp. 173-191.

Freestone, I.C. (2001a) Presentation at the 2001 AIHV Meeting, New York/Corning.

Freestone, I. C. (2001b) Post-depositional changes in archaeological ceramics and glasses. In (Eds. D. R. Brothwell and A. M. Pollard) *Handbook of Archaeological Sciences*. Chichester: John Wiley and Sons, Ltd., pp. 615–625.

Freestone, I. C. and Gorin-Rosen, Y. (1999) The Great glass slab at Bet She'arim, Israel: an early Islamic glassmaking experiment?. *Journal of Glass Studies* 41, pp. 105-116.

Freestone, I. C. , Gorin-Rosen, Y., and Hughes, M. J. (2000) Primary glass from Israel and the production of glass in late antiquity and the early Islamic period. *La route du verre*, TMO 33, Lyon: Maison de l'Orient, pp. 65-83.

Freestone, I. C., Stapleton, C. P., Rigby, V. (2001) The Production of Red Glass and Enamel in the Late Iron Age, Roman and Byzantine Periods. In (C. Entwistle, Ed.) *Through a Glass Brightly*. London: Oxbow.

Freestone, I. C. and Stapleton, C. P. (1998) Composition and Technology of Islamic Enamelled Glass of the Thirteenth and Fourteenth Centuries. In (Ed. Rachel Ward) *Gilded and Enamelled Glass from the Middle East*. London: British Museum Press, pp. 122-128.

Giberson, Jr., D. F. (2002) Core Vessel Technology: A New Model. In (P. B. Vandiver, M. Goodway, and J. L. Mass, Eds.) *Materials Issues in Art and Archaeology VI*, Materials Research Society Symposium Proceedings 712. Warrendale, PA: Materials Research Society, pp. 571-578.

Gratuze, B., Blet-Lemarquand, M. and Barrandon, J.-N. (2000) Mass spectrometry with laser sampling: a new tool to characterize archaeological materials. *Journal of Radioanalytical and Nuclear Chemistry* 247 (3), pp. 645-656.

Grose, D. F. (1989) *Early Ancient Glass*. New York: Hudson Hills Press.

Hartmann, G., Kappel, I., Grote, K., and Arndt, B. (1997) Chemistry and Technology of Prehistoric Glass from Lower Saxony and Hess. *Journal of Archaeological Science* 24: 547-559.

Hauptmann, A., Weisgerber, G., and Bachmann, H. G. (1988) Early Copper Metallurgy in Oman. In (R. Maddin, Ed.) *The Beginnings of the Use of Metals and Alloys*. Cambridge: MIT Press, p. 34-51.

Helvaci, C. (1988) The Beypazari trona deposit, Ankara Province, Turkey. In (J. R. Dyni and R. W. Jones, Eds.) *Proceedings of the First International Soda Ash Conference, Volume III*. Public Information Circular No. 40. Laramie: Wyoming State Geological Survey, pp. 67-103.

Henderson, J. (1985) The Raw materials of early glass production. *Oxford Journal of Archeology* 4 (3), pp. 267-291.

Henderson, J. (1988) Electron probe microanalysis of mixed-alkali glasses. *Archaeometry*, 30 (1), pp. 77-91.

Henderson, J. (1991) Technological characteristics of Roman enamels. *Jewellery Studies* 5, pp. 65-76.

Henderson, J. (2002) Tradition and experiment in first millennium A.D. glass production—the emergence of early Islamic glass technology in late antiquity. *Accounts of Chemical Research* 35 (8), pp. 594-602.

Henderson, J. and Warren S. E. (1983) Analysis of prehistoric lead glass. *Proceedings of the 22<sup>nd</sup> Symposium on Archaeometry, University of Bradford, Bradford, UK, March 30<sup>th</sup>-April 3<sup>rd</sup>, 1982*, pp. 168-180.

Hermann, G. (1968) Lapis lazuli: the early phases of its trade. *Iraq* 30, pp. 21-57.

Herz, N. and Garrison, E. G. (1998) *Geological Methods for Archaeology*. New York: Oxford University Press.

Heyworth, M. P., Hunter, J. R., and Warren, S. E. (1989) The Role of inductively coupled plasma spectrometry in glass provenance studies, in (Y. Maniatis, Ed.) *Archaeometry, Proceedings of the 25<sup>th</sup> International Symposium*. Oxford: Elsevier, pp. 661-669.

Jackson, C. M., Nicholson, P. T., and Gneisinger, W. (1998) Glassmaking at Tell el-Amarna: An Integrated Approach. *Journal of Glass Studies* 40, pp. 11-23.

Kaczmarczyk, A. (1986) The source of cobalt in ancient Egyptian pigments. In (J. S. Olin and M. J. Blackman) *Proceedings of the 24<sup>th</sup> International Archaeometry Symposium*. Washington, D. C.: Smithsonian Institute Press, pp. 369-376.

Knapp, A. B. (1988) *The History and Culture of Ancient Western Asia and Egypt*. Chicago: The Corsey Press.

Lamberg-Karlovsky, C. C. (1988) The "intercultural style" carved vessels, *Iranica Antiqua* 23, pp. 45-95.

Kohn, M. J., Valley, J. W., Elsenheimer, D., and Spicuzza, M. J. (1993) O isotope zoning in garnet and staurolite: evidence for closed-system mineral growth during regional metamorphism. *American Mineralogist* 78, pp. 988-1001.

Lamberg-Karlovsky, C. C. and Sabloff, J. A. (1995) *Ancient Civilizations: The Near East and Mesoamerica*. Prospect Heights, IL: Waveland Press.

Lambert, J. B., Johnson, S. C., Parkhurst, R. T., and Bronson, B. (1996) Analysis of 9<sup>th</sup> century Thai glass. *American Chemical Society Symposium Series* 625. Westerville, OH: American Chemical Society, pp. 10-22.

Larocque, A. C. L., Stimac, J. A., Keith, J. D. and Huminicki, M. A. E. (2000) Evidence for open-system behavior in immiscible Fe-S-O liquids in silicate magmas: implications for contributions of metals and sulfur to ore-forming fluids. *Canadian Mineralogist* 38, pp. 1233-1249.

Levine, L. D. and Young, Jr., T. C. (1977) *Mountains and Lowlands: Essays in the Archaeology of Greater Mesopotamia*. Bibliotheca Mesopotamica 7. Malibu: Udena.

Lightfoot, C. S. (1989) *A Catalogue of Glass Vessels in Afyon Museum*. British Archaeological Report International Series 530. Oxford: BAR.

Lightfoot, C. S. and Arslan, M. (1992) *Ancient Glass of Asia Minor: The Yuksel Erimtan Collection*. Ankara: Lightfoot and Arslan.

Lilyquist, C. and Brill, R. H. (1993) *Studies in Early Egyptian Glass*. New York: The Metropolitan Museum of Art.

Lloyd, S. (1984) *The Archaeology of Mesopotamia: From the Old Stone Age to the Persian Conquest*. New York: Thames and Hudson.

Lucas, A. (1926, reprinted 1989) *Ancient Egyptian Materials and Industries*. London: Histories and Mysteries of Man, Ltd.

Lupu, A. (1969) Metallurgical aspects of Chalcolithic copper working at Timna (Israel).

Marcus, M. I. (1991) The Mosaic glass vessels from Hasanlu, Iran: a study in large-scale stylistic trait distribution. *The Art Bulletin* 73 (4), pp. 536-560.

Marcus, M. I. (1996) *Emblems of Identity and Prestige: the Seals and Sealings from Hasanlu, Iran*. Philadelphia: University Museum, University of Pennsylvania.

Mass, J. L., Stone, R. E., and Wypyski, M. T. (1998) The Mineralogical and Metallurgical Origins of Roman Opaque Colored Glasses. In (P. McCray and W. D. Kingery, Eds.) *The Prehistory and History of Glassmaking Technology: Ceramics and Civilization*, Volume VIII. Westerville, OH: American Ceramic Society, pp. 121-144.

Mass, J. L., Wypyski, M. T., and Stone, R. E. (2002) Malkata and Lisht glassmaking technologies: towards a specific link between second millennium BC metallurgists and glassmakers. *Archaeometry* 44 (1), pp. 67-82.

McCray, W. P., Osborne, Z. A., and Kingery, W. D. (1995) The History and technology of Renaissance Venetian chalcedony glass. *Rivista della Stazione Sper. Vetro*.

McGovern, P. E. (1987) Silicate Industries of Late Bronze-Early Iron Age Palestine: Technological Interaction between Egypt and the Levant. In (M. Bimson and I. C. Freestone, Eds.) *Early Vitreous Materials*. British Museum Occasional Paper 56. London: British Museum Press, pp. 91-114.

McGovern, P. E., Fleming, S. J., and Swann, C. P. (1991) The Beads from Tomb B10a B27 at Dinkha Tepe and the Beginnings of Glassmaking in the Ancient Near East. *American Journal of Archaeology* 95, pp. 395-402.

Moorey, P. R. S. (1999) *Ancient Mesopotamian Materials and Industries: the Archaeological Evidence*. Winona Lake, IN: Eisenbrauns.

Muscarella, O. W. (1966) Hasanlu 1964. *Bulletin of the Metropolitan Museum of Art* 25, pp. 121-135.

Muhly, J. D. (1985) Sources of tin and the beginnings of bronze metallurgy. *American Journal of Archaeology* 89, pp. 275-291.

Muhly, J. D., Begemann, F., Oztunali, O., Pernicka E., Schmitt-Strecker, S., Wagner, G. A. (1991) The Bronze Age metallurgy of Anatolia and the question of local tin sources, in (E. Pernicka and G. A. Wagner, Eds.) *Archaeometry '90, International Symposium on Archaeometry, 2-6 April, 199, Heidelberg*. Basel, pp. 209-220.

Nenna, M.-D., Vichy, M., and Picon, M. (1997) L' Atelier de verrier de Lyon, du Ier siecle apres J.-C., et l' origine des verres "Romains" *Revue d' Archaeometrie* 21, pp. 81-87.

Neri, A. (1662) *The art of glass*. Translated by Merret, C. 1662. London: A.W. for O. Pulleyn.

Newton, R. & Davison, S. (1989) *Conservation of Glass*. Oxford: Butterworth-Heinemann.

Newton, R. (1989) Deterioration of glass. In (R. Newton and S. Davison, Eds.) *Conservation of Glass*. Butterworth-Neinemann, Oxford, UK.

Nicholson, P. T. (1995) Recent excavations at an ancient Egyptian glassworks: Tell el-Amarna 1993. *Journal of Glass Technology* 36 (4), pp. 125-128.

Nicholson, P. T. and Henderson, J. (2002) Glass. In (P. T. Nicholson and J. Henderson, Eds.) *Ancient Egyptian Materials*. Cambridge: Cambridge University Press, pp. 195-224.

Oppenheim, A. L. (1970) The Cuneiform Texts. In (Oppenheim, A. L., Brill, R. H., Barag, D., and von Saldern, A.) *Glass and Glassmaking in Ancient Mesopotamia: An Edition of the Cuneiform Texts Which Contain Instructions for Glassmakers with a Catalogue of Surviving Objects*. Corning, New York: The Corning Museum of Glass, pp. 1-104.

Oppenheim, A. L., Brill, R. H., Barag, D., and von Saldern, A. (1970) *Glass and Glassmaking in Ancient Mesopotamia: An Edition of the Cuneiform Texts Which Contain Instructions for Glassmakers with a Catalogue of Surviving Objects*. Corning, New York: The Corning Museum of Glass.

Peltenburg, E. (1971) Some early developments of vitreous materials. *World Archaeology* 3 (1), pp. 6-12.

Peltenberg, E. J. (1987) Early Faience: Recent Studies, Origins and Relations with Glass. In (M. Bimson and I. C. Freestone, Eds.) *Early Vitreous Materials*. British Museum Occasional Paper 56. London: British Museum Press, pp. 5-29.

Petrie, W. M. F. (1894) *Tell el-Amarna*. London: Methuen.

Phillips, D. L. and Koch, P. L. (2002) Incorporating concentration dependence in stable isotope mixing models. *Oecologia* 130, pp. 114-125.

Pigott, V. (1980) The Iron Age in western Iran. In (T. A. Wertheim and J. D. Muhly, Eds.) *The Coming of the Age of Iron*. New Haven: Yale University Press, pp. 417-461.

Pigott, V. (1999) *The Archaeometallurgy of the Asian Old World*. MASCA Research Papers in Science and Archaeology 16, University Museum Symposium Series 7, University Museum Monograph 89. Philadelphia: Museum University of Pennsylvania.

Potts, D. T. (1999) *The Archaeology of Elam*. Cambridge: Cambridge University Press.

Potts, T. (1994) *Mesopotamia and the East*. Oxford University Committee for Archaeology Monograph 37. Oxford: Institute of Archaeology.

Reed, S. B. J. (1996) *Electron Microprobe Analysis and Scanning Electron Microscopy in Geology*. Cambridge: Cambridge University Press.

Rehren, Th., Pusch, E., and Herold, A. (1998) Glass Coloring Works within a Copper-Centered Industrial Complex in Late Bronze Age Egypt. In (P. McCray and W. D. Kingery, Eds.) *The Prehistory and History of Glassmaking Technology: Ceramics and Civilization*, Volume VIII. Westerville, OH: American Ceramic Society, pp. 227-250.

Renfrew, A. C., Dixon, J. E., and Cann, J. R. (1976) Obsidian and early cultural contact in the Near East. *Proceedings of the Prehistoric Society* 32, pp. 30-72.

Rising, B. (1999) Analytical Procedures. In (Ed. Brill R. H.) *Chemical Analyses of Early Glasses Volume 2*. Corning, NY: Corning Museum of Glass, pp. 529-44.

Roaf, (1995) in (Curtis, J., Ed.) *Early Mesopotamia and Iran: Contact and Conflict, 3500-1600 B.C.* London: British Museum Press.

Roman, I. (1990) The Copper Ingots. In (B. Rothenberg, Ed.) *The Ancient Metallurgy of Copper*. Researches in the Arabah, 1959-1984, Volume 2. London: Institute for Archaeo-Metallurgical Studies, pp. 176-181.

Saitowitz, S. J., Reid, D. L., and van der Merwe, N. J. (1996) Glass bead trade from Islamic Egypt to South Africa c. AD 900-1250. *South African Journal of Science*, 92, pp. 101–104.

von Saldern, A. (1966) Mosaic glass from Hasanlu, Marlik, and Tell al-Rimah. *Journal of Glass Studies* 8, pp. 9-25.

Sanderson, D. S. W. and Hunter, J. R. (1981) Composition variability in vegetable ash. *Science and Archaeology* 23, pp. 27-30.

Santopadre, P. and Verità, M. (2000) Analyses of the production technologies of Italian vitreous materials of the Bronze-Age. *Journal of Glass Studies* 42, pp. 25–40.

Sayre, E. V. (1965) Summary of the Brookhaven Program of Analysis of Ancient Glass. *Application of Science in Examination of Works of Art*. Boston: Museum of Fine Arts, pp. 145-154.

Sayre, E. V. and Smith, R. W. (1961) Compositional categories of ancient glass. *Science* 133 (3467), pp. 1824-1826.

de Schauensee, M. (1988) Bronzeworking in the Iron Age: The View from Hasanlu, in (Curtis J., Ed.) *Bronzeworking Centres of Central Asia*. London: Kegan Paul International, pp. 45-62.

de Schauensee, M. (2001) A Note on three glass plaques from Hasanlu. *Iraq* 63, pp. 99-106.

Sheppard, S. M. F. (1986) Igneous Rocks: III. Isotopic Case Studies of Magmatism in Africa, Eurasia and Oceanic Islands, in (Eds. J. W. Valley, H. P. Taylor, Jr., and J. R. O'Neil) *Stable Isotopes: High Temperature Geological Processes*. Reviews in Mineralogy 16 Washington, DC: Mineralogical Society of America, pp. 319-371.

Shortland, A. J. (2002) The Use and origin of antimonate colorants in early Egyptian glass. *Archaeometry* 44 (4), pp. 517-530.

Shortland, A. J. and Tite, M. S. (2000) Raw materials of glass from Amarna and implications for the origins of Egyptian glass. *Archaeometry* 42 (1), pp. 141-151.

Smedley, J. W., Jackson, C.M., and Welch, C.M. (2001) Unraveling glass compositions: detecting the raw materials used for glassmaking at Little Birches, Staffordshire. In *Abstracts of Association Internationale pour l'Histoire du Verre, XV Congress, New York/Corning, October 15-20, 2001*, p. 25.

Spicuzza, M. J., Valley, J. W., and McConnell, V. S. (1998) Oxygen isotope analysis of whole rock via laser fluorination: an air-lock approach. *Geological Society of America Annual Meeting Program with Abstracts* 30 (7), p. A80.

Stapleton, C. P. (submitted) Glass colouring technology of mosaic vessels from the early Roman Empire. *Archaeometry*.

Stapleton, C. P. and Swanson, S. E. (2002a) Chemical analysis of glass artefacts from Iron Age levels at Hasanlu, northwestern Iran. *Journal of Glass Technology* 43C, pp. 151-157.

Stapleton, C. P. and Swanson, S. E. (2002b) Batch Material Processing and Glassmaking Technology of 9<sup>th</sup> Century B.C. Artifacts Excavated from the Site of Hasanlu, Northwest Iran. In (P. B. Vandiver, M. Goodway, and J. L. Mass, Eds.) *Materials Issues in Art and Archaeology VI*, Materials Research Society Symposium Proceedings 712. Warrendale, PA: Materials Research Society, pp. 315-321.

Stapleton, C. P., Freestone, I. C., and Bowman, S. G. E. (1999) Composition and origin of early mediaeval opaque red enamel from Britain and Ireland. *Journal of Archaeological Science* 26, pp. 913–921.

Stapleton, C. P., Swanson, S. E., and Ghazi, A. M. (submitted) The Raw materials used to colour 11<sup>th</sup>-9<sup>th</sup> c BC blue transparent glazes from Hasanlu, Iran. *Journal of Geoarchaeological and Bioarchaeological Studies*.

Starr, R. F. S. (1937) *Nuzi: Report on the Excavations at Yorgan Tepe Near Kirkuk, Iraq, 1927-1931, Volume I*. Cambridge, MA: Harvard University Press.

Starr, R. F. S. (1939) *Nuzi: Report on the Excavations at Yorgan Tepe Near Kirkuk, Iraq, 1927-1931, Volume II*. Cambridge, MA: Harvard University Press.

Stein, A. (1969) *Old Routes of Western Iran*. New York: Greenwood Press.

Swann, C. P., McGovern, P. E., and Fleming, S. J. (1993) Recent applications of PIXE spectrometry in archaeology part II, observations on early glassmaking in the Near East. *Nuclear Instruments and Methods in Physics Research B* 75, pp. 445–449.

Swanson, S. E. (1977) Relation of nucleation and crystal-growth rate to the development of granitic textures. *American Mineralogist* 62, pp. 966-978.

Swanson, S. E. (1979) The Effect of CO<sub>2</sub> on phase equilibria and crystal growth in the system KAlSi<sub>3</sub>O<sub>8</sub>-NaAlSi<sub>3</sub>O<sub>8</sub>-CaAl<sub>2</sub>Si<sub>2</sub>O<sub>8</sub>-SiO<sub>2</sub>-H<sub>2</sub>O-CO<sub>2</sub> to 8000 bars. *American Journal of Science* 279, pp. 703-720.

Taylor, Jr., H. P. (1968) The Oxygen isotope geochemistry of igneous rocks. *Contributions to Mineralogy and Petrology* 19, 1-17.

Taylor, Jr., H. P. and S. M. F. Sheppard, S. M. F. (1986) Igneous Rocks: I: Processes of Isotopic Fractionation and Isotope Systematics, in (Eds. J. W. Valley, H. P. Taylor, Jr., and J. R. O'Neil) *Stable Isotopes: High Temperature Geological Processes*. Reviews in Mineralogy 16 Washington, DC: Mineralogical Society of America, pp. 227-271.

Thornton C. P., Lamberg-Karlovsky C. C., Liezers M. and Young, S. M. M. (2002) On pins and needles: tracing the evolution of copper-base alloying at Tepe Yahha, Iran, via ICP-MS analysis of common-place items. *Journal of Archaeological Sciences* 29, pp. 1451-60

Tite M. S., Bimson M., and Cowell M. R. (1984) Technological Examination of Egyptian Blue. In (J. G. Lambert, Ed.) *Archaeological Chemistry III*, Advances in Chemistry Series 205. Washington, D. C.: American Chemical Society, pp. 215-242.

Turner, W. E. S. (1956) Studies of ancient glasses and glass-making processes. Part V. Raw materials and melting processes. *Transactions of the Society of Glass Technology* 40, pp. 277T-300T.

Tylecote, R. F. (1976) *A History of Metallurgy*. London: Metals Society.

Tylecote, R. F. and Boydell, P. J. (1978) Experiments on copper smelting. In (B. Rothenberg, Ed.) *Chalcolithic Copper Smelting*. London: International Association for Metallurgical Studies, pp. 27-49.

Valley, J. W., Kitchen, N., Kohn, M. J., Niendorf, C. R., and Spicuzza, M. J. (1995) UWG-2, a garnet standard for oxygen isotope ratios: Strategies for high precision and accuracy with laser heating. *Geochimica et Cosmochimica Acta* 59 (24), pp. 5223-5231.

Vandiver, P. B. (1982) Mid-Second Millennium B.C. Soda-Lime-Silicate Technology at Nuzi (Iraq). In (T. A. Wertime and S. F. Wertime, Eds.) *Early Pyrotechnology: The Evolution of the First Fire-Using Industries*. Washington, D. C.: Smithsonian Institution Press, pp. 73-92.

Vandiver, P. B. (1983a) Egyptian Faience Technology. In (A. Kaczmarczyk and R. E. M. Hedges) *Ancient Egyptian Faience*. Warminster: Aris and Phillips, pp. A1-A144.

Vandiver, P. (1983b) Glass technology at the mid-second millennium BC Hurrian site of Nuzi. *Journal of Glass Studies* 25, pp. 241–251.

Verità, M., Basso, R., Wypyski, M. T., and Koestler, R. J. (1994) X-ray microanalysis of ancient glassy materials: a comparative study of wavelength dispersive and energy dispersive techniques. *Archaeometry* 36 (2), pp. 241–251.

Voigt, M. M. (1977) The Subsistence Economy of a Sixth Millennium Village in the Ushnu-Solduz Valley, in (L. D. Levine and T. C. Young, Jr., Eds.) *Mountains and Lowlands: Essays in the Archaeology of Greater Mesopotamia*. Malibu: Udena, pp. 307-346.

Voigt, M. M. and Dyson, R. H. (1993) Chronology of Western Iran. In (R. W. Ehrich, Ed.) *Chronologies in Old World Archaeology*. Chicago: Chicago University Press, pp. 174-178.

Wedepohl, K. H. (1997) Chemical composition of medieval glass from excavations in West Germany. *Glastechnik Berichte Glass Science and Technology* 70 (8), pp. 246-255.

Weyl, W. A. (1951) *Coloured Glasses*. Sheffield: Society of Glass Technology.

White, A. (1983) Surface chemistry and dissolution kinetics of glassy rocks at 25 C. *Geochimica et Cosmochimica Acta* 47, pp. 805-815.

Winter, I. J. (1976) Phoenician and north Syrian ivory carving in historical context: questions of style and distribution. *Iraq* 38, pp.1-22.

Winter, I. J. (1977) Perspective on the "Local Style" of Hasanlu IVB: A Study in Receptivity. In (Eds., L. D. Levine and T. C. Young, Jr.) *Mountains and Lowlands*. Malibu: Undena, pp. 371-386, plates XV-XXVI.

Yener, K. A. (2000) *The Domestication of Metals: The Rise of Complex Metal Industries in Anatolia*. Boston: Brill.

Yener, K. A. and Vandiver, P. B. (1993) Tin processing at Goltepe, an early Bronze Age site in Anatolia. *American Journal of Archaeology* 97, pp. 207-238.

Yener, K. A., Ozbal, H., and Kaptan, E. (1989) Kestel: An Early Bronze Age Source of Tin Ore in the Taurus Mountains, Turkey. *Science* 244, pp. 117-264.

Yoffee, N. (1981) *Explaining Trade in Ancient Western Asia*. Monographs on the Ancient Near East 2. Malibu: Undena.

Young, Jr., T. C. (1967) The Iranian migration into the Zagros. *Iran* 5, pp. 11-34.

Zimansky, P. E. (1985) *Ecology and Empire: The Structure of the Urartian State*. Chicago: Oriental Institute, University of Chicago.